Marginal material stability

Yury Grabovsky   Lev Truskinovsky

Journal of Nonlinear science, Vol. 23, No. 5, pp. 891–969, 2013,
DOI: 10.1007/s00332-013-9173-6

Abstract

Marginal stability plays an important role in nonlinear elasticity because the associated *minimally stable* states usually delineate failure thresholds. In this paper we study the local (material) aspect of marginal stability. The *weak* notion of marginal stability at a point, associated with the loss of strong ellipticity, is classical. States that are marginally stable in the *strong* sense are located at the boundary of the quasi-convexity domain and their characterization is the main goal of this paper. We formulate a set of bounds for such states in terms of solvability conditions for an auxiliary *nucleation problem* formulated in the whole space and present nontrivial examples where the obtained bounds are tight.

Contents

1 Introduction **2**

2 Spinodal and binodal **7**
- 2.1 Generalized second variation . . . 8
- 2.2 Definitions of spinodal and binodal . . . 10
- 2.3 Equivalent variational characterizations . . . 11

3 Examples of equivalent problems **12**
- 3.1 Spinodal . . . 12
- 3.2 Binodal . . . 14
  - 3.2.1 Localized test functions . . . 16
  - 3.2.2 Periodic-decaying test fields . . . 19
  - 3.2.3 Laminates . . . 21

4 Characterization of spinodal and binodal **22**
- 4.1 Spinodal . . . 22
- 4.2 Binodal . . . 25
  - 4.2.1 Classical nucleation . . . 25

4.2.2 Microstructure nucleation . . . 33

5 Bi-quadratic energy **38**

5.1 Isolated cylindrical inclusions . . . 39

5.1.1 Euler-Lagrange equations . . . 40

5.1.2 Noether-Eshelby equations . . . 42

5.1.3 Optimal orientation . . . 44

5.1.4 Explicit bounds . . . 45

5.2 Interacting cylindrical inclusions . . . 48

5.2.1 Euler-Lagrange equations . . . 48

5.2.2 Noether-Eshelby equations . . . 50

5.2.3 Optimal orientation . . . 50

5.2.4 Optimal shapes . . . 52

5.3 Laminates . . . 57

6 Conclusions **57**

7 Acknowledgement **58**

A Proof of Lemma 3.3 **58**

B Proof of Lemma 3.7 **60**

C Proof of Theorem 3.9 **62**

D Proof of Theorem 3.14 **68**

E Proof of Lemma 4.4 **69**

F Proof of Theorem 4.6 **70**

G Proof of Lemma 5.5 **72**

1 Introduction

A classical problem of calculus of variation is to find global minimizers and identify in this way the most stable configurations known in physics as *ground states*. A more complex and less studied problem concerns finding all local minima which in physical terms means characterization of the set of *metastable states*. The task of finding all local minimizers is often obfuscated by the fact that local minima can be defined in different ways depending on the choice of the topology on the set of configurations. When such uncertainty exists, it indicates certain degeneracy of the theory and its resolution requires additional physical hypotheses external to the original variational problem.

In this paper we pose a new problem of identifying all minimally stable local minimizers that are usually interpreted in physical and mechanical literature as *marginally stable* states. As in the case of local minima the definition of marginally stable states depends on the choice of topology.

More specifically, we focuss on the study of variational functionals typical of nonlinear elasticity

$$E(\boldsymbol{y}) = \int_{\Omega} W(\nabla \boldsymbol{y}(\boldsymbol{x}))d\boldsymbol{x}, \tag{1.1}$$

where the energy density W is a continuous and bounded from below function on the space $\mathbb{M}$ of all $m \times d$ matrices, with d being the spatial dimension. For the variational problem (1.1) the two basic topologies are the $W^{1,\infty}$ norm topology and the $W^{1,\infty}$ sequential weak-* topology; the associated local minimizers will be called weak and strong[1], respectively. In elasticity theory the selection of topology is a physical assumption and the choice between our strong and week topologies may reflect, for instance, the presence of spatial inhomogeneities in the physical problem. To avoid these decisions we consider two topologies on equal grounds being aware that our choices are by no means exhaustive, for instance, both exclude cavitation.

The knowledge of marginally stable states is important in elasticity theory because reaching such states entails either *structural* or *material* failure [121, 32, 111, 8]. In applications it is important to identify states with disappearing reserve of stability in order to predict large and sometimes catastrophic changes associated with decomposition of these states.

Structural instabilities are global and are associated with such physical phenomena as buckling, barreling, microstructure collapse, etc. [64, 112, 83, 48, 57, 115, 21, 22]. In mathematical literature the notion of *weak global* stability is interpreted as non-negativity of the second variation [17, 113, 49]. The full understanding of this concept in the scalar case was already achieved in the classical work of Jacobi who characterized bifurcation points of the Euler-Lagrange equations for the second variation [95, 47, 49]. In the vectorial case the situation is more complicated, since the space of all solutions of the vectorial analog of the Jacobi equation is infinite dimensional.

Local instabilities manifest themselves at a point and are geometry independent. In mechanical terms they are usually interpreted as *material instabilities* that can manifest themselves through the nucleation of cracks, cavities, nuclei of a new phase, dislocation loops, shear bands, etc. [65, 13, 15, 90, 84, 92]. Reaching local marginal stability thresholds usually means termination of an equilibrium branch and often indicates transition from statics to dynamics.

It is important to mention that material instabilities, epitomized by marginally stable equilibria, serve as indicators that a system has reached the limit of applicability of classical continuum elasticity, in particular, that the description of local deformation in terms of affine Cauchy-Born scheme is about to fail. To advance beyond the limits of marginal stability the theory must be augmented either by admitting singularities or by incorporating internal

[1] Traditionally a strong local minimizer is associated with L^∞ topology. Our abuse of terminology should not cause problems, since in this paper we discuss only the necessary conditions. Clearly, all necessary conditions for a $W^{1,\infty}$ sequential weak-* local minimizer will also be necessary for a L^∞ local minimizer.

length scales. In the first case additional hypotheses of physical nature must be added allowing one to locate (track) these singularities in space. In the second case, these singularities must be appropriately regularized and captured as high gradient regions in the framework of some meso-scopic theory. Even more radical solution is to consider directly the micro-scopic theory which is usually discrete or to build hybrid discrete-continuum numerical schemes. All these extension of the classical elasticity allow one to see how marginal instability ultimately resolves itself.

Recently it has become clear that marginally stable states also play a crucial role in quasi-static evolution of distributed mechanical systems with nonconvex energy, e.g. [105, 109]. In particular, marginally stable states are fundamentally important for self organization towards criticality as observed in plasticity, friction, earthquakes, fracture, martensitic phase transitions and damage propagation [133, 4, 110, 109]. Such driven systems exhibit a capability of *locking* themselves in marginally stable states and the corresponding locus is known in different mechanical settings as yield limit, dynamic friction limit, Griffith limit, or martinsitic hysteresis limit.

The simplest examples of *material instabilities* that can be linked to the two topologies studied in this paper can be found in the theory of fluid equilibria where the loss of weak local stability is associated with spinodal decomposition, and the corresponding marginally stable states lie on the *spinodal* [82], while the loss of strong local stability is associated with nucleation of a new phase, and the corresponding stability threshold is called the *binodal* [124]. In this paper we propose a far reaching generalization of these physical concepts in the context of calculus of variation. In the absence of better choices we continue using the terms *spinodal* and *binodal* as the indicators of weak and strong marginally stable states, respectively.

In the classical calculus of variation, dealing with either scalar or one-dimensional problems, the physical ideas of spinodal and binodal correspond to the notions of local and global convexity limits. The spinodal is then a manifold where Hessian degenerates, while the binodal can be associated with appropriate zeros of the Weierstrass excess function [47, 49].

The general vectorial criterion of *weak local* stability is given by the Legendre-Hadamard condition whose relation to ellipticity loss of the Euler-Lagrange equations and associated bifurcations has been thoroughly studied [125, 9, 39, 33, 72, 10, 101]. In the context of nonlinear elasticity, the locus of weak marginally stable deformation gradients which we call *elastic spinodal* can often be fully characterized analytically [71, 134, 35].

The mathematical notion of *strong local*, or material stability in vectorial problems is expressed by the quasiconvexity condition [94, 12, 111, 15, 36]. Unlike the Legendre-Hadamard condition, this constraint is non-local and is much harder to explicate [77]. The quasiconvexification is known explicitly only in a few very special cases [68, 76, 75, 6, 103, 36] and our goal is to solve a simpler problem of computing the *elastic binodal*, without getting into a task of relaxing a non-quasiconvex energy.

We first observe that the *spinodal* and the *binodal regions*, where our two notions of local stability are *strictly violated*, can be characterized in terms of the parametric variational inequalities:

$$\mathfrak{S} = \left\{ \boldsymbol{F} \in \mathbb{M} : \inf_{\boldsymbol{\phi} \in C_0^1(B_1;\mathbb{R}^m)} \int_{B_1} (W_{\boldsymbol{FF}}(\boldsymbol{F})\nabla\boldsymbol{\phi}(\boldsymbol{z}), \nabla\boldsymbol{\phi}(\boldsymbol{z}))d\boldsymbol{z} < 0 \right\}, \tag{1.2}$$

for the spinodal region and

$$\mathfrak{B} = \left\{ \boldsymbol{F} \in \mathbb{M} : \inf_{\boldsymbol{\phi} \in C_0^1(B_1;\mathbb{R}^m)} \int_{B_1} \{W(\boldsymbol{F} + \nabla\boldsymbol{\phi}(\boldsymbol{z})) - W(\boldsymbol{F})\}d\boldsymbol{z} < 0 \right\}. \tag{1.3}$$

for the binodal region, where $W_{\boldsymbol{F}}(\boldsymbol{F})$ denote the array of partial derivatives $\partial W/\partial F_{i\alpha}$ with $i = 1, \ldots, m$ and $\alpha = 1, \ldots, d$. These definitions, however, cannot be considered as universal tools allowing one to characterize either spinodal or binodal regions directly by solving the corresponding Euler-Lagrange equations. Even if minimizers can be determined in this way, such characterization is usually not the simplest.

One way to obtain a constructive definition of spinodal and binodal regions is to formulate problems equivalent to (1.2) and (1.3) in extended spaces of admissible test functions where all unnecessary smoothness and growth conditions are eliminated. Different formulations defining the same critical sets form an *equivalence class*. We show that in the case of weak local minima, a particular equivalent reformulation of the original problem allows one to fully characterize the spinodal region in the space of gradients and to localize the spinodal as its boundary.

Similarly exhaustive reformulation in the case of a general binodal remains elusive. Here, in contrast with the classical bifurcation theory, which is fully adequate in the case of the spinodal [121, 101, 111], the implied *generalized bifurcation problem* cannot be understood by linearization. In the absence of a general solution of such nonlinear bifurcational problem we focus in this paper on the task of characterizing different subsets of binodal region and constructing in this way some bounds separating (strongly) unstable states from the (strongly) stable ones.

We use the crucial observation that in order to characterize the binodal we do not need to know the value of the infimum in (1.2) and (1.3) but only its sign. This simplifies the equivalence criterion and allows one to formulate alternative parametrized variational inequalities that are more amenable to analysis. In particular, we show that in this way one can characterize a subset of "unsafe loading conditions" by solving auxiliary problems formulated either for a system of *partial differential equations* or an *algebraic system*. More specifically, we show that by probing a homogeneous configuration with the test functions from sufficiently large spaces one can obtain a partial characterization of the binodal (see earlier related work reviewed in [89, 27, 28, 29]). How tight are the ensuing bounds depends on specifics of the non-convexity of the energy density function.

The main tool in our analysis of the binodal is the notion of stability with respect to *nucleation* which we formulate, building on some earlier insights [86, 85, 106, 107, 108, 68, 67, 45, 46, 44], in terms of solvability conditions for an auxiliary problem in all physical space. The infinite size of the domain reflects the fact that marginalization of an equilibrium in strong topology is a manifestation of *local* instability. Here it is appropriate to mention similar development in the theory of shape optimization where non convex functionals arise naturally and where our nucleation problem can be linked to the computation of 'topological' or 'Hadamard derivatives' [116, 5].

The nucleation problem can be formulated in different but *equivalent* ways depending on the assumed behavior of the test functions at infinity and we raise the problem of maximal extension of the space of test functions in order to obtain the broadest possible notion of the energy-neutral nucleus. In particular, we observe that seemingly natural requirement of the energy density decay at infinity is inadequate for capturing non-compact nuclei represented by cylinders and plates or by the sets of interacting nuclei spreading to infinity.

To supplement the PDE-based bounds we also consider a nucleation problem for gradient Young measures of the sequences of test functions converging only weakly [130, 131, 14, 18, 102, 120]. Finding the optimal Young measures in the general case is hardly possible, however, simple algebraic bounds on the binodal can be obtained by energy minimization with respect to a subclass of Young measures represented by laminates. This leads to the concept of partially relaxed energy density which can be used in the *secondary* nucleation PDE-based problem. The generalized bifurcations in the resulting PDE can be interpreted as nucleation of composite precipitates [106, 107, 108, 135, 74, 73] and our work establishes a rigorous connection between the corresponding 'polydomain nucleation problem' and the task of identifying the limits of strong stability.

In addition to isolated inclusions we also consider arrays of *interacting* inclusions that are periodic in some directions and decay in others. In physical terms the periodicity assumption means that the elastic interaction between individual inclusions is necessary for optimality and that we are dealing here with a *cooperative phenomenon*. The most dramatic example of collective nucleation is provided by multi-rank laminates. While the resulting bounds are in no way exhaustive they may be very useful in applications, where one has no hope of computing the explicit quasiconvex envelopes.

To illustrate our formal development, we consider two examples in full detail. In the first example we deal with the simplest energy exhibiting two incompatible (non rank one connected) wells. The material is isotropic and the double well structure is imposed only on the $\mathrm{Tr}\,\boldsymbol{F}$ dependence of the energy. In the second example we consider general isotropic energy with two quadratic wells which has been broadly studied in composite theory and in the theory of martensitic transformations. For these two examples we show that the PDE-based methods combined with the laminate-based methods allow one to locate the *entire* elastic binodal. It is, of course, not surprising since in both cases quasi-convexification is known to coincide with rank one convexification.

Several important issues are not addressed in this paper. For instance, it is known that both weak and strong versions of material stability have nontrivial heterogeneous versions when the point of interest is located on the Neumann part of the external boundary [2, 3, 23, 17, 114, 111, 93] or on an internal point of inhomogeneity [37, 83, 63]. In the case of weak local minima the corresponding theory is rather well developed [114, 111, 93] and the associated concept of *surface spinodal* is straightforward. For strong local minimizers, one needs to find the limits of the quasiconvexification-on-the-boundary set [17, 113, 111, 11] which makes an explicit characterization of the *surface binodal* a formidable challenge. Although the associated instabilities play an important role in applications, e.g., [119, 66], we left this interesting subject outside the scope of the present paper. Similarly, we did not attempt the differential characterization of the binodal (Clausius-Clapeyron type relations) and did not specifically study the nucleation conditions at the non-smooth part of the binodal associated with simultaneous activation of distinct nucleation mechanisms.

While we succeeded in building some conceptual links between the notions of spinodal and binodal, the ensuing stability limits remain fundamentally unconnected in the framework of classical nonlinear elasticity which does not have an internal length scale. The situation changes fundamentally if one considers regularized theory where the jumps of deformation gradients are replaced by smooth transition layers. In such settings (e.g. gradient theory, phase field theory, etc.) binodal and spinodal become parts of a *single* stability diagram where the (regularized) spinodal indicates the actual bifurcation of a homogeneous configuration while the (regularized) binodal marks the transition between the trivial and the nontrivial branches of the global minimization path (see [19, 122] for 1D examples). These issues deserve a careful separate study.

This paper is organized as follows. In Section 2 we introduce the concepts of elastic spinodal and elastic binodal as the boundaries of the larger sets on which certain variational functionals are non-negative. To identify these boundaries one needs to solve a *bifurcation problem* in the case of the spinodal and a *nucleation problem* in the case of the binodal. In Section 3 we present several examples of equivalent formulations of the bifurcation and nucleation problems and propose the *existence* and the *computability* of solutions as possible selection criteria. In Section 4 we obtain an explicit characterization of the spinodal and binodal sets for some classes of test functions. In particular, we study the case when the binodal is detectable by solving a system of PDEs complemented with additional conditions allowing one to specify locations of gradient discontinuities. A case study for an important class of bi-quadratic energies with two isotropic wells is presented in the last Section 5 where we deal with *arbitrary* space dimensions and make the nucleation-based bounds on the binodal fully explicit. While similar calculations have been performed many times before [68, 89, 45, 46, 28, 29] their direct relation to the notion of quasiconvexity was not rigorously established.

2 Spinodal and binodal

Consider a rather general variational functional used in non-linear elasticity theory

$$E(\boldsymbol{y}) = \int_{\Omega} W(\nabla \boldsymbol{y}(\boldsymbol{x}))d\boldsymbol{x} - \int_{\partial\Omega_N} (\boldsymbol{t}(\boldsymbol{x}), \boldsymbol{y})dS(\boldsymbol{x}), \tag{2.1}$$

where Ω is a smooth open and bounded domain in $\mathbb{R}^d$, and $\partial\Omega_N$ is the Neumann part of the boundary. We assume that the values of $\boldsymbol{y}(\boldsymbol{x})$ are prescribed on the Dirichlet part $\partial\Omega_D = \partial\Omega \setminus \partial\Omega_N$. Further regularity assumptions will be stated below. We observe that in general it is possible to absorb the boundary term into the volume integral by replacing the energy density with an appropriate more general Lagrangian

$$E(\boldsymbol{y}) = \int_{\Omega} L(\boldsymbol{x}, \boldsymbol{y}(\boldsymbol{x}), \nabla \boldsymbol{y}(\boldsymbol{x}))d\boldsymbol{x}. \tag{2.2}$$

To formulate our two notions of local stability (or metastability) we define $\mathrm{Var} = \{\boldsymbol{u} \in C^1(\overline{\Omega}; \mathbb{R}^m) : \boldsymbol{u}(\boldsymbol{x}) = \boldsymbol{0},\ \boldsymbol{x} \in \partial\Omega_D\}$. The weakly and strongly stable states are defined as follows.

Definition 2.1. *A sequence $\boldsymbol{u}_n \in \mathrm{Var}$ is called an **admissible weak variation** if $\|\boldsymbol{u}_n\|_{C^1} \to 0$, as $n \to \infty$.*

Definition 2.2. *We say that $\boldsymbol{y}(\boldsymbol{x})$ is a **weak local minimum** if for all admissible weak variations $\boldsymbol{u}_n$ we have $E(\boldsymbol{y} + \boldsymbol{u}_n) \geq E(\boldsymbol{y})$ when n is sufficiently large.*

Definition 2.3. *A sequence $\boldsymbol{s}_n \in \mathrm{Var}$ is called an **admissible strong variation** if $\|\boldsymbol{s}_n\|_{C^0} \to 0$, as $n \to \infty$.*

Definition 2.4. *We say that $\boldsymbol{y}(\boldsymbol{x})$ is a strong local minimum if for all admissible strong variations $\boldsymbol{s}_n$ we have $E(\boldsymbol{y} + \boldsymbol{s}_n) \geq E(\boldsymbol{y})$ when n is sufficiently large.*

2.1 Generalized second variation

Suppose that we are testing stability of a given configuration $\boldsymbol{y} \in C^1(\overline{\Omega}; \mathbb{R}^m)$. We always assume that the energy density $L(\boldsymbol{x}, \boldsymbol{y}, \boldsymbol{F})$ is of class C^2 on the extended graph $\{(\boldsymbol{x}, \boldsymbol{y}(\boldsymbol{x}), \nabla \boldsymbol{y}(\boldsymbol{x})) : \boldsymbol{x} \in \overline{\Omega}\}$ of $\boldsymbol{y}(\boldsymbol{x})$. Consider a general (weak or strong) admissible variation[2] $\{\boldsymbol{g}_\epsilon\} \subset \mathrm{Var}$. We can expand the energy increment as follows

$$\Delta E(\boldsymbol{g}_\epsilon) = E(\boldsymbol{y} + \boldsymbol{g}_\epsilon) - E(\boldsymbol{y}) = \delta E(\boldsymbol{g}_\epsilon) + \delta^2 E(\boldsymbol{g}_\epsilon), \tag{2.3}$$

where

$$\delta E(\boldsymbol{g}_\epsilon) = \int_{\Omega} \{(L_{\boldsymbol{F}}, \nabla \boldsymbol{g}_\epsilon) + (L_{\boldsymbol{y}}, \boldsymbol{g}_\epsilon)\} d\boldsymbol{x}.$$

The second term

$$\delta^2 E(\boldsymbol{g}_\epsilon) = \int_{\Omega} L^\star(\boldsymbol{x}, \boldsymbol{g}_\epsilon, \nabla \boldsymbol{g}_\epsilon) d\boldsymbol{x},$$

where

$$L^\star(\boldsymbol{x}, \boldsymbol{u}, \boldsymbol{H}) = L(\boldsymbol{x}, \boldsymbol{y}(\boldsymbol{x}) + \boldsymbol{u}, \nabla \boldsymbol{y}(\boldsymbol{x}) + \boldsymbol{H}) - L(\boldsymbol{x}) - (L_{\boldsymbol{F}}(\boldsymbol{x}), \boldsymbol{H}) - (L_{\boldsymbol{y}}(\boldsymbol{x}), \boldsymbol{u}),$$

can be formally interpreted as the "generalized second variation." Indeed, for the weak variations of the form

$$\boldsymbol{g}_\epsilon = \epsilon \boldsymbol{u}, \qquad \boldsymbol{u} \in C^1(\overline{\Omega}; \mathbb{R}^m) \cap \mathrm{Var}, \tag{2.4}$$

[2] Variations can either be sequences as in the Definitions 2.1 and 2.3 or continuum families, such as $\boldsymbol{G}_\epsilon$, where the limit as $n \to \infty$ is replaced by the limit as $\epsilon \to 0$.

we have

$$\delta^2 E(\boldsymbol{g}_\epsilon) = \frac{\epsilon^2}{2}\int_\Omega \{(L_{\boldsymbol{F}\boldsymbol{F}}\nabla\boldsymbol{u}, \nabla\boldsymbol{u}) + 2(L_{\boldsymbol{y}\boldsymbol{F}}\nabla\boldsymbol{u}, \boldsymbol{u}) + (L_{\boldsymbol{y}\boldsymbol{y}}\boldsymbol{u}, \boldsymbol{u})\}d\boldsymbol{x} + o(\epsilon^2).$$

Since the linear term $\delta E(\boldsymbol{g}_\epsilon)$ in the expansion (2.3) vanishes due to the Euler-Lagrange equation, the requirement $\Delta E(\boldsymbol{g}_\epsilon) \geq 0$ implies, for the class of special weak variations (2.4), the non-negativity of the classical second variation

$$\int_\Omega \{(L_{\boldsymbol{F}\boldsymbol{F}}\nabla\boldsymbol{u}, \nabla\boldsymbol{u}) + 2(L_{\boldsymbol{y}\boldsymbol{F}}\nabla\boldsymbol{u}, \boldsymbol{u}) + (L_{\boldsymbol{y}\boldsymbol{y}}\boldsymbol{u}, \boldsymbol{u})\}d\boldsymbol{x} \geq 0 \tag{2.5}$$

where $\boldsymbol{u} \in \mathrm{Var}$ is arbitrary. The condition of non-negativity of the generalized second variation condition can be also specified if we consider a special class of strong variations

$$\boldsymbol{g}_\eta = \eta\boldsymbol{\phi}((\boldsymbol{x} - \boldsymbol{x}_0)/\eta), \qquad \boldsymbol{x}_0 \in \Omega, \qquad \boldsymbol{\phi} \in C_0^1(B_1; \mathbb{R}^m), \tag{2.6}$$

where B_r denotes the ball of radius r centered at the origin. Then, if $\nabla\boldsymbol{y}(\boldsymbol{x})$ is continuous at $\boldsymbol{x}_0$, the generalized second variation has the form

$$\delta^2 E(\boldsymbol{g}_\eta) = \eta^d \int_{B_1} W^\circ(\nabla\boldsymbol{y}(\boldsymbol{x}_0), \nabla\boldsymbol{\phi}(\boldsymbol{z}))d\boldsymbol{z} + o(\eta^d).$$

Here

$$W^\circ(\boldsymbol{F}, \boldsymbol{H}) = \mathcal{E}_L(\boldsymbol{x}_0, \boldsymbol{y}(\boldsymbol{x}_0), \boldsymbol{F}, \boldsymbol{F} + \boldsymbol{H}), \tag{2.7}$$

and

$$\mathcal{E}_L(\boldsymbol{x}, \boldsymbol{y}, \boldsymbol{F}, \boldsymbol{F}') = L(\boldsymbol{x}, \boldsymbol{y}, \boldsymbol{F}') - L(\boldsymbol{x}, \boldsymbol{y}, \boldsymbol{F}) - (L_{\boldsymbol{F}}(\boldsymbol{x}, \boldsymbol{y}, \boldsymbol{F}), \boldsymbol{F}' - \boldsymbol{F})$$

is the classical Weierstrass excess function for the Lagrangian L [132, 49]. We see that $W^\circ(\boldsymbol{F}, \boldsymbol{H})$ can be expressed entirely in terms of the localized version of the Lagrangian

$$W(\boldsymbol{F}) = L(\boldsymbol{x}_0, \boldsymbol{y}(\boldsymbol{x}_0), \boldsymbol{F}), \tag{2.8}$$

where the dependence on $\boldsymbol{x}_0 \in \Omega$ is suppressed in the notation. We note that if the Lagrangian $L(\boldsymbol{x}, \boldsymbol{y}, \boldsymbol{F})$ comes from the energy of the form (2.1) then our definition of $W(\boldsymbol{F})$ differs from the original $W(\boldsymbol{F})$ by at most a linear term, which does not affect any of the subsequent equations.

The requirement $\Delta E(\boldsymbol{g}_\eta) \geq 0$ for the class of special strong variations (2.6) is equivalent to the quasiconvexity at $\nabla\boldsymbol{y}(\boldsymbol{x}_0)$, [94, 12]:

$$\int_{B_1} W^\circ(\nabla\boldsymbol{y}(\boldsymbol{x}_0), \nabla\boldsymbol{\phi}(\boldsymbol{z}))d\boldsymbol{z} \geq 0, \tag{2.9}$$

for all $\boldsymbol{\phi} \in C_0^1(B_1; \mathbb{R}^m)$. Notice that the infinitesimal perturbation (2.6) at a point $\boldsymbol{x}_0 \in \Omega$ is transformed by rescaling (zooming in) into a finite perturbation prescribed on the unit ball. It is well known that the condition (2.9) does not depend on the support of $\boldsymbol{\phi}(\boldsymbol{x})$ and the unit ball B_1 can be replaced by any bounded domain in $\mathbb{R}^d$. The smoothness of $\boldsymbol{\phi}(\boldsymbol{x})$ is also not important, in particular, the condition (2.9) would be unchanged if we require that $\boldsymbol{\phi}$ be of class C^∞, or if we allow $\boldsymbol{\phi}$ to be merely Lipschitz continuous.

The removal of the linear term in (2.3) is natural since we consider stability of an equilibrium state and this step is straightforward in the case of weak local minima. For strong local minima, the removal of the linear term is also useful because finite perturbations in a small domain create small perturbations outside this domain, and the latter become invisible if the linear part of the functional is removed. This was first realized by Weierstrass in a one dimensional setting.

We emphasize that while the quasiconvexity condition (2.9) is *domain-local*, i.e. it depends only on the behavior of the deformation $\boldsymbol{y}(\boldsymbol{x})$ in any neighborhood of the point $\boldsymbol{x}_0$, the second variation condition (2.5) is *domain-global*. The two conditions, however, have a non-trivial intersection that can be achieved either by performing the "localization" $\boldsymbol{u}(\boldsymbol{x}) \mapsto \eta\boldsymbol{v}((\boldsymbol{x}-\boldsymbol{x}_0)/\eta)$ in (2.5) with $\boldsymbol{v} \in C_0^1(B_1;\mathbb{R}^m)$ or by the "weakening" $\boldsymbol{\phi}(\boldsymbol{z}) \mapsto \epsilon\boldsymbol{v}(\boldsymbol{z})$, in (2.9) with $\boldsymbol{v} \in C_0^1(B_1;\mathbb{R}^m)$. Independently of whether we take a limit $\epsilon \to 0$ in (2.9) or a limit $\eta \to 0$ in (2.5) we obtain

$$\int_{B_1} (W_{\boldsymbol{FF}}(\nabla\boldsymbol{y}(\boldsymbol{x}_0))\nabla\boldsymbol{v}(\boldsymbol{z}), \nabla\boldsymbol{v}(\boldsymbol{z}))d\boldsymbol{z} \geq 0 \tag{2.10}$$

for all $\boldsymbol{v} \in C_0^1(B_1;\mathbb{R}^m)$.

2.2 Definitions of spinodal and binodal

The necessary conditions (2.9) and (2.10) of strong and weak stability motivate the following definitions of *spinodal* and *binodal*.

Definition 2.5. *The deformation gradient $\boldsymbol{F} \in \mathbb{M}$ is called* ***weakly locally stable*** *if*

$$\int_{B_1} (W_{\boldsymbol{FF}}(\boldsymbol{F})\nabla\boldsymbol{v}(\boldsymbol{z}), \nabla\boldsymbol{v}(\boldsymbol{z}))d\boldsymbol{z} \geq 0 \tag{2.11}$$

for all $\boldsymbol{v} \in C_0^1(B_1;\mathbb{R}^m)$. The set

$$\mathfrak{S} = \{\boldsymbol{F} \in \mathbb{M} : \boldsymbol{F} \textit{ is not weakly locally stable}\}$$

is called the ***spinodal region****.*

Definition 2.6. *The boundary surface $\mathfrak{Spin} = \partial\mathfrak{S}$ of the spinodal region is called the* ***spinodal****.*

Definition 2.7. *The deformation gradient $\boldsymbol{F} \in \mathbb{M}$ is called* ***strongly locally stable*** *if*

$$\int_{B_1} W^\circ(\boldsymbol{F}, \nabla\boldsymbol{\phi}(\boldsymbol{z}))d\boldsymbol{z} \geq 0, \tag{2.12}$$

for all $\boldsymbol{\phi} \in C_0^1(B_1;\mathbb{R}^m)$*. The set*

$$\mathfrak{B} = \{\boldsymbol{F} \in \mathbb{M} : \boldsymbol{F} \text{ is not strongly locally stable}\} \tag{2.13}$$

is called the ***binodal region****.*

Definition 2.8. *The boundary surface* $\mathfrak{Bin} = \partial\mathfrak{B}$ *of the binodal region is called the* ***binodal****.*

Our goal is to formulate conditions on $\boldsymbol{F}$ under which the inequalities (2.11) and (2.12) become violated. The spinodal and the binodal regions can be characterized in terms of the parametric variational inequalities already mentioned in the Introduction which we rewrite here for convenience

$$\mathfrak{S} = \left\{\boldsymbol{F} \in \mathbb{M} : \inf_{\boldsymbol{v}\in C_0^1(B_1;\mathbb{R}^m)} \int_{B_1} (W_{\boldsymbol{FF}}(\boldsymbol{F})\nabla\boldsymbol{v}(\boldsymbol{z}), \nabla\boldsymbol{v}(\boldsymbol{z}))d\boldsymbol{z} < 0\right\}, \tag{2.14}$$

$$\mathfrak{B} = \left\{\boldsymbol{F} \in \mathbb{M} : \inf_{\boldsymbol{\phi}\in C_0^1(B_1;\mathbb{R}^m)} \int_{B_1} W^\circ(\boldsymbol{F}, \nabla\boldsymbol{\phi}(\boldsymbol{z}))d\boldsymbol{z} < 0\right\}. \tag{2.15}$$

One way to characterize the spinodal and binodal is to compute the infima in (2.14) and (2.15). The infimum in (2.14) is not hard to compute explicitly. The infimum in (2.15) can be expressed in terms of the quasiconvex envelope [34]

$$QW(\boldsymbol{F}) = \frac{1}{|B_1|} \inf_{\boldsymbol{\phi}\in C_0^1(B_1;\mathbb{R}^m)} \int_{B_1} W(\boldsymbol{F} + \nabla\boldsymbol{\phi}(\boldsymbol{z}))d\boldsymbol{z}, \tag{2.16}$$

however, the general problem of finding the function $QW(\boldsymbol{F})$ is notoriously difficult, except for the scalar case $\min(m, d) = 1$, where $QW = CW$ is the convex envelope of $W(\boldsymbol{F})$.

The crucial observation is that in order to construct the set $\mathfrak{B}$ it is *not necessary* to compute the quasiconvex envelope. The reason is that we do not need to know the value of the infinum in (2.15) but only its sign which means that the problem is much easier. In particular, there is a possibility to *modify* both the functional and the set of admissible functions in (2.15) without changing the corresponding set $\mathfrak{B}$. If such modified variational problem possesses minimizers, which can then be identified as solutions of the Euler-Lagrange equation, then the corresponding points on the binodal can also be identified.

2.3 Equivalent variational characterizations

We now make formal definitions of equivalent variational characterizations of the spinodal and binodal.

Definition 2.9. *Let* $\mathcal{F} \subset W^{1,\infty}(\mathbb{R}^d;\mathbb{R}^m)$ *and let* $I(\boldsymbol{F}, \boldsymbol{\phi})$ *be a functional on* $\mathcal{F}$*. We say that the pair* $(I, \mathcal{F})$ ***bounds the spinodal (binodal)*** *if for every* $\boldsymbol{F} \notin \mathfrak{S}$ *(*$\boldsymbol{F} \notin \mathfrak{B}$*)*

$$\inf_{\boldsymbol{\phi}\in\mathcal{F}} I(\boldsymbol{F}, \boldsymbol{\phi}) \geq 0. \tag{2.17}$$

We say that the pair $(I, \mathcal{F})$ ***characterizes the spinodal (binodal)*** *if, in addition to (2.17), for every $\boldsymbol{F} \in \mathfrak{S}$ ($\boldsymbol{F} \in \mathfrak{B}$)*

$$\inf_{\boldsymbol{\phi}\in\mathcal{F}} I(\boldsymbol{F}, \boldsymbol{\phi}) < 0. \tag{2.18}$$

We already know that the pair

$$\mathcal{F} = C_0^1(B_1; \mathbb{R}^m), \qquad I(\boldsymbol{F}, \boldsymbol{v}) = \int_{B_1} (W_{\boldsymbol{FF}}(\boldsymbol{F})\nabla\boldsymbol{v}(\boldsymbol{z}), \nabla\boldsymbol{v}(\boldsymbol{z}))d\boldsymbol{z}$$

characterizes the spinodal, while the pair

$$\mathcal{F} = C_0^1(B_1; \mathbb{R}^m), \qquad I(\boldsymbol{F}, \boldsymbol{\phi}) = \int_{B_1} W^\circ(\boldsymbol{F}, \nabla\boldsymbol{\phi}(\boldsymbol{z}))d\boldsymbol{z}$$

characterizes the binodal. Another well-known example of the binodal characterizing pair is $(\mathcal{Y}_c^0, \Lambda^\circ)$ [70], where $\mathcal{Y}_c^0$ is the space of homogeneous compactly supported gradient Young measures with zero first moment and Λ° is a linear functional on $\mathcal{Y}_c^0$ defined by

$$\Lambda^\circ(\nu) = \int_{\mathbb{M}} W^\circ(\boldsymbol{F} + \boldsymbol{H})d\nu(\boldsymbol{H}), \qquad \nu \in \mathcal{Y}_c^0. \tag{2.19}$$

Since none of these characterizations of the binodal is practical, our goal will be to present other pairs $(\mathcal{F}, I)$ that characterize the binodal. As we have already mentioned, we are interested in finding the spaces $\mathcal{F}$ that allow one to characterize the binodal in terms of computable solutions of a system of PDEs.

We also observe that the notions of pairs characterizing and bounding the binodal may go beyond a simple extension of a function space. For example, nucleation of a precipitate containing martensitic twins microstructure in a shape memory alloy [106, 107, 108, 135, 74, 73], suggests that the set $\mathcal{F}$ may contain parametrized families of Young measures. Then the functional I in the pair $(\mathcal{F}, I)$ will be derived as a limit of the original functional on the sequences generating the Young measures.

3 Examples of equivalent problems

In this section we present several examples of spinodal-characterizing, binodal-characterizing and binodal-bounding pairs that are different from those given in (2.14) and (2.15) and are better suited for obtaining explicit constraints for the sets $\mathfrak{Spin}$ and $\mathfrak{Bin}$.

3.1 Spinodal

In the case of spinodal, the functional in (2.11) is quadratic, and hence, it is natural to extend the space $C_0^1(B_1, \mathbb{R}^m)$ to the space

$$\mathcal{S}_0 = \{\boldsymbol{v} \in L^2_{\mathrm{loc}}(\mathbb{R}^d; \mathbb{R}^m) : \nabla\boldsymbol{v} \in L^2(\mathbb{R}^d; \mathbb{M})\}. \tag{3.1}$$

Then the pair $(\mathcal{S}_0, I_0)$ is spinodal-characterizing, where

$$I_0(\boldsymbol{F}, \boldsymbol{\phi}) = \int_{\mathbb{R}^d} (W_{\boldsymbol{F}\boldsymbol{F}}(\boldsymbol{F})\nabla\boldsymbol{v}(\boldsymbol{z}), \nabla\boldsymbol{v}(\boldsymbol{z}))d\boldsymbol{z} \geq 0, \qquad \boldsymbol{v} \in \mathcal{S}_0. \tag{3.2}$$

Let us show that generically, when $d > 1$ the associated Euler-Lagrange equation

$$\nabla \cdot (W_{\boldsymbol{F}\boldsymbol{F}}(\boldsymbol{F})\nabla\boldsymbol{v}) = \boldsymbol{0}, \qquad \boldsymbol{v} \in \mathcal{S}_0 \tag{3.3}$$

does not have non-zero solutions. Indeed, taking the Fourier transform of (3.3) we obtain [125, 121, 111]

$$\boldsymbol{A}(\boldsymbol{m}; \boldsymbol{F})\widehat{\boldsymbol{v}}(\boldsymbol{m}) = \boldsymbol{0},$$

where the acoustic tensor $\boldsymbol{A}(\boldsymbol{m}; \boldsymbol{F})$ at $\boldsymbol{F}$ is defined as the linear map on $\mathbb{R}^m$ given by

$$\boldsymbol{a} \mapsto \boldsymbol{A}(\boldsymbol{m}; \boldsymbol{F})\boldsymbol{a} = (W_{\boldsymbol{F}\boldsymbol{F}}(\boldsymbol{F})(\boldsymbol{a} \otimes \boldsymbol{m}))\boldsymbol{m}. \tag{3.4}$$

As we can see the L^2 function $\widehat{\boldsymbol{v}}(\boldsymbol{m}) \otimes \boldsymbol{m}$ must be supported on the union of rays $\mathbb{R}\boldsymbol{n}$, where $|\boldsymbol{n}| = 1$ solves $\det \boldsymbol{A}(\boldsymbol{n}; \boldsymbol{F}) = 0$. Generically, this union is a closed and nowhere dense subset of $\mathbb{R}^d$, when $d > 1$. Hence $\widehat{\nabla\boldsymbol{v}}(\boldsymbol{m}) = \boldsymbol{0}$ for a.e. $\boldsymbol{m} \in \mathbb{R}^d$, and the problem (3.3) has only trivial solutions in $\mathcal{S}_0$. The reason for non-existence in (3.3) is that the eigenfunctions of the second order differential operator with constant coefficients are single Fourier modes $e^{i(\boldsymbol{n},\boldsymbol{z})}\boldsymbol{a}$, where $\boldsymbol{a}$ is an eigenvector of the acoustic tensor and these eigenfunctions do not belong to $\mathcal{S}_0$.

The set of functions containing the eigen-modes of the linear operator (3.3) should be sufficient to characterize the spinodal. One possible choice is the set of functions

$$\mathcal{F}_{\mathfrak{S}} = \{\phi((\boldsymbol{z}, \boldsymbol{n}))\boldsymbol{a} : \phi \in H^1(\mathbb{R})\}, \tag{3.5}$$

whose distributional Fourier transform is supported on a single ray $\mathbb{R}\boldsymbol{n}$.

Observe that the functions from (3.5) decay at infinity only in one direction $\boldsymbol{n}$ and the quadratic functional in (3.2) is no longer defined. To fix this problem we can approximate functions (3.5) by a sequence of functions $\boldsymbol{v}_\eta \in \mathcal{S}_0$ and consider an equivalent functional

$$I(\boldsymbol{F}, \boldsymbol{v}) = \frac{\int_{\mathbb{R}^d} (W_{\boldsymbol{F}\boldsymbol{F}}(\boldsymbol{F})\nabla\boldsymbol{v}, \nabla\boldsymbol{v})d\boldsymbol{z}}{\int_{\mathbb{R}^d} |\nabla\boldsymbol{v}|^2 d\boldsymbol{z}}, \qquad \boldsymbol{v} \in \mathcal{S}_0. \tag{3.6}$$

Indeed, it is obvious that $I(\boldsymbol{F}, \boldsymbol{v}) \geq 0$ for all $\boldsymbol{v} \in \mathcal{S}_0$ if and only if (3.2) holds. Let $\rho(\boldsymbol{x})$ be a smooth compactly supported function then

$$\lim_{\eta \to 0} I(\boldsymbol{F}, \rho(\eta\boldsymbol{z})\phi((\boldsymbol{z}, \boldsymbol{n}))\boldsymbol{a}) = (\boldsymbol{A}(\boldsymbol{n}; \boldsymbol{F})\boldsymbol{a}, \boldsymbol{a}). \tag{3.7}$$

This formula follows from the relation

$$\lim_{\eta \to 0} \int_{\mathbb{R}^d} (W_{\boldsymbol{F}\boldsymbol{F}}(\boldsymbol{F})\nabla\boldsymbol{v}_\eta, \nabla\boldsymbol{v}_\eta)d\boldsymbol{z} = (\boldsymbol{A}(\boldsymbol{n}; \boldsymbol{F})\boldsymbol{a}, \boldsymbol{a}) \left(\int_{\mathbb{R}} \phi'(t)^2 dt\right) \left(\int_{(\mathbb{R}\boldsymbol{n})^\perp} \rho(\boldsymbol{u})^2 dS(\boldsymbol{u})\right),$$

where

$$\boldsymbol{v}_\eta(\boldsymbol{z}) = \eta^{\frac{d-1}{2}}\rho(\eta\boldsymbol{z})\phi((\boldsymbol{z},\boldsymbol{n}))\boldsymbol{a}.$$

It is now easy to show that the pair $(\mathcal{F}_{\mathfrak{S}}, I_{\mathfrak{S}})$ with

$$I_{\mathfrak{S}}(\boldsymbol{F}, \phi((\boldsymbol{z},\boldsymbol{n}))\boldsymbol{a}) = (\boldsymbol{A}(\boldsymbol{n};\boldsymbol{F})\boldsymbol{a},\boldsymbol{a}). \tag{3.8}$$

characterizes the spinodal. The Plancherel's identity applied to (3.2) implies

$$\int_{\mathbb{R}^d}(\boldsymbol{A}(\boldsymbol{m};\boldsymbol{F})\widehat{\boldsymbol{v}}(\boldsymbol{m}),\widehat{\boldsymbol{v}}(\boldsymbol{m}))d\boldsymbol{m} \ge 0. \tag{3.9}$$

It is obvious now, that if the acoustic tensor $\boldsymbol{A}(\boldsymbol{n};\boldsymbol{F}) \ge 0$ in the sense of quadratic forms for all $\boldsymbol{n} \in \mathbb{S}^{d-1}$, then (3.9) and hence (3.2) holds. Conversely, (3.7) shows that (3.2) implies non-negativity of the acoustic tensor.

Remark 3.1. *Due to the homogeneity of the functional $I_{\mathfrak{S}}$ we can also write*

$$\inf_{\boldsymbol{\phi}\in\mathcal{F}_{\mathfrak{S}}} I_{\mathfrak{S}}(\boldsymbol{F},\boldsymbol{\phi}) = -Ind_{\mathfrak{S}^c}(\boldsymbol{F}) \tag{3.10}$$

where $Ind_{\mathfrak{S}^c}(\boldsymbol{F})$ is the indicator function[3] *of the complement to the spinodal region $\mathfrak{S}$.*

3.2 Binodal

Here we proceed in parallel with the analysis for the spinodal. We begin by extending the space of admissible test functions from $C_0^1(B_1;\mathbb{R}^m)$ to the space

$$\mathcal{S} = \{\boldsymbol{\phi} \in W^{1,\infty}(\mathbb{R}^d;\mathbb{R}^m) : \nabla\boldsymbol{\phi} \in L^2(\mathbb{R}^d;\mathbb{M})\}, \tag{3.11}$$

for which the integral

$$I^\circ(\boldsymbol{F},\boldsymbol{\phi}) = \int_{\mathbb{R}^d} W^\circ(\boldsymbol{F},\nabla\boldsymbol{\phi}(\boldsymbol{z}))d\boldsymbol{z} \tag{3.12}$$

is convergent. We emphasize the additional assumption of uniform boundedness of $\boldsymbol{\phi}$ and $\nabla\boldsymbol{\phi}$ in the definition of the space $\mathcal{S}$. From a technical standpoint the assumption $\boldsymbol{\phi} \in \mathcal{S}_0$ is insufficient to ensure convergence of the integral (3.12).

Interestingly, the phenomenon of cavitation [13, 118], which is outside the scope of this paper, can be interpreted as existence of unbounded Sobolev test fields $\boldsymbol{\phi} \in W^{1,p}(\mathbb{R}^d;\mathbb{R}^m)$ that in the hard device can lower the energy of a homogeneous state, which is not in the binodal region. Thus, examples in [96, 104] feature cavitation for globally polyconvex energies, whose binodal regions are empty sets.

THEOREM **3.2.** *The pair $(\mathcal{S}, I^\circ)$ characterizes the binodal.*

[3]The indicator function of a set equals to zero on the set and $+\infty$ on its complement.

Proof. If the inequality (2.12) fails for some $\boldsymbol{\phi} \in C_0^\infty(B_1;\mathbb{R}^m)$ then the inequality $I^\circ(\boldsymbol{F},\boldsymbol{\phi}) \geq 0$ also fails, since $\boldsymbol{\phi} \in \mathcal{S}$, if extended by zero outside of B_1.

First we prove $I^\circ(\boldsymbol{F},\boldsymbol{\phi}) \geq 0$, assuming that (2.12) holds. For each $R > 0$ let $\eta_R \in C_0^\infty(B_{2R})$ be a cut-off function such that η_R takes values between 0 and 1, $\eta_R(\boldsymbol{x}) = 1$ for all $\boldsymbol{x} \in B_R$ and $|\nabla\eta_R(\boldsymbol{x})| \leq C/R$ for all $\boldsymbol{x} \in \mathbb{R}^d$ with constant C independent of R. We extend $\eta_R(\boldsymbol{x})$ by zero to the complement of B_{2R}. The theorem will be proved if we show that for each $\boldsymbol{\phi} \in \mathcal{S}$ there exists a constant[4] $\boldsymbol{c} \in \mathbb{R}^m$ and a sequence $R_k \to \infty$, such that

$$\lim_{k\to\infty}\int_{\mathbb{R}^d} W^\circ(\boldsymbol{F},\nabla(\eta_{R_k}(\boldsymbol{\phi}-\boldsymbol{c}))d\boldsymbol{z} = \int_{\mathbb{R}^d} W^\circ(\boldsymbol{F},\nabla\boldsymbol{\phi})d\boldsymbol{z}, \tag{3.13}$$

Indeed, if $\boldsymbol{F}$ satisfies (2.12) then

$$\int_{\mathbb{R}^d} W^\circ(\boldsymbol{F},\nabla(\eta_{R_k}(\boldsymbol{\phi}-\boldsymbol{c})))d\boldsymbol{z} = \int_{B_{2R_k}} W^\circ(\boldsymbol{F},\nabla(\eta_{R_k}(\boldsymbol{\phi}-\boldsymbol{c})))d\boldsymbol{z} \geq 0$$

for all $k \in \mathbb{N}$, and hence the relation (3.13) implies the inequaltity $I^\circ(\boldsymbol{F},\boldsymbol{\phi}) \geq 0$.

To prove (3.13) we use the inequality

$$|W^\circ(\boldsymbol{F},\boldsymbol{G}+\boldsymbol{H}) - W^\circ(\boldsymbol{F},\boldsymbol{G})| \leq C(|\boldsymbol{G}||\boldsymbol{H}| + |\boldsymbol{H}|^2) \tag{3.14}$$

that holds for all $|\boldsymbol{G}| \leq M$ and $|\boldsymbol{H}| \leq M$, where the constant C depends on M, $\boldsymbol{F}$ and W. Taking $M = \|\boldsymbol{\phi}\|_{1,\infty}$, we have

$$|W^\circ(\boldsymbol{F},\nabla(\eta_R(\boldsymbol{\phi}-\boldsymbol{c}))) - W^\circ(\boldsymbol{F},\eta_R\nabla\boldsymbol{\phi})| \leq C\left(\frac{1}{R}|\boldsymbol{\phi}-\boldsymbol{c}||\nabla\boldsymbol{\phi}| + \frac{1}{R^2}|\boldsymbol{\phi}-\boldsymbol{c}|^2\right),$$

where the constant C is independent of $\boldsymbol{x}$ and R. Lemma 3.3 below implies there exists a constant $\boldsymbol{c} \in \mathbb{R}^m$ and a subsequence R_k, such that

$$\lim_{k\to\infty}\int_{\mathbb{R}^d} W^\circ(\boldsymbol{F},\nabla(\eta_{R_k}(\boldsymbol{\phi}-\boldsymbol{c}))d\boldsymbol{z} = \lim_{k\to\infty}\int_{\mathbb{R}^d} W^\circ(\boldsymbol{F},\eta_{R_k}\nabla\boldsymbol{\phi})d\boldsymbol{z}.$$

The inequality $W^\circ(\boldsymbol{F},\boldsymbol{H}) \leq C|\boldsymbol{H}|^2$ holds for all $|\boldsymbol{H}| \leq M$, where the constant C depends M. Using this inequality with $M = \|\boldsymbol{\phi}\|_{1,\infty}$ permits the application of the Lebesgue dominated convergence theorem, resulting in (3.13). □

Now we formulate the Lemma which we needed in Theorem 3.2.

LEMMA **3.3.** *For any $\boldsymbol{\phi} \in \mathcal{S}$ there exists a constant $\boldsymbol{c} \in \mathbb{R}^m$, such that*

$$\varliminf_{R\to\infty}\int_{A_R}\left\{\frac{1}{R}|\boldsymbol{\phi}-\boldsymbol{c}||\nabla\boldsymbol{\phi}| + \frac{1}{R^2}|\boldsymbol{\phi}-\boldsymbol{c}|^2\right\}d\boldsymbol{x} = 0,$$

where $A_R = B_{2R} \setminus B_R$.

[4]When $d \geq 3$ there is a canonical choice of the constant $\boldsymbol{c}$, such that $\boldsymbol{\phi} - \boldsymbol{c} \in L^{2d/d-2}(\mathbb{R}^d;\mathbb{R}^m)$ (see Theorem A.1). When $d = 1$ the choice of the constant is irrelevant. However, when $d = 2$ there is no canonical choice of the constant $\boldsymbol{c}$, which can not be chosen arbitrarily.

The proof of the lemma is in Appendix A.

Remark 3.4. *In the statement of Lemma 3.3 the liminf can be replaced by limit as $R \to \infty$ (as we can see from the proof), except when $d = 2$. When $d = 2$, the use of liminf is essential. Indeed, let $\phi(\boldsymbol{x}) = u(|\boldsymbol{x}|)$, where*

$$u(r) = 2\sin(\ln\ln r) + \frac{\cos(\ln\ln r)}{\ln r}, \qquad r \geq e. \tag{3.15}$$

We compute

$$\langle\phi\rangle_{A_R} = \frac{2}{3R^2}\int_R^{2R} ru(r)dr = \frac{2}{3R^2}(r^2\sin(\ln\ln r))\,|_R^{2R} = 2\sin(\ln\ln R) + o(1),$$

as $R \to \infty$. We see that $\langle\phi\rangle_{A_R}$ has no limit as $R \to \infty$ and that we can choose any $c \in [-2, 2]$ so that there is a sequence R_k for which $\langle\phi - c\rangle_{A_{R_k}} \to 0$, as $k \to \infty$.

3.2.1 Localized test functions

While the space $\mathcal{S}$ is adequate for test fields produced by compact precipitates, it does not contain functions of the form (3.5) corresponding to nucleation of slabs. The proof of equivalence in Theorem 3.2, and especially Lemma 3.3 suggests that the test functions $\boldsymbol{\phi}$ must satisfy

$$\varliminf_{R\to\infty} \frac{\displaystyle\int_{A_R(h(R))}\left\{\frac{1}{h(R)^2}|\boldsymbol{\phi} - \boldsymbol{c}|^2 + |\nabla\boldsymbol{\phi}|^2\right\}d\boldsymbol{x}}{\displaystyle\int_{B_R}|\nabla\boldsymbol{\phi}|^2 d\boldsymbol{x}} = 0, \tag{3.16}$$

for some constant $\boldsymbol{c} \in \mathbb{R}^m$, where $h(R)$ is a monotone increasing function, such that $h(R)/R \to 0$, as $R \to \infty$. Here

$$A_R(h) = \{\boldsymbol{x} \in \mathbb{R}^d : R - h < |\boldsymbol{x}| < R\}.$$

Without attempting to achieve the maximal extension, we can simplify the foregoing exposition by pointing out that in all of our applications we use only the functions $\boldsymbol{\phi}(\boldsymbol{x})$ for which

$$\lim_{R\to\infty} \frac{\displaystyle\int_{A_R(h(R))}|\nabla\boldsymbol{\phi}|^2 d\boldsymbol{x}}{\displaystyle\int_{B_R}|\nabla\boldsymbol{\phi}|^2 d\boldsymbol{x}} = 0 \tag{3.17}$$

for every monotone increasing function $h(R) = o(R)$. This property can be restated as a *relative uniform continuity* of the function

$$K(R) = \int_{B_R}|\nabla\boldsymbol{\phi}|^2 d\boldsymbol{x}.$$

The notion of relative uniform continuity is the same as the classical notion of uniform continuity, except the absolute errors are replaced with relative errors. More precisely, $K(R)$ is relatively uniformly continuous if for every $\epsilon > 0$ there exist $\delta > 0$ such that for any $R_1 > R_2 > 1$ for which $(R_1 - R_2)/R_1 < \delta$, we have $(K(R_1) - K(R_2))/K(R_1) < \epsilon$. We can also restate this property using classical uniform continuity. Observe that the exponential function converts absolute errors into relative errors. Therefore, the relative uniform continuity of $K(R)$ is equivalent to the classical uniform continuity of $f(x) = \ln K(e^x)$ on $[0, +\infty)$.

Definition 3.5. *We say that the test function $\boldsymbol{\phi} \in W^{1,\infty}(\mathbb{R}^d; \mathbb{R}^m)$ is **localized** if $K(R)$ is relatively uniformly continuous at infinity and there exists a constant $\boldsymbol{c} \in \mathbb{R}^m$, and a monotone increasing function $h(R) = o(R)$ such that*

$$\varliminf_{R \to \infty} \frac{1}{K(R)h(R)^2} \int_{A_R(h(R))} |\boldsymbol{\phi} - \boldsymbol{c}|^2 d\boldsymbol{x} = 0. \tag{3.18}$$

It is easy to see that any localized test function $\boldsymbol{\phi}$ satisfies (3.16). One can also construct radial test functions $\phi(\boldsymbol{x}) = u(|\boldsymbol{x}|)$ that satisfy (3.16) but are not localized in the sense of Definition 3.5.

Remark 3.6. *If $d = 1$ or 2, then the condition (3.18) is a consequence of (3.17) for any choice of $\boldsymbol{c}$. If $d \geq 3$, then the condition (3.18) is not a consequence of (3.17). Indeed, if $d = 1$ we have*

$$\frac{1}{h(R)^2} \int_{A_R(h(R))} |\boldsymbol{\phi} - \boldsymbol{c}|^2 d\boldsymbol{x} \leq \frac{\|\boldsymbol{\phi} - \boldsymbol{c}\|_\infty^2}{h(R)},$$

and (3.18) follows as long as $h(R) \to \infty$, as $R \to \infty$. When $d = 2$, we consider two cases. If

$$\varliminf_{R \to \infty} K(R) < +\infty$$

then $\boldsymbol{\phi} \in \mathcal{S}$ and (3.18) follows from Lemma 3.7 below. If $K(R) \to +\infty$, as $R \to \infty$, then

$$\frac{1}{h(R)^2} \int_{A_R(h(R))} |\boldsymbol{\phi} - \boldsymbol{c}|^2 d\boldsymbol{x} \leq 3\pi \|\boldsymbol{\phi} - \boldsymbol{c}\|_\infty^2 \frac{R}{h(R)}.$$

We can now choose $h(R) = o(R)$ that grows sufficiently fast, so that $R/(K(R)h(R)) \to 0$, along some subsequence $R_k \to \infty$. This is proved formally in Lemma B.1. If $d \geq 3$, then the functions $\phi(\boldsymbol{x}) = |\boldsymbol{x}|^{-\alpha}$ satisfy (3.17) but not (3.18), when $0 < \alpha < (d-2)/2$.

The terminology "localized test function" reflects the fact that these functions retain those features of the original smooth, compactly supported test functions that are essential for defining the binodal via the localization (2.6). The definition suggests that we may regard the test function $\boldsymbol{\phi}$ (or more precisely, $\boldsymbol{\phi} - \boldsymbol{c}$) as supported on a compact set $K \subset B_R$ for a sufficiently large R. This corresponds, via (2.6) to variations supported on a small ball $B_{\eta R}(\boldsymbol{x}_0) \subset \Omega$.

If we now wish to distinguish between the the binodal and the interior of the binodal region we need to further restrict our attention to the functions satisfying "zero volume fraction condition"

$$\lim_{R\to\infty} \fint_{B_R} |\nabla\boldsymbol{\phi}|^2 d\boldsymbol{x} = 0 \tag{3.19}$$

In the minimization of the blow up functional (3.12), the condition (3.19) represents additional constraint on the behavior of the test function $\boldsymbol{\phi}$ at infinity.

It is now natural to extend the space of admissible test functions from the space $\mathcal{S}$ to

$$\mathcal{S}_* = \{\boldsymbol{\phi} : \boldsymbol{\phi} \text{ is localized and satisfies (3.19)}\}.$$

Lemma **3.7.** *$\mathcal{S} \subset \mathcal{S}_*$.*

The proof is in the Appendix B.

It is clear that for $\boldsymbol{\phi} \in \mathcal{S}_*$ the integral (3.12) does not have to converge. By analogy with (3.6) we replace it with the normalized functional

$$I_*(\boldsymbol{F}, \boldsymbol{\phi}) = \overline{\lim_{R\to\infty}} \frac{\displaystyle\int_{B_R} W^\circ(\boldsymbol{F}, \nabla\boldsymbol{\phi}) d\boldsymbol{x}}{\displaystyle\int_{B_R} |\nabla\boldsymbol{\phi}|^2 d\boldsymbol{x}}. \tag{3.20}$$

Observe that for any $\boldsymbol{\phi} \in \mathcal{S}_*$ the functional $I_*(\boldsymbol{F}, \boldsymbol{\phi})$ is finite, since $\nabla\boldsymbol{\phi}(\boldsymbol{x})$ is uniformly bounded.

Theorem **3.8.** *The pair $(\mathcal{S}_*, I_*)$ characterizes the binodal.*

Proof. If the inequality (2.12) fails for some $\boldsymbol{\phi} \in C_0^\infty(B_1; \mathbb{R}^m)$ then $I_*(\boldsymbol{F}, \boldsymbol{\phi}) < 0$, since $\boldsymbol{\phi} \in \mathcal{S}_*$. Now assume that (2.12) is satisfied. Our goal is to prove that $I_*(\boldsymbol{F}, \boldsymbol{\phi}) \geq 0$ for all $\boldsymbol{\phi} \in \mathcal{S}_*$. Let us fix $\boldsymbol{\phi} \in \mathcal{S}_*$. Let $h(R)$ and $\boldsymbol{c} \in \mathbb{R}^m$ be as in the Definition 3.5. Let $\eta_R(\boldsymbol{x})$ be a Lipschitz cut-off function such that $0 \leq \eta_R(\boldsymbol{x}) \leq 1$, $\eta_R(\boldsymbol{x}) = 0$, when $|\boldsymbol{x}| \geq R$ and $\eta_R(\boldsymbol{x}) = 1$, when $|\boldsymbol{x}| \leq R - h(R)$. In addition we can choose $\eta_R(\boldsymbol{x})$ such that $|\nabla\eta_R(\boldsymbol{x})| \leq 1/h(R)$. We have due to (3.14)

$$\int_{B_R} |W^\circ(\boldsymbol{F}, \nabla(\eta_R(\boldsymbol{\phi} - \boldsymbol{c}))) - W^\circ(\boldsymbol{F}, \nabla\boldsymbol{\phi})| d\boldsymbol{x} \leq C \int_{A_R(h(R))} \left\{ \frac{|\boldsymbol{\phi} - \boldsymbol{c}|^2}{h(R)^2} + |\nabla\boldsymbol{\phi}|^2 \right\} d\boldsymbol{x}.$$

Therefore,

$$I_*(\boldsymbol{F}, \boldsymbol{\phi}) \geq \underline{\lim_{R\to\infty}} \frac{\int_{B_R} W^\circ(\boldsymbol{F}, \nabla(\eta_R(\boldsymbol{\phi} - \boldsymbol{c}))) d\boldsymbol{x}}{\int_{B_R} |\nabla\boldsymbol{\phi}|^2 d\boldsymbol{x}} \geq 0.$$

The theorem is proved. □

The next logical step is to write down explicit conditions on $\boldsymbol{\phi} \in \mathcal{S}_*$ minimizing (3.20). However, the definition of the functional $I_*(\boldsymbol{F}, \boldsymbol{\phi})$ makes it difficult to study its minima by classical variational methods. It is not even clear if the space $\mathcal{S}_*$ is a vector space. It is then natural to search for subsets of $\mathcal{S}_*$ that are vector spaces on which the functional $I_*(\boldsymbol{F}, \boldsymbol{\phi})$ can be represented by a classical variational integral without violating the binodal characterization property.

3.2.2 Periodic-decaying test fields

The analysis of spinodal in Section 3.1 suggests to consider the test fields that are periodic (or constant) in some directions and decaying in the remaining ones. More precisely, we choose our test functions $\boldsymbol{\phi}(\boldsymbol{x})$ to be in $\mathcal{S}$ "along" a k dimensional subspace $\mathcal{L}$ of $\mathbb{R}^d$ and to have $(d-k)$ periods in the orthogonal complement $\mathcal{L}^\perp$.

More precisely, we assume that

$$\boldsymbol{\phi}(\boldsymbol{x}+\boldsymbol{u}_j)=\boldsymbol{\phi}(\boldsymbol{x}), \qquad \{\boldsymbol{u}_1,\ldots,\boldsymbol{u}_{d-k}\}\subset\mathcal{L}^\perp \text{ is a basis of periods.} \tag{3.21}$$

Let $\{\boldsymbol{e}_1,\ldots,\boldsymbol{e}_k\}$ be an orthonormal basis of $\mathcal{L}$ and $\{\boldsymbol{e}_{k+1},\ldots,\boldsymbol{e}_d\}$ an orthonormal basis of $\mathcal{L}^\perp$. We define

$$\boldsymbol{\psi}(\boldsymbol{t},\boldsymbol{p})=\boldsymbol{\phi}\left(\sum_{j=1}^{k}t_j\boldsymbol{e}_j+\sum_{j=k+1}^{d}p_{j-k}\boldsymbol{e}_j\right), \quad \boldsymbol{t}=(t_1,\ldots,t_k)\in\mathbb{R}^k, \quad \boldsymbol{p}=(p_1,\ldots,p_{d-k})\in Q_{d-k}, \tag{3.22}$$

where Q_{d-k} is the period cell in $\boldsymbol{p}$ variables. We assume that $\boldsymbol{\psi}\in\mathcal{S}_k(Q_{d-k})$, where

$$\mathcal{S}_k(Q_{d-k})=\{\boldsymbol{\psi}\in W^{1,\infty}(Y_k;\mathbb{R}^m):[\boldsymbol{\psi_t}\ \boldsymbol{\psi_p}]\in L^2(Y_k;\mathbb{R}^{m\times d})\}, \qquad Y_k=\mathbb{R}^k\times Q_{d-k}.$$

Hence, we introduce the space of "periodic-decaying" test functions

$$\mathcal{C}_k=\left\{\boldsymbol{\phi}(\boldsymbol{x})=\boldsymbol{\psi}(\boldsymbol{R}\boldsymbol{x},\boldsymbol{Q}\boldsymbol{x}):\boldsymbol{\psi}\in\mathcal{S}_k(Q_{d-k}),\ \begin{bmatrix}\boldsymbol{R}\\ \boldsymbol{Q}\end{bmatrix}\in SO(d),\ Q_{d-k}-\text{a parallelepiped}\right\}.$$

The $k\times d$ matrix $\boldsymbol{R}$ has rows $\boldsymbol{e}_1,\ldots,\boldsymbol{e}_k$, while $(d-k)\times d$ matrix $\boldsymbol{Q}$ has rows $\boldsymbol{e}_{k+1},\ldots,\boldsymbol{e}_d$. Observe that the sets $\mathcal{C}_k$ are the unions of the family of vector spaces smoothly parametrized by a finite dimensional manifold $\mathcal{G}_{d,k}\times GL(d-k,\mathbb{R})/SL(d-k,\mathbb{Z})$. The first factor is the Grassmannian of k-dimensional subspaces $\mathcal{L}\subset\mathbb{R}^d$, while the second factor is the set of all distinct oriented Bravais lattices in $\mathbb{R}^{d-k}$. Here $GL(n,\mathbb{R})$ denotes the set of all invertible real $n\times n$ matrices, while $SL(n,\mathbb{Z})$ denotes the set of all $n\times n$ matrices with integer components and determinant equal to 1. Such matrices map the lattice $\mathbb{Z}^n$ onto itself.

We remark that in the case $k=1$ the functions $\boldsymbol{\phi}\in\mathcal{C}_1$ correspond to the physical idea of the nucleation of either a homogeneous plate [89, 88, 27] or a composite plate [106, 107, 108, 30] while the case $k=d$ can be viewed as nucleation of a fully localized precipitate [86, 85, 67, 28, 29].

We also distinguish special subspaces of $\mathcal{C}_k$ generated by functions $\boldsymbol{\psi}\in\mathcal{S}_k(Q_{d-k})$ that do not depend on the $\boldsymbol{p}$ variables explicitly. We denote these subspaces by $\widetilde{\mathcal{S}}_k$ and $\widetilde{\mathcal{C}}_k$, respectively.

$$\widetilde{\mathcal{S}}_k=\{\boldsymbol{\psi}\in W^{1,\infty}(\mathbb{R}^k;\mathbb{R}^m):\nabla\boldsymbol{\psi}\in L^2(\mathbb{R}^k;\mathbb{R}^{m\times k})\};$$

$$\widetilde{\mathcal{C}}_k=\left\{\boldsymbol{\phi}(\boldsymbol{x})=\boldsymbol{\psi}(\boldsymbol{R}\boldsymbol{x}):\boldsymbol{\psi}\in\widetilde{\mathcal{S}}_k,\ \boldsymbol{R}:\mathbb{R}^d\to\mathbb{R}^k,\ \boldsymbol{R}\boldsymbol{R}^T=\boldsymbol{I}_k\right\}.$$

For example, the test functions in $\widetilde{\mathcal{C}}_1$ must have the form

$$\boldsymbol{\phi}(\boldsymbol{x})=\boldsymbol{f}((\boldsymbol{n},\boldsymbol{x})), \qquad \boldsymbol{f}\in W^{1,\infty}(\mathbb{R};\mathbb{R}^m), \quad \boldsymbol{f}'\in L^2(\mathbb{R};\mathbb{R}^m), \tag{3.23}$$

where $\boldsymbol{n} \in \mathbb{S}^{d-1}$ is constant but arbitrary. In physical terms these test functions correspond to the nucleation of long and thin platelets.

THEOREM **3.9.** *For any $1 \le k \le d$ we have $\mathcal{C}_k \subset \mathcal{S}_*$ and*

$$I_*(\boldsymbol{F},\boldsymbol{\phi}) = \frac{\displaystyle\int_{Y_k} W^\circ(\boldsymbol{F},\boldsymbol{\psi_t R}+\boldsymbol{\psi_p Q})d\boldsymbol{p}d\boldsymbol{t}}{\displaystyle\int_{Y_k}(|\boldsymbol{\psi_t}|^2+|\boldsymbol{\psi_p}|^2)d\boldsymbol{p}d\boldsymbol{t}} = \frac{\displaystyle\int_Y W^\circ(\boldsymbol{F},\nabla\boldsymbol{\phi})d\boldsymbol{x}}{\displaystyle\int_Y|\nabla\boldsymbol{\phi}|^2d\boldsymbol{x}}, \tag{3.24}$$

for any $\boldsymbol{\phi} \in \mathcal{C}_k$, where $Y = [\boldsymbol{R}^T\ \boldsymbol{Q}^T]Y_k = \mathcal{L} \times \boldsymbol{Q}^T Q_{d-k}$.

The proof is in Appendix C.

Suppose now that $\boldsymbol{A} \in GL(d-k,\mathbb{R})$ maps Q_{d-k} onto $[0,1]^{d-k}$. If $\boldsymbol{\psi} \in \mathcal{S}_k(Q_{d-k})$, then

$$\boldsymbol{\psi}(\boldsymbol{t},\boldsymbol{p}) = \boldsymbol{\psi}_0(\boldsymbol{t},\boldsymbol{A}\boldsymbol{p}),$$

where $\boldsymbol{\psi}_0 \in \mathcal{S}_k([0,1]^{d-k}) \stackrel{\text{def}}{=} \mathcal{S}_k^0$. Since the denominator in (3.24) is always non-negative, the conclusion of our analysis is that the functional

$$J_k(\boldsymbol{F},\boldsymbol{\psi},\boldsymbol{R},\boldsymbol{Q},\boldsymbol{A}) = \int_{Y_k^0} W^\circ(\boldsymbol{F},\boldsymbol{\psi_t}(\boldsymbol{t},\boldsymbol{p})\boldsymbol{R}+\boldsymbol{\psi_p}(\boldsymbol{t},\boldsymbol{p})\boldsymbol{A}\boldsymbol{Q})d\boldsymbol{p}d\boldsymbol{t} \tag{3.25}$$

defined on $\mathcal{S}_k^0$ is the desired replacement of the functional in (2.12). Here $Y_k^0 = \mathbb{R}^k \times [0,1]^{d-k}$. Next we show that the spaces $\mathcal{C}_k$ contain enough test functions to characterize the binodal.

THEOREM **3.10.** *For any $1 \le k \le d$, any orthogonal splitting $[\boldsymbol{R}^T\ \boldsymbol{Q}^T] \in SO(d)$ of $\mathbb{R}^d$, and any $\boldsymbol{A} \in GL(d-k,\mathbb{R})$ the pairs $(\mathcal{S}_k^0, J_k)$ characterize the binodal.*

Proof. Theorem 3.9 implies that if for given $\boldsymbol{R}$, $\boldsymbol{Q}$ and $\boldsymbol{A}$ there exists $\boldsymbol{\psi} \in \mathcal{S}_k^0$ for which $J_k(\boldsymbol{F},\boldsymbol{\psi},\boldsymbol{R},\boldsymbol{Q}) < 0$, then the corresponding function $\boldsymbol{\phi}(\boldsymbol{x}) = \boldsymbol{\psi}(\boldsymbol{R}\boldsymbol{x},\boldsymbol{A}\boldsymbol{Q}\boldsymbol{x}) \in \mathcal{S}_*$ satisfies $I_*(\boldsymbol{F},\boldsymbol{\phi}) < 0$. By Theorem 3.8 we conclude that $\boldsymbol{F} \in \mathfrak{B}$.

Now assume that $\boldsymbol{F} \in \mathfrak{B}$. Then there exists $\boldsymbol{\phi} \in C_0^1(B_1;\mathbb{R}^m)$ for which the inequality (2.12) fails. Let us first extend the function $\boldsymbol{\phi}(\boldsymbol{x})$ by zero to all of $\mathbb{R}^d$. Let us split the space $\mathbb{R}^d$ into an orthogonal sum $\mathbb{R}^d = \boldsymbol{R}^T\mathbb{R}^k \oplus \boldsymbol{Q}^T\mathbb{R}^{d-k}$. Let $\boldsymbol{\psi}_0(\boldsymbol{t},\boldsymbol{u}) = \boldsymbol{\phi}(\boldsymbol{R}^T\boldsymbol{t}+\boldsymbol{Q}^T\boldsymbol{u})$. Let Q_{d-k} be the period cell mapped by $\boldsymbol{A} \in GL(d-k,\mathbb{R})$ onto $[0,1]^{d-k}$. Let $\boldsymbol{c} \in Q_{d-k}$ be the center of Q_{d-k} and $a > 0$ be so large that $\boldsymbol{\psi}_0(\boldsymbol{t},\boldsymbol{u}) = \boldsymbol{0}$, if $\boldsymbol{u} \notin a(Q_{d-k}-\boldsymbol{c})$. Let $\widetilde{\boldsymbol{\psi}}(\boldsymbol{t},\boldsymbol{u})$ be the $a(Q_{d-k}-\boldsymbol{c})$-periodic extension of $\boldsymbol{\psi}_0(\boldsymbol{t},\boldsymbol{u})$. Let $\boldsymbol{\psi}(\boldsymbol{t},\boldsymbol{p}) = a^{-1}\widetilde{\boldsymbol{\psi}}(a\boldsymbol{t},a\boldsymbol{A}^{-1}\boldsymbol{p})$. Then $\boldsymbol{\psi} \in \mathcal{S}_k^0$. Also

$$J_k(\boldsymbol{F},\boldsymbol{\psi},\boldsymbol{R},\boldsymbol{Q},\boldsymbol{A}) = a^{-d}|\det\boldsymbol{A}|\int_{B_1} W^\circ(\boldsymbol{F},\nabla\boldsymbol{\phi})d\boldsymbol{z} < 0.$$

□

Remark 3.11. *We observe that if* $\boldsymbol{\phi} \in \mathcal{C}_k$ *and* $\lambda > 0$*, then* $\boldsymbol{\phi}_\lambda = \lambda\boldsymbol{\phi}(\boldsymbol{x}/\lambda) \in \mathcal{C}_k$*, and*

$$\int_Y W^\circ(\boldsymbol{F}, \nabla\boldsymbol{\phi}_\lambda)d\boldsymbol{x} = \lambda^d \int_Y W^\circ(\boldsymbol{F}, \nabla\boldsymbol{\phi})d\boldsymbol{x}.$$

Therefore,

$$\inf_{\boldsymbol{\phi}\in\mathcal{C}_k} J_k(\boldsymbol{F}, \boldsymbol{\phi}) = -Ind_{\mathfrak{B}^c}(\boldsymbol{F}),$$

where $Ind_{\mathfrak{B}^c}(\boldsymbol{F})$ *is the indicator function of the complement of the binodal region.*

If $\boldsymbol{\phi} \in \widetilde{\mathcal{C}}_k$ then the functional J_k reduces to

$$\widetilde{J}_k(\boldsymbol{F}, \boldsymbol{\psi}, \boldsymbol{R}) = \int_{\mathbb{R}^k} W^\circ(\boldsymbol{F}, \nabla\boldsymbol{\psi}(\boldsymbol{t})\boldsymbol{R})d\boldsymbol{t}. \tag{3.26}$$

Observe that the pairs $(\widetilde{\mathcal{C}}_k, \widetilde{J}_k)$ only *bound* the binodal, while the pairs $(\mathcal{S}_k^0, J_k)$ *characterize* it.

3.2.3 Laminates

Crossing the binodal may not be detectable by solving the Euler-Lagrange equations in one of the above problems. For instance, one can show that in the example considered in Section 5 with $d = 2$ there are parts of the binodal that can only be detected by test functions whose gradient is supported on three specific gradients [56]. To construct such objects we need sequences of test functions in $\mathcal{C}_1$ that converge only weakly. The limiting value of the functional J_1 will then be expressed in terms of the finitely many parameters describing the geometry and piecewise-constant elastic fields in the limiting configuration.

More precisely, we consider elastic fields described by finitely supported probability measures [31, 69]

$$\nu = \sum_{j=1}^r \lambda_j \delta_{\boldsymbol{H}_j}, \qquad \sum_{j=1}^r \lambda_j = 1, \quad \lambda_j > 0. \tag{3.27}$$

Given such a measure it is in general difficult to *verify* if ν is a gradient Young measure. However, one may easily *construct* a large class of such Young measures via the process of lamination [97].

Definition 3.12. *Let* $1 \le j_0 \le r$*,* $s \in (0, 1)$*,* $\theta \in [0, 1]$ *and* $\{\boldsymbol{B}_1, \boldsymbol{B}_2\} \subset \mathbb{M}$ *are such that* $\boldsymbol{B}_1 - \boldsymbol{B}_2$ *is rank-1 and* $\boldsymbol{H}_{j_0} = s\boldsymbol{B}_1 + (1 - s)\boldsymbol{B}_2$*. We say that the probability measure*

$$\nu' = \nu + \theta\lambda_{j_0}(s\delta_{\boldsymbol{B}_1} + (1 - s)\delta_{\boldsymbol{B}_2} - \delta_{\boldsymbol{H}_{j_0}})$$

is obtained from ν *by* ***lamination****.*

Definition 3.13. *A* ***finite rank laminate*** *is a finitely supported probability measure (3.27) for which there exists a sequence of probability measures* $\nu_1, \ldots, \nu_m$*, such that* $\nu_1 = \delta_{\boldsymbol{H}}$*,* $\nu_m = \nu$ *and for each* $k = 1, \ldots, m - 1$ *the measure* ν_{k+1} *is obtained from* ν_k *by lamination.*

For a measure ν given by (3.27) we define its "center of mass" by

$$\bar{\nu} = \sum_{j=1}^{r} \lambda_j \boldsymbol{H}_j.$$

We observe that if ν' is obtained from ν by lamination then $\overline{\nu'} = \bar{\nu}$. Hence, the matrix $\boldsymbol{H}$ in the definition of a finite rank laminate Young measure is equal to $\bar{\nu}$.

THEOREM **3.14.** *Suppose ν is a finite rank laminate with $\bar{\nu} = \boldsymbol{a} \otimes \boldsymbol{n}$. Then there exists a sequence $\{\boldsymbol{\phi}_n\} \subset \mathcal{C}_1$, such that $\boldsymbol{\phi}_n \to \boldsymbol{\phi}_0$ uniformly, where $\boldsymbol{\phi}_0(\boldsymbol{x})$ is given by*

$$\boldsymbol{\phi}_0(\boldsymbol{x}) = \begin{cases} \boldsymbol{a}, & \text{if } (\boldsymbol{n}, \boldsymbol{x}) \geq 1, \\ \boldsymbol{0}, & \text{if } (\boldsymbol{n}, \boldsymbol{x}) \leq 0, \\ (\boldsymbol{n}, \boldsymbol{x})\boldsymbol{a}, & \text{if } 0 < (\boldsymbol{n}, \boldsymbol{x}) < 1, \end{cases} \tag{3.28}$$

and such that

$$\lim_{n\to\infty} J_1(\boldsymbol{F}, \boldsymbol{\phi}_n, \boldsymbol{R}, \boldsymbol{Q}, \boldsymbol{I}) = J(\boldsymbol{F}, \nu) = \int_{\mathbb{M}} W^\circ(\boldsymbol{F}, \boldsymbol{H}) d\nu(\boldsymbol{H}) = \sum_{j=1}^{r} \lambda_j W^\circ(\boldsymbol{F}, \boldsymbol{H}_j), \tag{3.29}$$

where the $1 \times d$ matrix $\boldsymbol{R}$ can be identified with the unit vector $\boldsymbol{n}$.

The proof of Theorem 3.14 can be found in Appendix D.

We can now define the space

$$\mathfrak{L} = \{\nu - \text{finite rank laminate Young measure, rank}(\bar{\nu}) = 1\}.$$

Corollary 3.15. *The pair $(\mathfrak{L}, J(\boldsymbol{F}, \nu))$ bounds the binodal.*

Proof. If $\boldsymbol{F} \notin \mathfrak{B}$ then $J_1(\boldsymbol{F}, \boldsymbol{\phi}_n, \boldsymbol{R}, \boldsymbol{Q}, \boldsymbol{I}) \geq 0$ for any $n \geq 1$, where the sequence $\{\boldsymbol{\phi}_n\}$ is as in Theorem 3.14. The formula (3.29) then implies that $J(\boldsymbol{F}, \nu) \geq 0$. Hence, the pair $(\mathfrak{L}, J(\boldsymbol{F}, \nu))$ bounds the binodal. Obviously, this result also follows from the fact that any quasiconvex function is rank-one convex. □

4 Characterization of spinodal and binodal

In this section we use our equivalent formulations to derive explicit necessary conditions characterizing spinodal and bounding the binodal.

4.1 Spinodal

We recall from (3.8) that the deformation gradient $\boldsymbol{F}$ is weakly locally stable if and only if

$$I_{\mathfrak{S}}(\boldsymbol{F}, \phi((\boldsymbol{x}, \boldsymbol{n}))\boldsymbol{a}) = (\boldsymbol{A}(\boldsymbol{n}; \boldsymbol{F})\boldsymbol{a}, \boldsymbol{a}) \geq 0, \text{ for all } \boldsymbol{a} \in \mathbb{R}^m, \ \boldsymbol{n} \in \mathbb{S}^{d-1}. \tag{4.1}$$

The conditions of weak marginal stability can then be interpreted as the emergence of $\boldsymbol{a} \neq \boldsymbol{0}$ and $\boldsymbol{n} \in \mathbb{S}^{d-1}$ such that

$$I_{\mathfrak{S}}(\boldsymbol{F}, \phi((\boldsymbol{x},\boldsymbol{n}))\boldsymbol{a}) = 0.$$

If the above equality is satisfied because $\boldsymbol{F}$ crosses into the spinodal region, then the pair $(\boldsymbol{a},\boldsymbol{n})$ must be minimizing for $I_{\mathfrak{S}}(\boldsymbol{F}, \phi((\boldsymbol{x},\boldsymbol{n}))\boldsymbol{a})$. Therefore, the equilibrium equations

$$\nabla_{\boldsymbol{a}} I_{\mathfrak{S}}(\boldsymbol{F}, \phi((\boldsymbol{x},\boldsymbol{n}))\boldsymbol{a}) = \boldsymbol{0}, \tag{4.2}$$

$$\nabla_{\boldsymbol{n}} I_{\mathfrak{S}}(\boldsymbol{F}, \phi((\boldsymbol{x},\boldsymbol{n}))\boldsymbol{a}) = \boldsymbol{0} \tag{4.3}$$

must hold.

Remark 4.1. *The space $\mathcal{F}_{\mathfrak{S}}$ defined by (3.5) has $m+d-1$ degrees of freedom $\boldsymbol{a} \in \mathbb{R}^m$ and $\boldsymbol{n} \in \mathbb{S}^{d-1}$. The equation (4.2) describes equilibrium with respect to the variation of the local values of the field, as in the Euler-Lagrange equation. The equation (4.3) describes equilibrium with respect to "configurational" degrees of freedom $\boldsymbol{n}$ that describe the large-scale structure of the field (directions in which $\boldsymbol{\phi} \in \mathcal{F}_{\mathfrak{S}}$ does not decay at infinity). In this respect it is analogous to the Noether-Eshelby equation which is usually used to find configuration of singularities, [100, 42, 43, 91, 49, 62]. Indeed, the lack of proper decay of the field $\boldsymbol{\phi}(\boldsymbol{x})$ can be regarded as a singularity at infinity.*

One can see that equations (4.2)–(4.3) always have a family of trivial solutions $(\boldsymbol{a},\boldsymbol{n})$, characterized by $\boldsymbol{a} = \boldsymbol{0}$. Hence, we may regard the problem of finding the non-trivial solutions of (4.2)–(4.3) as a bifurcation problem. Explicitly, equations (4.2)–(4.3) read

$$\boldsymbol{A}(\boldsymbol{n};\boldsymbol{F})\boldsymbol{a} = \boldsymbol{0}, \qquad \boldsymbol{A}^*(\boldsymbol{a};\boldsymbol{F})\boldsymbol{n} = \boldsymbol{0}, \tag{4.4}$$

where $\boldsymbol{A}^*(\boldsymbol{a};\boldsymbol{F})$ is the co-acoustic tensor defined as the linear map on $\mathbb{R}^d$ given by

$$\boldsymbol{m} \mapsto \boldsymbol{A}^*(\boldsymbol{a};\boldsymbol{F})\boldsymbol{m} = (W_{\boldsymbol{FF}}(\boldsymbol{F})(\boldsymbol{a} \otimes \boldsymbol{m}))^T \boldsymbol{a}. \tag{4.5}$$

Observe that the equations in (4.4) are not independent. There is one relation between the left-hand sides in (4.4)

$$(\boldsymbol{A}^*(\boldsymbol{a};\boldsymbol{F})\boldsymbol{n},\boldsymbol{n}) = (\boldsymbol{A}(\boldsymbol{n};\boldsymbol{F})\boldsymbol{a},\boldsymbol{a}).$$

Equations in (4.4) are also homogeneous in $\boldsymbol{a}$ and $\boldsymbol{n}$ and therefore, they can be regarded as $m+d-1$ constraints on $md+(m-1)+(d-1)$ unknowns. As such they describe a co-dimension 1 surface in $\mathbb{M}$, which we can interpret as "an equation of spinodal".

While the points on the spinodal satisfy (4.4) the converse need not be true, i.e. some other points inside the spinodal region may satisfy (4.4). It is possible to reduce the size of the system (4.4) by eliminating $\boldsymbol{a}$ in the case when $\mathrm{rank}(\boldsymbol{A}(\boldsymbol{n})) = m-1$. In that case the vector $\boldsymbol{a}$ spanning its kernel is determined up to a scalar multiple, or, if we normalize it to the unit length, up to a sign. Then

$$\mathrm{cof}(\boldsymbol{A}(\boldsymbol{n})) = \alpha \boldsymbol{a} \otimes \boldsymbol{a}, \qquad \alpha = \mathrm{Tr}\,\mathrm{cof}(\boldsymbol{A}(\boldsymbol{n})) \neq 0. \tag{4.6}$$

Using Einstein summation convention, the second equation in (4.4) and the first equation in (4.6) can be written as

$$W_{F_{i\alpha}F_{j\beta}}a_ia_jn_\beta = 0, \qquad a_ia_j = \frac{1}{\alpha}\mathrm{cof}(\boldsymbol{A}(\boldsymbol{n}))_{ij},$$

respectively. Hence, we obtain

$$W_{F_{i\alpha}F_{j\beta}}\mathrm{cof}(\boldsymbol{A}(\boldsymbol{n}))_{ij}n_\beta = 0. \tag{4.7}$$

We can write (4.7) in index-free notations

$$(\mathrm{cof}(\boldsymbol{A}(\boldsymbol{n};\boldsymbol{F})), \mathbb{B}(\boldsymbol{n},\boldsymbol{\eta};\boldsymbol{F})) = 0, \qquad \mathrm{Tr}\,\mathrm{cof}(\boldsymbol{A}(\boldsymbol{n};\boldsymbol{F})) \neq 0. \tag{4.8}$$

for all $\boldsymbol{\eta} \in \mathbb{R}^d$, if we introduce a bi-linear matrix-valued form

$$\mathbb{B}(\boldsymbol{n},\boldsymbol{\eta};\boldsymbol{F})_{ij} = W_{F_{i\alpha}F_{j\beta}}(\boldsymbol{F})n_\alpha\eta_\beta.$$

Conversely, if we take $\boldsymbol{\eta} = \boldsymbol{n}$ in (4.8) we obtain $\det \boldsymbol{A}(\boldsymbol{n}) = 0$. Hence, there exists $\boldsymbol{a} \neq \boldsymbol{0}$, such that the first equation in (4.4) is satisfied. The relation (4.6) also holds, since $\mathrm{Tr}\,\mathrm{cof}(\boldsymbol{A}(\boldsymbol{n})) \neq 0$. Thus, the second equation in (4.4) and the first equation in (4.8) are equivalent. We remark that the side condition $\mathrm{Tr}\,\mathrm{cof}(\boldsymbol{A}(\boldsymbol{n})) \neq 0$ in (4.8) is important, since for generic fully anisotropic tensors $W_{\boldsymbol{FF}}$ the set $\{\boldsymbol{F} \in \mathbb{M} : \mathrm{rank}(\boldsymbol{A}(\boldsymbol{n};\boldsymbol{F})) \leq m-2 \text{ for some } |\boldsymbol{n}| = 1\}$ has full dimension, if $d \geq 3$. We regard conditions (4.8) and (4.4) as generically equivalent, since at the spinodal we expect, in the generic case, the *single* smallest eigenvalue of $\boldsymbol{A}(\boldsymbol{n})$ to attain its minimum value of 0.

It turns out that there are no other domain-local constraints on $\nabla\boldsymbol{y}(\boldsymbol{x})$ than $\nabla\boldsymbol{y}(\boldsymbol{x}) \notin \mathfrak{S}$ that follow from stability with respect to weak variations under the assumption of non-degeneracy of $\boldsymbol{A}(\boldsymbol{n};\boldsymbol{F})$. Indeed, due to [113] and the van Hove's theorem [125], the homogeneous deformation $\boldsymbol{y}_0(\boldsymbol{x}) = \boldsymbol{F}\boldsymbol{x}$ is a weak local minimizer of (2.1) on the unit ball with Dirichlet boundary conditions, provided $\boldsymbol{A}(\boldsymbol{n};\boldsymbol{F}) > 0$ for all $|\boldsymbol{n}| = 1$.

Example 4.2.

As a simple illustration, consider the energy [24, 1]

$$W(\boldsymbol{F}) = f(\mathrm{Tr}\,\boldsymbol{\varepsilon}) + \mu\left|\boldsymbol{\varepsilon} - \frac{1}{d}(\mathrm{Tr}\,\boldsymbol{\varepsilon})\boldsymbol{I}\right|^2, \qquad \boldsymbol{\varepsilon} = \frac{1}{2}(\boldsymbol{F} + \boldsymbol{F}^T), \qquad \mu > 0. \tag{4.9}$$

In this model the acoustic tensor can be written explicitly

$$\boldsymbol{A}(\boldsymbol{n}) = \mu(|\boldsymbol{n}|^2\boldsymbol{I} - \boldsymbol{n}\otimes\boldsymbol{n}) + \left(f''(\mathrm{Tr}\,\boldsymbol{\varepsilon}) + 2\mu\left(1 - \frac{1}{d}\right)\right)\boldsymbol{n}\otimes\boldsymbol{n}.$$

From (4.5) we immediately find that $\boldsymbol{A}^*(\boldsymbol{a}) = \boldsymbol{A}(\boldsymbol{a})$. The system (4.4) then becomes

$$\begin{cases} \mu|\boldsymbol{n}|^2\boldsymbol{a} + \left(f''(\mathrm{Tr}\,\boldsymbol{\varepsilon}) + \mu\left(1 - \frac{2}{d}\right)\right)(\boldsymbol{a},\boldsymbol{n})\boldsymbol{n} = \boldsymbol{0}, \\ \mu|\boldsymbol{a}|^2\boldsymbol{n} + \left(f''(\mathrm{Tr}\,\boldsymbol{\varepsilon}) + \mu\left(1 - \frac{2}{d}\right)\right)(\boldsymbol{a},\boldsymbol{n})\boldsymbol{a} = \boldsymbol{0}. \end{cases}$$

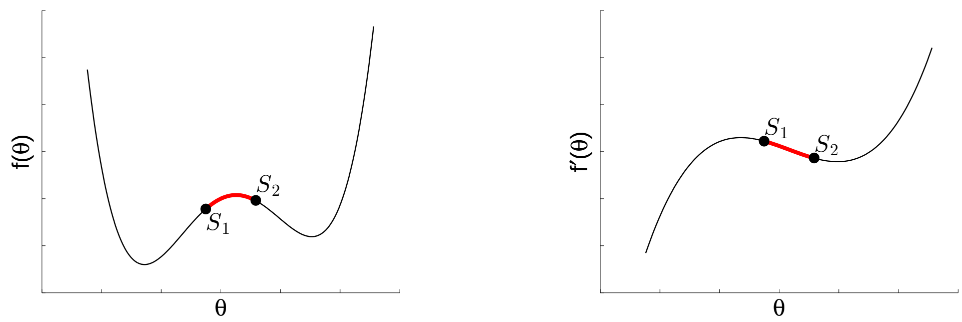

Figure 1: The double-well energy $f(\theta)$ from the example in Remark 4.2. Spinodal region is the projection of the bold part of the graph onto the θ-axis and spinodal points are S_1 and S_2.

We see that $\boldsymbol{a}$ must be a scalar multiple of $\boldsymbol{n}$ and the system reduces to

$$f''(\operatorname{Tr}\boldsymbol{\varepsilon}) + 2\mu\left(1 - \frac{1}{d}\right) = 0. \tag{4.10}$$

The equation (4.8) can be written as

$$d\mu^{d-1}\left(f''(\operatorname{Tr}\boldsymbol{\varepsilon}) + 2\mu\left(1 - \frac{1}{d}\right)\right)\boldsymbol{n} = \mathbf{0}.$$

and it is clear that this equation is equivalent to (4.10). The actual spinodal in this example is the union of hyperplanes of the form $\operatorname{Tr}\boldsymbol{\varepsilon} = \theta$, where θ is any zero of $\phi(\theta) = f''(\theta)+2\mu(1-1/d)$, around which $\phi(\theta)$ changes sign. The latter condition of transversality has to be imposed externally, since it is not captured by the equation (4.10). Our general theorems will feature such external transversality conditions, enabling us to assert the marginal stability of $\boldsymbol{F}$. If the function $f(\theta)$ has a double-well shape and its second derivative is shaped like a parabola, then the spinodal and the spinodal region are shown in Figure 1. We see how according to (4.10) the spinodal lies in the region, where $f'' < 0$.

4.2 Binodal

In this section we consider different explicit characterizations of the binodal. In particular we distinguish the PDE problem associated with nucleation of *classical inclusions* from the algebraic problem associated with nucleation of *laminates*.

4.2.1 Classical nucleation

To obtain specific constraints on the value of $\boldsymbol{F}$ we need to study necessary conditions of equilibrium for the functionals J_k, $k = 1, \ldots, d$, defined by (3.25). Before writing these conditions it is necessary to identify independent degrees of freedom associated with the spaces $\mathcal{C}_k$: $\psi \in \mathcal{S}_k^0$, the subspace $\boldsymbol{\mathcal{L}} \subset \mathbb{R}^d$, described by the $k \times d$ matrix $\boldsymbol{R}$ satisfying $\boldsymbol{R}\boldsymbol{R}^T = \boldsymbol{I}_k$, and the shape and orientation of the period cells Q_{d-k} described by the matrix $\boldsymbol{A} \in GL(d-k, \mathbb{R})$. As in the case of the spinodal we identify the finite dimensional parameters $\boldsymbol{R}$ and $\boldsymbol{A}$ as *configurational* degrees of freedom associated with "singularities at infinity[5]" The lack of rank-1 convexity of $W(\boldsymbol{F})$ allows the field variable $\boldsymbol{\psi} \in \mathcal{S}_k^0$ to possess additional configurational degrees of freedom associated with singularities allowed by the Euler-Lagrange equations at finite $\boldsymbol{x} \in \mathbb{R}^d$.

Our next two theorems introduce the classical Euler-Lagrange equations and the configurational Noether-Eshelby equations [100, 42, 43, 91, 49, 62].

THEOREM **4.3.** *Assume that for* $\boldsymbol{F} \in \mathfrak{Bin}$ *there exists* $1 \le k \le d$, *orientation* $[\boldsymbol{R}^T\ \boldsymbol{Q}^T] \in SO(d)$, *a period cell shape* Q_{d-k} *(i.e.* $\boldsymbol{A} \in GL(d-k, \mathbb{R})$*) and a non-zero function* $\boldsymbol{\psi} \in \mathcal{S}_k^0$ *such that* $J_k(\boldsymbol{F}, \boldsymbol{\psi}, \boldsymbol{R}, \boldsymbol{Q}, \boldsymbol{A}) = 0$, *while*

$$J_k \ge 0$$

for all test functions $\boldsymbol{\phi} \in \mathcal{C}_k$. *Then*

$$\boldsymbol{F} + \nabla\boldsymbol{\phi}(\boldsymbol{x}) \notin \mathfrak{B} \text{ for a.e. } \boldsymbol{x} \in \mathbb{R}^d, \tag{4.11}$$

and the test field $\boldsymbol{\phi}(\boldsymbol{x}) = \boldsymbol{\psi}(\boldsymbol{R}\boldsymbol{x}, \boldsymbol{A}\boldsymbol{Q}\boldsymbol{x})$ *has to satisfy the Euler-Lagrange and the Noether-Eshelby equations in* $\mathbb{R}^d$

$$\begin{cases} \nabla \cdot \boldsymbol{P}(\boldsymbol{F} + \nabla\boldsymbol{\phi}) = \boldsymbol{0}, \\ \nabla \cdot \boldsymbol{P}^*(\boldsymbol{F} + \nabla\boldsymbol{\phi}) = \boldsymbol{0}, \end{cases} \tag{4.12}$$

where $\boldsymbol{P}(\boldsymbol{F}) = W_{\boldsymbol{F}}(\boldsymbol{F})$ *and* $\boldsymbol{P}^*(\boldsymbol{F}) = W(\boldsymbol{F})\boldsymbol{I} - \boldsymbol{F}^T\boldsymbol{P}(\boldsymbol{F})$. [6] *The optimal orientation and the period cell shape are determined by the additional conditions*

$$\int_Y \widehat{\boldsymbol{P}}^*(\nabla\boldsymbol{\phi})d\boldsymbol{x} = \boldsymbol{0}, \tag{4.13}$$

where $\widehat{\boldsymbol{P}}^*(\boldsymbol{H}) = W^\circ(\boldsymbol{F}, \boldsymbol{H})\boldsymbol{I} - \boldsymbol{H}^T W^\circ_{\boldsymbol{H}}(\boldsymbol{F}, \boldsymbol{H})$.

Proof. By assumption, $\boldsymbol{\phi}$ is the minimizer of the functional

$$\boldsymbol{\phi} \mapsto \int_Y \widehat{W}(\nabla\boldsymbol{\phi})d\boldsymbol{x}$$

over all $\boldsymbol{\phi} \in \mathcal{C}_k$, where

$$\widehat{W}(\boldsymbol{H}) = W^\circ(\boldsymbol{F}, \boldsymbol{H}). \tag{4.14}$$

[5] The functions in the much larger space $\mathcal{S}_*$ would possess infinitely many configurational degrees of freedom at infinity corresponding to the infinite variety of possible asymptotic behaviors of $\boldsymbol{\phi} \in \mathcal{S}_*$.

[6] In elasticity theory the tensors $\boldsymbol{P}(\boldsymbol{F})$ and $\boldsymbol{P}^*(\boldsymbol{F})$ are called the Piola Kirchhoff tensor and the Eshelby tensor, respectively.

The classical optimality conditions [12] then imply (4.11) and (4.12). Indeed,

$$\widehat{\boldsymbol{P}}(\boldsymbol{H}) = \widehat{W}_{\boldsymbol{H}}(\boldsymbol{H}) = \boldsymbol{P}(\boldsymbol{F}+\boldsymbol{H}) - \boldsymbol{P}(\boldsymbol{F}),$$

which means that the Euler-Lagrange for the energy density (4.14) coincides with first equation in (4.12). We also compute

$$\widehat{\boldsymbol{P}}^*(\boldsymbol{H}) = \boldsymbol{P}^*(\boldsymbol{F}+\boldsymbol{H}) + \boldsymbol{F}^T\boldsymbol{P}(\boldsymbol{F}+\boldsymbol{H}) + \boldsymbol{N}(\boldsymbol{H}), \tag{4.15}$$

where

$$\boldsymbol{N}(\boldsymbol{H}) = \boldsymbol{H}^T\boldsymbol{P}(\boldsymbol{F}) - (\boldsymbol{H}, \boldsymbol{P}(\boldsymbol{F}))\boldsymbol{I} - W(\boldsymbol{F})\boldsymbol{I}.$$

Therefore, the Noether-Eshelby equation $\nabla \cdot \widehat{\boldsymbol{P}}^*(\nabla\boldsymbol{\phi}) = \boldsymbol{0}$ for the energy density (4.14) is equivalent to the second equation in (4.12), since $\nabla \cdot \boldsymbol{N}(\nabla\boldsymbol{\phi}) = \boldsymbol{0}$ for any smooth vector field $\boldsymbol{\phi}$. Finally, (4.11) follows from a simple observation that $\boldsymbol{H}$ is a point of quasiconvexity for $\widehat{W}$ if and only if $\boldsymbol{F}+\boldsymbol{H}$ is a point of quasiconvexity for W.

The additional integral constraint (4.13) comes from variations in $\boldsymbol{R}$, $\boldsymbol{Q}$ and $\boldsymbol{A}$. If we fix $\boldsymbol{\psi}$ and $\boldsymbol{A}$, and vary $[\boldsymbol{R}^T\ \boldsymbol{Q}^T] \in SO(d)$ we obtain

$$\int_Y \nabla\boldsymbol{\phi}^T\widehat{\boldsymbol{P}}(\nabla\boldsymbol{\phi})d\boldsymbol{x} \in \mathrm{Sym}(\mathbb{R}^d). \tag{4.16}$$

Fixing $\boldsymbol{\psi}$, $\boldsymbol{R}$ and $\boldsymbol{Q}$ and varying $\boldsymbol{A}$ results in

$$\int_Y \boldsymbol{Q}\nabla\boldsymbol{\phi}^T\widehat{\boldsymbol{P}}(\nabla\boldsymbol{\phi})\boldsymbol{Q}^T d\boldsymbol{x} = \boldsymbol{0}. \tag{4.17}$$

By assumption

$$\int_Y W^\circ(\boldsymbol{F}, \nabla\boldsymbol{\phi})d\boldsymbol{x} = \frac{1}{|\det\boldsymbol{A}|}J_k(\boldsymbol{F}, \boldsymbol{\psi}, \boldsymbol{R}, \boldsymbol{Q}, \boldsymbol{A}) = 0.$$

This, together with (4.17) implies

$$\int_Y \boldsymbol{Q}\widehat{\boldsymbol{P}}^*(\nabla\boldsymbol{\phi})\boldsymbol{Q}^T d\boldsymbol{x} = \boldsymbol{0}.$$

Hence, in order to prove the theorem we need to show that

$$\int_Y \boldsymbol{R}\widehat{\boldsymbol{P}}^*(\nabla\boldsymbol{\phi})\boldsymbol{Q}^T d\boldsymbol{x} = \boldsymbol{0}, \qquad \int_Y \boldsymbol{R}\widehat{\boldsymbol{P}}^*(\nabla\boldsymbol{\phi})\boldsymbol{R}^T d\boldsymbol{x} = \boldsymbol{0},$$

since, according to (4.16) $\int_Y \widehat{\boldsymbol{P}}^* d\boldsymbol{x} \in \mathrm{Sym}(\mathbb{R}^d)$. The relation (4.13) then follows from Lemma 4.4 below. □

LEMMA **4.4.** *The equations (4.12) imply that*

$$\int_Y \widehat{\boldsymbol{P}}^*(\nabla\boldsymbol{\phi})\boldsymbol{R}^T d\boldsymbol{x} = \boldsymbol{0}. \tag{4.18}$$

The proof is in the Appendix E.

Several remarks are in order. The first remark concerns the necessary condition (4.11).

Definition 4.5. *If $\boldsymbol{\phi} \in \mathcal{C}_k \setminus \{\mathbf{0}\}$ satisfies (4.12) and (4.13), but fails (4.11) then $\boldsymbol{\phi}$ is called a* ***spurious solution****.*

The failure of quasiconvexity means that it is possible to modify the function $\boldsymbol{\phi}$ locally, such that the modified function still belongs to $\mathcal{C}_k$, but gives a negative value to the functional J_k. This implies that $\boldsymbol{F} \in \mathfrak{B}$. In other words, spurious solutions do not correspond to points $\boldsymbol{F}$ on the binodal. Conversely, if $\boldsymbol{\phi} \in \mathcal{C}_k$ satisfies (4.11), then obviously $\boldsymbol{F} \notin \mathfrak{B}$.

The Eshelby-Noether equation $(4.12)_2$ is the condition of equilibrium with respect to the degrees of freedom associated with the singularities of $\boldsymbol{\psi} \in \mathcal{S}_k^0$. Indeed, in the absence of singularities a well-know Noether identity [100]

$$\nabla \cdot \boldsymbol{P}^*(\nabla\boldsymbol{\phi}) = -(\nabla\boldsymbol{\phi})^T \nabla \cdot \boldsymbol{P}(\nabla\boldsymbol{\phi}) \tag{4.19}$$

says that $(4.12)_2$ is a consequence of $(4.12)_1$. If the singularities of $\boldsymbol{\psi} \in \mathcal{S}_k^0$ are smooth surfaces of jump discontinuity then the PDE $(4.12)_2$ can be replaced with an algebraic equation on the singular surface Σ [42, 43, 91, 49, 62, 21]

$$[\![\boldsymbol{P}^*]\!]\boldsymbol{n} = \mathbf{0}, \qquad \boldsymbol{x} \in \Sigma, \tag{4.20}$$

where $[\![\boldsymbol{P}^*]\!] = \boldsymbol{P}^*_+ - \boldsymbol{P}^*_-$, is the jump of $\boldsymbol{P}^*(\boldsymbol{F} + \nabla\boldsymbol{\phi}(\boldsymbol{x}))$ across Σ. Here $\boldsymbol{n}$ is a unit normal to Σ. The region into which $\boldsymbol{n}$ points is called the "+" region, while the region from which $\boldsymbol{n}$ points is called the "−" region. It is well-known, the d algebraic equations (4.20) can be reduced to a single scalar Maxwell relation [38, 42]

$$p^* = [\![W]\!] - (\{\!\!\{\boldsymbol{P}\}\!\!\}, [\![\boldsymbol{F}]\!]) = 0, \qquad \boldsymbol{x} \in \Sigma, \tag{4.21}$$

where $\{\!\!\{\boldsymbol{P}\}\!\!\} = (\boldsymbol{P}_+ + \boldsymbol{P}_-)/2$, interestingly (4.21) survives even in dynamics [123]. Now, if all the singularities of $\boldsymbol{\phi}(\boldsymbol{x})$ are smooth surfaces of jump discontinuity the system (4.12) is equivalent to the system $(4.12)_1$, (4.21). However, while the relation (4.21) will be convenient in the analysis of the example in Section 5, in the general theory we are not making any assumptions on the nature of singularities of $\nabla\boldsymbol{\phi}(\boldsymbol{x})$, and the equation $(4.12)_2$ must be retained along with $(4.12)_1$.

It is clear that the verification of (4.11) may be difficult without the complete knowledge of the binodal. Yet, even partial knowledge of the binodal region can be used to demonstrate that condition (4.11) fails, thereby ruling out some of the spurious solutions of (4.12)–(4.13). For instance, there are several easy-to-evaluate consequences of (4.11), especially on a smooth surface of jump discontinuity Σ of $\nabla\boldsymbol{\phi}$. These conditions are discussed in detail in [61]. One important example is the roughening equilibrium equation [58]

$$[\![\boldsymbol{P}(\boldsymbol{F} + \nabla\boldsymbol{\phi})]\!]^T [\![\nabla\boldsymbol{\phi}]\!]\boldsymbol{n} = \mathbf{0}, \quad \boldsymbol{x} \in \Sigma. \tag{4.22}$$

This condition and the optimal orientation condition (4.13) are related via a localization argument. Indeed, consider the pair of fields $\boldsymbol{F}_\pm = \boldsymbol{F} + \nabla\boldsymbol{\phi}_\pm(\boldsymbol{x}_0)$ at a point $\boldsymbol{x}_0$ on the surface of jump discontinuity. This implies a configuration, where an infinite slab carrying the field $\boldsymbol{F}_-$ is embedded in the infinite space where the field is $\boldsymbol{F}_+$. Such a configuration solves the $(4.12)_1$ if and only if

$$\begin{cases} [\![\boldsymbol{F}]\!] = \boldsymbol{a} \otimes \boldsymbol{n}, \text{ for some } \boldsymbol{a} \in \mathbb{R}^m \\ [\![\boldsymbol{P}]\!]\boldsymbol{n} = \boldsymbol{0}, \end{cases} \tag{4.23}$$

where $\boldsymbol{n}$ is the normal to the boundary of the slab. It solves $(4.12)_2$ if and only if (4.21) is satisfied and it satisfies (4.13) if and only if (4.22) holds.

Another consequence of (4.11) is the roughening stability inequality [58]. It is stated as

$$\mathbb{C}_\pm(\boldsymbol{a}, \boldsymbol{n}) = \begin{bmatrix} \boldsymbol{A}_\pm(\boldsymbol{n}) & \boldsymbol{B}_\pm(\boldsymbol{a}, \boldsymbol{n}) + [\![\boldsymbol{P}]\!] \\ \boldsymbol{B}_\pm(\boldsymbol{a}, \boldsymbol{n})^T + [\![\boldsymbol{P}]\!]^T & \boldsymbol{A}^*_\pm(\boldsymbol{a}) \end{bmatrix} \geq 0 \tag{4.24}$$

in the sense of quadratic forms on the orthogonal complement of $\mathbb{R}[\boldsymbol{a}, -\boldsymbol{n}]$. Here $\boldsymbol{A}_\pm(\boldsymbol{n}) = \boldsymbol{A}(\boldsymbol{n}; \boldsymbol{F}_\pm)$, $\boldsymbol{A}^*_\pm(\boldsymbol{a}) = \boldsymbol{A}^*(\boldsymbol{a}; \boldsymbol{F}_\pm)$ and

$$\boldsymbol{B}_\pm(\boldsymbol{a}, \boldsymbol{n})\boldsymbol{m} = \boldsymbol{A}(\boldsymbol{n}, \boldsymbol{m}; \boldsymbol{F}_\pm)\boldsymbol{a} = (W_{\boldsymbol{F}\boldsymbol{F}}(\boldsymbol{F}_\pm)(\boldsymbol{a} \otimes \boldsymbol{m}))\boldsymbol{n}$$

is the bilinear form satisfying $\boldsymbol{B}_\pm(\boldsymbol{a}, \boldsymbol{n})\boldsymbol{n} = \boldsymbol{A}_\pm(\boldsymbol{n})\boldsymbol{a}$ and $\boldsymbol{B}^T_\pm(\boldsymbol{a}, \boldsymbol{n})\boldsymbol{a} = \boldsymbol{A}^*_\pm(\boldsymbol{a})\boldsymbol{n}$.

The second remark concerns condition (4.13). Its compact general form comprises two relations: (4.18), which is a consequence of (4.12), and

$$\int_Y \widehat{\boldsymbol{P}}^*(\nabla\boldsymbol{\phi})\boldsymbol{Q}^T d\boldsymbol{x} = \boldsymbol{0}, \tag{4.25}$$

which is an algebraic condition of optimality with respect to orientation and period cell shape. We observe that there is an analogy between equations (4.12), (4.17) and the first equation in (4.4), and between (4.16) and the second equation in (4.4). Observe that if we dot the first equation in (4.4) with $\boldsymbol{a}$ we obtain that $I_{\mathfrak{S}}(\boldsymbol{F}, \phi((\boldsymbol{x}, \boldsymbol{n}))\boldsymbol{a}) = 0$ implying that generically $\boldsymbol{F}$ must lie in $\overline{\mathfrak{S}}$—the closure of the spinodal region. However, it cannot describe the spinodal alone. Indeed, if $\boldsymbol{F}$ in the spinodal region is such that the function $\mathbb{S}^{d-1} \ni \boldsymbol{n} \mapsto \det \boldsymbol{A}(\boldsymbol{n}; \boldsymbol{F})$ changes sign then there will be an entire neighborhood of $\boldsymbol{F}$ where this is true. Therefore, for each $\boldsymbol{F}$ with this property we can find $\boldsymbol{n} \neq \boldsymbol{0}$ with $\det \boldsymbol{A}(\boldsymbol{n}; \boldsymbol{F}) = 0$. This shows that existence of non-trivial solutions of the first equation in (4.4) describes entire subregions of the spinodal region. The second equation in (4.4) eliminates most of these solutions and describes a co-dimension 1 surface containing the spinodal.

Our next theorem relates the existence of non-zero solutions to the system (4.12)–(4.13), i.e. the generalized bifurcation, with the marginal stability of $\boldsymbol{F}$. More precisely, we show that generically, the existence of nontrivial solutions implies that $\boldsymbol{F}$ must be either on the binodal or inside the binodal region. The solutions corresponding to the latter possibility are "spurious", and one must use both the partial knowledge of $\mathfrak{B}$ and computable consequences of (4.11), (see [61]), in order to eliminate them.

THEOREM **4.6.** *Suppose* $1 \leq k \leq d$ *and* $\boldsymbol{\phi} \in \mathcal{C}_k$ *solves (4.12) and satisfies (4.13). Then* $J_k(\boldsymbol{F}, \boldsymbol{\psi}, \boldsymbol{R}, \boldsymbol{Q}, \boldsymbol{A}) = 0$.

The proof is given in the Appendix F

Corollary 4.7. *If (4.12) has solution* $(\boldsymbol{\psi}, \boldsymbol{R}, \boldsymbol{Q}, \boldsymbol{A})$ *such that* $\boldsymbol{\psi} \neq \boldsymbol{0}$*, and*

$$\frac{\partial J_k(\boldsymbol{F}, \boldsymbol{\psi}, \boldsymbol{R}, \boldsymbol{Q}, \boldsymbol{A})}{\partial \boldsymbol{F}} \neq \boldsymbol{0} \tag{4.26}$$

then $\boldsymbol{F}$ *must lie in the closure of* $\mathfrak{B}$*.*

The Corollary 4.7 implies that $\boldsymbol{F}$ can not lie in the interior of the complement of $\mathfrak{B}$, so $\boldsymbol{F} \in \mathfrak{Bin}$. Therefore non-trivial solution of (4.12) corresponds to $\boldsymbol{F} \in \mathfrak{Bin}$ if and only if it is not spurious.

We give the following definition in order to distinguish parts of the binodal that could be identified by the test functions from $\mathcal{C}_k$.

Definition 4.8. *We say that* $\boldsymbol{F}$ *belongs to the* ***nucleation set*** $\mathfrak{N}_k$ *if there exists a fundamental domain* $Y = \mathcal{L} \times \boldsymbol{Q}^T Q_{d-k}$ *such that the system (4.12) has a non-zero solution* $\boldsymbol{\phi} \in \mathcal{C}_k$ *satisfying (4.13).*

In Section 5 we show that sometimes the sets $\mathfrak{N}_k$ can be characterized without a complete knowledge of the binodal set $\mathfrak{B}$.

Example 4.9.

As a simple illustration of a case where binodal can be fully characterized by our method, consider again the energy (4.9). The Euler-Lagrange equation from (4.12) becomes

$$\mu \Delta \boldsymbol{\phi} + \nabla \left(f'(\operatorname{Tr} \boldsymbol{F} + \nabla \cdot \boldsymbol{\phi}) + \frac{\mu(d-2)}{d} \nabla \cdot \boldsymbol{\phi} \right) = 0. \tag{4.27}$$

Taking divergence of this equation we obtain

$$\Delta \Phi'(\operatorname{Tr} \boldsymbol{F} + \nabla \cdot \boldsymbol{\phi}) = 0, \qquad \Phi(\theta) = f(\theta) + \frac{\mu(d-1)}{d} \theta^2. \tag{4.28}$$

By assumption, $\nabla \cdot \boldsymbol{\phi}(\boldsymbol{x})$, and hence $\Phi'(\operatorname{Tr} \boldsymbol{F} + \nabla \cdot \boldsymbol{\phi}(\boldsymbol{x}))$ is bounded on $\mathbb{R}^d$. Therefore, $\Phi'(\operatorname{Tr} \boldsymbol{F} + \nabla \cdot \boldsymbol{\phi}(\boldsymbol{x})) = \text{const}$. Taking the curl of (4.27) we obtain

$$\Delta(\nabla \boldsymbol{\phi} - (\nabla \boldsymbol{\phi})^T) = \boldsymbol{0}$$

in the sense of distributions. Hence, the boundedness of $\nabla \boldsymbol{\phi}(\boldsymbol{x})$ implies that $\nabla \boldsymbol{\phi} - (\nabla \boldsymbol{\phi})^T = 2\boldsymbol{M}$, where $\boldsymbol{M}$ is a constant anti-symmetric matrix. Therefore, $\boldsymbol{\phi}(\boldsymbol{x}) = \boldsymbol{M}\boldsymbol{x} + \nabla h(\boldsymbol{x})$ for some locally integrable function $h(\boldsymbol{x})$. The boundedness of $\boldsymbol{\phi}(\boldsymbol{x})$ implies that $\boldsymbol{M} = \boldsymbol{0}$. Indeed, if $\boldsymbol{M} \neq \boldsymbol{0}$, there exists a unit vector $\boldsymbol{e}_1$ such that $\boldsymbol{M}\boldsymbol{e}_1 \neq \boldsymbol{0}$. Let $\boldsymbol{e}_2 = \boldsymbol{M}\boldsymbol{e}_1/|\boldsymbol{M}\boldsymbol{e}_1|$. Then, the unit vector $\boldsymbol{e}_2$ is orthogonal to $\boldsymbol{e}_1$, by anti-symmetry of $\boldsymbol{M}$, and $(\boldsymbol{M}\boldsymbol{e}_1, \boldsymbol{e}_2) = |\boldsymbol{M}\boldsymbol{e}_1| > 0$. For any $R > 0$ let $\boldsymbol{x}_R(t) = R\boldsymbol{e}_1 \cos t + R\boldsymbol{e}_2 \sin t$ be a closed loop. We conclude that

$$\left| \int_0^{2\pi} (\boldsymbol{\phi}(\boldsymbol{x}_R(t)), \dot{\boldsymbol{x}}_R(t)) dt \right| \leq 2\pi R \|\boldsymbol{\phi}\|_\infty.$$

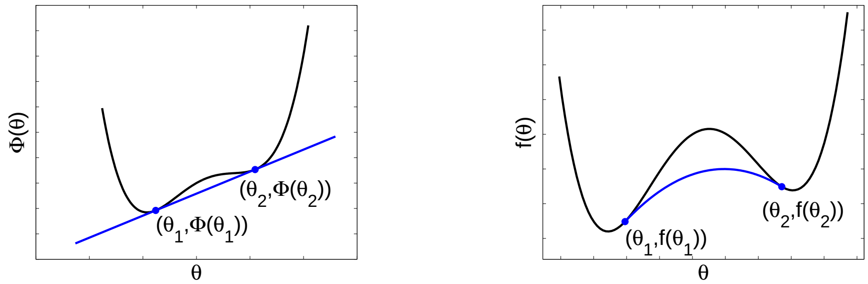

Figure 2: Common tangent to the graph of the function $\Phi(\theta)$ from Example 4.9 and its image on the graph of the function $f(\theta)$.

At the same time we have

$$\int_0^{2\pi}(\nabla h(\boldsymbol{x}_R(t)),\dot{\boldsymbol{x}}_R(t))dt=0,\qquad \int_0^{2\pi}(\boldsymbol{M}\boldsymbol{x}_R(t),\dot{\boldsymbol{x}}_R(t))dt=2\pi R^2(\boldsymbol{M}\boldsymbol{e}_1,\boldsymbol{e}_2).$$

Thus, $\boldsymbol{\phi}(\boldsymbol{x})=\nabla h(\boldsymbol{x})$, while $\Phi'(\mathrm{Tr}\,\boldsymbol{F}+\Delta h)=C=\text{const}$. We claim that $C=\Phi'(\mathrm{Tr}\,\boldsymbol{F})$. Indeed, if $C\neq\mathrm{Tr}\,\boldsymbol{F}$, then for every $\boldsymbol{x}\in\mathbb{R}^d$ the number $\nabla\cdot\boldsymbol{\phi}(\boldsymbol{x})=\Delta h(\boldsymbol{x})$ must belong to a finite set of solutions of the equation $\Phi'(\mathrm{Tr}\,\boldsymbol{F}+\eta)=C$, none of which is zero. Hence, $|\nabla\boldsymbol{\phi}(\boldsymbol{x})|>\delta>0$ for all $\boldsymbol{x}\in\mathbb{R}^d$ for some positive number δ. But then, condition (3.19) will not be satisfied. If the graph of function $f(\theta)$ has the shape shown in Figure 1 then the equation

$$\Phi'(\mathrm{Tr}\,\boldsymbol{F}+\eta)=\Phi'(\mathrm{Tr}\,\boldsymbol{F}) \tag{4.29}$$

will either have a unique solution $\eta=0$, or three solutions, two of which η_1 and η_2 are non-zero. In the former case the Euler-Lagrange PDE $(4.12)_1$ has only trivial solutions in $\mathcal{S}_*$. In the latter case condition (4.11) helps us to rule out some of the spurious solutions. Observe that one of the three solutions of (4.29) is always inside the spinodal region. Hence, assuming that $\mathrm{Tr}\,\boldsymbol{F}$ is not in the spinodal region we only need to consider solutions of the form

$$\Delta h=\eta\chi_\Omega(\boldsymbol{x}), \tag{4.30}$$

where η is the unique non-zero solution of (4.29) for which $\mathrm{Tr}\,\boldsymbol{F}+\eta$ is not in the spinodal region, and Ω is an arbitrary measurable subset of $\mathbb{R}^d$, satisfying "zero volume fraction condition"

$$\lim_{R\to\infty}\frac{|\Omega\cap B_R|}{|B_R|}=0,$$

so that the corresponding solution $\boldsymbol{\phi}$ satisfy (3.19). In this case any choice of an open and bounded subset $\Omega\subset\mathbb{R}^d$ provides a solution $\boldsymbol{\phi}\in\mathcal{S}$ to $(4.12)_1$ via the solution $h\in H^2(\mathbb{R}^d)$ of (4.30).

The equation $(4.12)_2$ is difficult to use directly in this example. Instead we restrict the class of solutions of the bifurcation system (4.12) only to those, where the set Ω has smooth boundary. In this case the equation $(4.12)_2$ can be replaced by the Maxwell relation (4.21)

$$f(\mathrm{Tr}\,\boldsymbol{F}+\eta)-f(\mathrm{Tr}\,\boldsymbol{F})-f'(\mathrm{Tr}\,\boldsymbol{F})\eta+\mu\left|[\![\nabla\nabla h]\!]-\frac{1}{d}[\![\Delta h]\!]\boldsymbol{I}\right|^2=0.$$

Observe that due to the assumed smoothness of the boundary of $\partial\Omega$ and elliptic regularity we conclude that $[\![\nabla\nabla h]\!]$ must be a rank-1 matrix on $\partial\Omega$. Hence, $[\![\nabla\nabla h]\!]=\eta\boldsymbol{n}(\boldsymbol{x})\otimes\boldsymbol{n}(\boldsymbol{x})$, $\boldsymbol{x}\in\partial\Omega$. Thus, we obtain

$$f(\mathrm{Tr}\,\boldsymbol{F}+\eta)-f(\mathrm{Tr}\,\boldsymbol{F})-f'(\mathrm{Tr}\,\boldsymbol{F})\eta+\mu\eta^2\left(1-\frac{1}{d}\right)=0.$$

Rewriting this in terms of the function $\Phi(\theta)$ we obtain

$$\Phi(\mathrm{Tr}\,\boldsymbol{F}+\eta)-\Phi(\mathrm{Tr}\,\boldsymbol{F})-\Phi'(\mathrm{Tr}\,\boldsymbol{F})\eta=0. \tag{4.31}$$

Equations (4.29) and (4.31) have a geometric interpretation. They say that the straight line connecting the points $(\mathrm{Tr}\,\boldsymbol{F},\Phi(\mathrm{Tr}\,\boldsymbol{F}))$ and $(\mathrm{Tr}\,\boldsymbol{F}+\eta,\Phi(\mathrm{Tr}\,\boldsymbol{F}+\eta))$ on the graph of $\Phi(\theta)$ must be a common tangent at both points. Figure 2 shows that if $f(\theta)$ is as shown on Figure 1 then there is a unique common tangent to the graph of $\Phi(\theta)$, touching it at the points $\theta=\theta_1$ and $\theta=\theta_2$. Thus, either $\mathrm{Tr}\,\boldsymbol{F}=\theta_1$ and $\Delta h(\boldsymbol{x})=(\theta_2-\theta_1)\chi_\Omega(\boldsymbol{x})$, or $\mathrm{Tr}\,\boldsymbol{F}=\theta_2$ and $\Delta h(\boldsymbol{x})=(\theta_1-\theta_2)\chi_\Omega(\boldsymbol{x})$.

Suppose now that Ω is an arbitrary $(d-k)$-periodic array of arbitrary smooth inclusions where

$$\Delta h(\boldsymbol{x})=[\![\theta]\!]\chi_\Omega(\boldsymbol{x}). \tag{4.32}$$

Computing Fourier transform in $\boldsymbol{t}$ variables and Fourier coefficients in $\boldsymbol{p}$ variables in (4.32) we can easily verify that $\boldsymbol{\phi}\in\mathcal{C}_k$. It remains to verify condition (4.13). We have, after straightforward calculations, taking into account (4.29) and (4.31)

$$\frac{1}{\mu}\widehat{\boldsymbol{P}}^*=\left(|\nabla\nabla h|^2-(\Delta h)^2\right)\boldsymbol{I}+2\left(\Delta h\nabla\nabla h-(\nabla\nabla h)^2\right).$$

Integration by parts gives

$$\int_Y|\nabla\nabla h|^2d\boldsymbol{x}=\int_Y(\Delta h)^2d\boldsymbol{x},\qquad\int_Y(\nabla\nabla h)^2d\boldsymbol{x}=\int_Y\Delta h\nabla\nabla h d\boldsymbol{x}.$$

Therefore, (4.13) is satisfied. Hence, the sets $\mathfrak{N}_k$ are all the same for all k and are given by

$$\mathfrak{N}_k=\{\boldsymbol{F}:\mathrm{Tr}\,\boldsymbol{F}\in\{\theta_1,\theta_2\}\},$$

where θ_1, θ_2 are determined as θ-coordinates of the two points of common tangency, as shown in Figure 2. In [60] we show that in this example $\mathfrak{Bin}=\mathfrak{N}_k$. It is also clear that if the graph of $\Phi(\theta)$ admits more than one common tangent, then the system (4.12)–(4.13) will also have spurious solutions corresponding to the interior points of the binodal region.

4.2.2 Microstructure nucleation

The main difference between the Legendre-Hadamard condition and the quasiconvexity condition is that in the former case the set of test functions (3.5) "exhausts" possible localized instabilities. This leads to algebraic system (4.8), whose nontrivial solutions signal instability whenever $\boldsymbol{F}$ crosses the spinodal. Similarly, it may be intuitively appealing to think that crossing the binodal *always* manifests itself through the bifurcation in (4.12)–(4.13) in the class of decaying-periodic fields. However, we know that some points $\boldsymbol{F}$ on the binodal can be revealed only by studying nucleation of finite rank laminates. In this case the functional

$$J(\boldsymbol{F},\nu)=\sum_{j=1}^{r}\lambda_j W^{\circ}(\boldsymbol{F},\boldsymbol{H}_j) \tag{4.33}$$

is non-negative for any finite rank laminate ν, with $\bar{\nu}=\boldsymbol{a}\otimes\boldsymbol{n}$, while achieving its minimum value of zero at a specific finite rank laminate, $\boldsymbol{a}\neq\boldsymbol{0}$ and $\boldsymbol{n}\in\mathbb{S}^{d-1}$. Finding the corresponding bounds for the binodal leads to an algebraic problem formulated below.

We recall that on each step of the construction of the measure ν in Definition 3.13 by means of lamination we introduced free parameters that can be varied in order to minimize $J(\boldsymbol{F},\nu)$ given by (4.33). The equilibrium equations obtained from such a minimization are constraints on the matrices $\boldsymbol{H}_j$ and weights λ_j in (3.27) get more and more complicated with the growth of the rank of the laminate. Below, we exhibit the recursive structure of the ensuing algebraic system by examining the passage from rank-1 to rank-two laminates.

The rank-1 laminate corresponds to $\nu_1=\delta_{\boldsymbol{a}\otimes\boldsymbol{n}}$. This Young measure is attained on the special test field $\boldsymbol{\phi}_0\in\widetilde{\mathcal{C}}_1$ given by (3.28). In that case

$$J(\boldsymbol{F},\nu_1)=\widetilde{J}_1(\boldsymbol{F},\boldsymbol{\phi}_0,\boldsymbol{n})=W^{\circ}(\boldsymbol{F},\boldsymbol{a}\otimes\boldsymbol{n}).$$

The field value $\boldsymbol{F}$ is marginally stable if the following equations are satisfied

$$\begin{cases} W^{\circ}(\boldsymbol{F},\boldsymbol{a}\otimes\boldsymbol{n})=0,\\ \nabla_{\boldsymbol{a}}W^{\circ}(\boldsymbol{F},\boldsymbol{a}\otimes\boldsymbol{n})=\boldsymbol{0},\\ \nabla_{\boldsymbol{n}}W^{\circ}(\boldsymbol{F},\boldsymbol{a}\otimes\boldsymbol{n})=\boldsymbol{0}.\end{cases} \tag{4.34}$$

This system places $\boldsymbol{F}$ on the jump set $\mathfrak{J}$ (see [58]). The second rank laminate ν_2 is obtained from ν_1 by means of lamination in the sense of Definition 3.12.

$$\nu_2=(1-\theta)\delta_{\boldsymbol{a}\otimes\boldsymbol{n}}+\theta s\delta_{\boldsymbol{H}_1}+\theta(1-s)\delta_{\boldsymbol{H}_2},\qquad s\boldsymbol{H}_1+(1-s)\boldsymbol{H}_2=\boldsymbol{a}\otimes\boldsymbol{n},\quad \boldsymbol{H}_2-\boldsymbol{H}_1=\boldsymbol{b}\otimes\boldsymbol{m}.$$

Observe that $J(\boldsymbol{F},\nu_2)$ is affine in θ. Hence, it is minimized either at $\theta=0$ corresponding to a rank-1 laminate or at $\theta=1$. The goal of using rank-r laminates is to capture points on the binodal that cannot be captured using rank-$(r-1)$ laminates. Therefore, we only need to consider the case $\theta=1$. Then

$$J(\boldsymbol{F},\nu_2)=sW^{\circ}(\boldsymbol{F},\boldsymbol{a}\otimes\boldsymbol{n}-(1-s)\boldsymbol{b}\otimes\boldsymbol{m})+(1-s)W^{\circ}(\boldsymbol{F},\boldsymbol{a}\otimes\boldsymbol{n}+s\boldsymbol{b}\otimes\boldsymbol{m}).$$

The field value $\boldsymbol{F}$ is marginally stable when the laminate with $s \in [0,1]$, $\{\boldsymbol{a},\boldsymbol{b}\} \subset \mathbb{R}^m \setminus \{\boldsymbol{0}\}$, and $\{\boldsymbol{n},\boldsymbol{m}\} \subset \mathbb{S}^{d-1}$ delivers the global minimum to $J(\boldsymbol{F},\nu_2)$, which is equal to 0. Observe that both $s=0$ and $s=1$ correspond to rank-1 laminates, and are therefore excluded from the analysis of rank-2 laminates. Hence, we are interested only in the case when $s \in (0,1)$. If the minimum of $J(\boldsymbol{F},\nu_2)$ is attained at a rank-2 laminate, then the following system of equations must hold

$$\begin{cases} sW(\boldsymbol{F}_1)+(1-s)W(\boldsymbol{F}_2)-W(\boldsymbol{F})-(\boldsymbol{P}(\boldsymbol{F}),\boldsymbol{a}\otimes\boldsymbol{n})=0 \\ W(\boldsymbol{F}_2)-W(\boldsymbol{F}_1)-(s\boldsymbol{P}(\boldsymbol{F}_1)+(1-s)\boldsymbol{P}(\boldsymbol{F}_2),\boldsymbol{F}_2-\boldsymbol{F}_1)=0 \\ (s\boldsymbol{P}(\boldsymbol{F}_1)+(1-s)\boldsymbol{P}(\boldsymbol{F}_2)-\boldsymbol{P}(\boldsymbol{F}))\boldsymbol{n}=\boldsymbol{0} \\ (s\boldsymbol{P}(\boldsymbol{F}_1)+(1-s)\boldsymbol{P}(\boldsymbol{F}_2)-\boldsymbol{P}(\boldsymbol{F}))^T\boldsymbol{a}=\boldsymbol{0} \\ (\boldsymbol{P}(\boldsymbol{F}_2)-\boldsymbol{P}(\boldsymbol{F}_1))\boldsymbol{m}=\boldsymbol{0} \\ (\boldsymbol{P}(\boldsymbol{F}_2)-\boldsymbol{P}(\boldsymbol{F}_1))^T\boldsymbol{b}=\boldsymbol{0} \end{cases} \tag{4.35}$$

where

$$\boldsymbol{F}_1=\boldsymbol{F}+\boldsymbol{a}\otimes\boldsymbol{n}-(1-s)\boldsymbol{b}\otimes\boldsymbol{m}, \qquad \boldsymbol{F}_2=\boldsymbol{F}+\boldsymbol{a}\otimes\boldsymbol{n}+s\boldsymbol{b}\otimes\boldsymbol{m}$$

are the values of the deformation gradient in the internal laminate. There are $2m+2d$ independent equations in (4.35) with $2m+2d-1$ unknowns s, $\boldsymbol{a}$, $\boldsymbol{b}$, $\boldsymbol{m}$ and $\boldsymbol{n}$, where $\boldsymbol{n}$ and $\boldsymbol{m}$ are constrained to be unit vectors. We conclude that the system (4.35) restricts $\boldsymbol{F}$ to a co-dimension 1 surface corresponding to nucleation of second rank laminates.

Next we observe that

$$\boldsymbol{F}_2-\boldsymbol{F}_1=\boldsymbol{b}\otimes\boldsymbol{n}. \tag{4.36}$$

Therefore, in view of either the 5th or the 6th equation in (4.35), we can rewrite the second equation in (4.35) as the Maxwell relation

$$W(\boldsymbol{F}_2)-W(\boldsymbol{F}_1)-(\boldsymbol{P}(\boldsymbol{F}_2),\boldsymbol{F}_2-\boldsymbol{F}_1)=0, \tag{4.37}$$

The system (4.35) can then be decomposed into two systems: the *micro-level* system and the *macro-level* system. The micro-level system consists of the 5th and the 6th equation in (4.35), as well as (4.36) and (4.37):

$$\begin{cases} W(\boldsymbol{F}_2)-W(\boldsymbol{F}_1)-(\boldsymbol{P}(\boldsymbol{F}_2),\boldsymbol{F}_2-\boldsymbol{F}_1)=0 \\ (\boldsymbol{P}(\boldsymbol{F}_2)-\boldsymbol{P}(\boldsymbol{F}_1))\boldsymbol{m}=\boldsymbol{0} \\ (\boldsymbol{P}(\boldsymbol{F}_2)-\boldsymbol{P}(\boldsymbol{F}_1))^T\boldsymbol{b}=\boldsymbol{0} \\ \boldsymbol{F}_2-\boldsymbol{F}_1=\boldsymbol{b}\otimes\boldsymbol{n}. \end{cases} \tag{4.38}$$

This is exactly the same system as in (4.34) defining the jump set $\mathfrak{J}$. In particular, $\{\boldsymbol{F}_1,\boldsymbol{F}_2\} \subset \mathfrak{J}$. The structure of the macro-level system becomes clear if we introduce the notations

$$\overline{\boldsymbol{F}}=s\boldsymbol{F}_1+(1-s)\boldsymbol{F}_2, \quad \overline{\boldsymbol{P}}=s\boldsymbol{P}(\boldsymbol{F}_1)+(1-s)\boldsymbol{P}(\boldsymbol{F}_2), \quad \overline{W}=sW(\boldsymbol{F}_1)+(1-s)W(\boldsymbol{F}_2). \tag{4.39}$$

Then the macro-level system can be written as follows

$$\begin{cases} \overline{W} - W(\boldsymbol{F}) - (\boldsymbol{P}(\boldsymbol{F}), \overline{\boldsymbol{F}} - \boldsymbol{F}) = 0 \\ (\overline{\boldsymbol{P}} - \boldsymbol{P}(\boldsymbol{F}))\boldsymbol{n} = \boldsymbol{0} \\ (\overline{\boldsymbol{P}} - \boldsymbol{P}(\boldsymbol{F}))^T \boldsymbol{a} = \boldsymbol{0} \\ \overline{\boldsymbol{F}} - \boldsymbol{F} = \boldsymbol{a} \otimes \boldsymbol{n}. \end{cases} \tag{4.40}$$

Observe that the system (4.40) has a structure very similar to structure of the system defining the jump set $\mathfrak{J}$, except the energy density $W(\boldsymbol{F})$ is replaced by a modified function $\overline{W}(\boldsymbol{F})$. To define this function we first introduce the set

$$\widehat{\mathfrak{J}} = \{s\boldsymbol{F}_1 + (1-s)\boldsymbol{F}_2 : s \in [0,1],\ \boldsymbol{F}_1, \boldsymbol{F}_2 \text{ solve (4.38)}\}.$$

Next, for $\overline{\boldsymbol{F}} \notin \widehat{\mathfrak{J}}$ we assume that $\overline{W}(\overline{\boldsymbol{F}}) = W(\overline{\boldsymbol{F}})$, while for $\overline{\boldsymbol{F}} \in \widehat{\mathfrak{J}}$ we define

$$\overline{W}(\overline{\boldsymbol{F}}) = \min_{\overline{\boldsymbol{F}} = s\boldsymbol{F}_1 + (1-s)\boldsymbol{F}_2} \{sW(\boldsymbol{F}_1) + (1-s)W(\boldsymbol{F}_2) : \boldsymbol{F}_1, \boldsymbol{F}_2 \text{ solve (4.38)}\}. \tag{4.41}$$

One can see that $\overline{W}(\boldsymbol{F})$ is a Lipschitz continuous function that agrees with $W(\boldsymbol{F})$ on the complement of $\widehat{\mathfrak{J}}$.

We claim now that $\boldsymbol{F}$ is located on the jump set of $\overline{W}(\boldsymbol{F})$, i.e.

$$\overline{W}(\overline{\boldsymbol{F}}) = \overline{W}, \qquad \overline{W}_{\boldsymbol{F}}(\overline{\boldsymbol{F}}) = \overline{\boldsymbol{P}}, \tag{4.42}$$

where $\overline{\boldsymbol{F}}$, $\overline{\boldsymbol{P}}$ and $\overline{W}$ are given by (4.39). We say that the point $\overline{\boldsymbol{F}} \in \widehat{\mathfrak{J}}$ is regular if the minimum in the definition of $\overline{W}(\overline{\boldsymbol{F}})$ is achieved at a unique pair $\boldsymbol{F}_1$, $\boldsymbol{F}_2$.

THEOREM **4.10.** *Assume that $\boldsymbol{F} \notin \widehat{\mathfrak{J}}$ and $\overline{\boldsymbol{F}} \in \widehat{\mathfrak{J}}$ is regular, i.e. there are unique values $\boldsymbol{F}_1$, $\boldsymbol{F}_2$ and s minimizing (4.41). Then, $\boldsymbol{F}_1$ and $\boldsymbol{F}_2$ are on the jump set $\mathfrak{J}$ of the energy $W(\boldsymbol{F})$, and $\boldsymbol{F}$ and $\overline{\boldsymbol{F}}$ are on the jump set $\overline{\mathfrak{J}}$ of the energy $\overline{W}(\boldsymbol{F})$ if and only if $\boldsymbol{F}$, $\boldsymbol{F}_1$, $\boldsymbol{F}_2$ and s solve (4.35).*

Proof. By definition of $\boldsymbol{F}_1$, $\boldsymbol{F}_2$ the system (4.38) is satisfied. The system (4.40) places $\boldsymbol{F}$ and $\overline{\boldsymbol{F}}$ are on the jump set $\overline{\mathfrak{J}}$ of the energy $\overline{W}(\boldsymbol{F})$ if and only if (4.42) holds. To prove (4.42) we perturb a regular point $\overline{\boldsymbol{F}}$ within $\widehat{\mathfrak{J}}$. Then, the values $\boldsymbol{F}_1$, $\boldsymbol{F}_2$ and, hence, $\boldsymbol{b}$ and $\boldsymbol{m}$ will also be smoothly perturbed. Therefore,

$$\delta\overline{\boldsymbol{F}} = \delta\boldsymbol{F}_2 - s\delta[\![\boldsymbol{F}]\!] - (\delta s)[\![\boldsymbol{F}]\!],$$

where $[\![\boldsymbol{F}]\!] = \boldsymbol{F}_2 - \boldsymbol{F}_1$. We also get

$$\delta\overline{W} = (\boldsymbol{P}(\boldsymbol{F}_2), \delta\boldsymbol{F}_2) - (\delta s)[\![W]\!] - s((\boldsymbol{P}(\boldsymbol{F}_2), \delta\boldsymbol{F}_2) - (\boldsymbol{P}(\boldsymbol{F}_1), \delta\boldsymbol{F}_1)).$$

Replacing $[\![W]\!] = W(\boldsymbol{F}_2) - W(\boldsymbol{F}_1)$ with $(\boldsymbol{P}(\boldsymbol{F}_1), [\![\boldsymbol{F}]\!])$ and $\delta\boldsymbol{F}_1$ with $\delta\boldsymbol{F}_2 - \delta[\![\boldsymbol{F}]\!]$ we obtain

$$\delta\overline{W} = (\boldsymbol{P}(\boldsymbol{F}_1), \delta\overline{\boldsymbol{F}}) + (1-s)([\![\boldsymbol{P}]\!], \delta\boldsymbol{F}_2) = (\boldsymbol{P}(\boldsymbol{F}_1), \delta\overline{\boldsymbol{F}}) + (1-s)([\![\boldsymbol{P}]\!], \delta\overline{\boldsymbol{F}}),$$

since

$$([\![\boldsymbol{P}]\!],[\![\boldsymbol{F}]\!])=([\![\boldsymbol{P}]\!],\delta[\![\boldsymbol{F}]\!])=0,$$

due to (4.38). Thus,

$$\overline{W}_{\boldsymbol{F}}(\overline{\boldsymbol{F}})=s\boldsymbol{P}(\boldsymbol{F}_1)+(1-s)\boldsymbol{P}(\boldsymbol{F}_2)=\overline{\boldsymbol{P}}.$$

□

We conclude that the set of field values $\boldsymbol{F}$ for which the system (4.35) has a non-trivial solutions can be interpreted as the jump set $\overline{\mathfrak{J}}$ for $\overline{W}(\boldsymbol{F})$ defined by (4.41). By replacing the function $W(\boldsymbol{F})$ with $\overline{W}(\boldsymbol{F})$, and by iterating this process, we can continue to define higher order jump sets for laminates of any rank. By analogy with (4.26) we also have a simple non-degeneracy condition.

THEOREM **4.11.** *If a finite rank laminate ν given (3.27) minimizes $J(\boldsymbol{F},\nu)$ with the minimal value of zero then $\boldsymbol{F}$ must lie in the closure of $\mathfrak{B}$, provided*

$$\boldsymbol{A}(\boldsymbol{n};\boldsymbol{F})\boldsymbol{a}\neq\boldsymbol{0}. \tag{4.43}$$

Proof. To prove the theorem it is enough to show that (4.43) guarantees that $\dfrac{\partial J(\boldsymbol{F},\nu)}{\partial\boldsymbol{F}}\neq\boldsymbol{0}$. Indeed, we compute

$$\frac{\partial J(\boldsymbol{F},\nu)}{\partial\boldsymbol{F}}=\overline{\boldsymbol{P}}-\boldsymbol{P}(\boldsymbol{F})-W_{\boldsymbol{F}\boldsymbol{F}}(\boldsymbol{a}\otimes\boldsymbol{n})\neq\boldsymbol{0},\qquad \overline{\boldsymbol{P}}=\int_{\mathbb{M}}\boldsymbol{P}(\boldsymbol{F}+\boldsymbol{H})d\nu(\boldsymbol{H}). \tag{4.44}$$

It is clear that if

$$\nu'=\sum_{j=1}^{r}\lambda_j\delta_{\boldsymbol{H}_j'}$$

is a finite rank laminate with $\bar{\nu}'=\boldsymbol{0}$, then the measure

$$\nu=\sum_{j=1}^{r}\lambda_j\delta_{\boldsymbol{H}_j'+\boldsymbol{a}\otimes\boldsymbol{n}}$$

is also a finite rank laminate with $\bar{\nu}=\boldsymbol{a}\otimes\boldsymbol{n}$. Hence, if $\boldsymbol{H}_j'$ are fixed, then the function

$$j(\boldsymbol{a},\boldsymbol{n},\nu')=\sum_{j=1}^{r}\lambda_jW^{\circ}(\boldsymbol{F},\boldsymbol{H}_j'+\boldsymbol{a}\otimes\boldsymbol{n})$$

must be minimized in $\boldsymbol{a}$. Hence,

$$\boldsymbol{0}=\nabla_{\boldsymbol{a}}j(\boldsymbol{a},\boldsymbol{n},\nu')=(\overline{\boldsymbol{P}}-\boldsymbol{P}(\boldsymbol{F}))\boldsymbol{n}.$$

Therefore, according to (4.44),

$$\frac{\partial J(\boldsymbol{F},\nu)}{\partial\boldsymbol{F}}\boldsymbol{n}=\boldsymbol{A}(\boldsymbol{n};\boldsymbol{F})\boldsymbol{a}.$$

The theorem is now proved. □

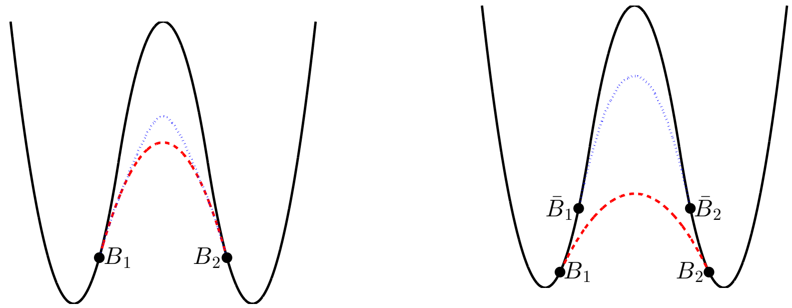

Figure 3: Possible relations between the envelopes $\overline{W}(\boldsymbol{F})$ and $QW(\boldsymbol{F})$.

Observe that by minimizing $j(\boldsymbol{a}, \boldsymbol{n}, \nu')$ in $\boldsymbol{n}$ we also obtain

$$(\overline{\boldsymbol{P}} - \boldsymbol{P}(\boldsymbol{F}))^T \boldsymbol{a} = \boldsymbol{0}, \tag{4.45}$$

which is the macro-level roughening equilibrium condition $(4.40)_3$. For an example where a part of the binodal can be captured only via the equations (4.35) we refer to [56].

The fact that the binodal of $\overline{W}(\boldsymbol{F})$ must lie in the closure of the binodal region of $W(\boldsymbol{F})$ is illustrated in Figures 3. The original energy $W(\boldsymbol{F})$ is shown by a solid line, the quasiconvexification—by a dashed line and $\overline{W}(\boldsymbol{F})$—by a dotted line. The left figure illustrates the case, where the jump set (points B_1 and B_2 in the figure) captures the binodal, without $\overline{W}(\boldsymbol{F})$ necessarily capturing the values of $QW(\boldsymbol{F})$. In the vicinity of points B_1 and B_2 the dashed and dotted lines may or may not coincide. The right figure shows a different situation, where the jump set is strictly inside the binodal region, while the binodal (points B_1 and B_2 in the figure) can only be delivered by studying other nucleation patterns, for instance, precipitates of a more general shape or higher rank laminates.

Remark 4.12. *By the rank-one convexity of the quasiconvex envelope we have $QW(\boldsymbol{F}) \leq \overline{W}(\boldsymbol{F})$ and $Q\overline{W}(\boldsymbol{F}) = QW(\boldsymbol{F})$. The points $\boldsymbol{F}$ corresponding to the non-trivial solutions of (4.12)–(4.13) with $W(\boldsymbol{F})$ replaced by $\overline{W}(\boldsymbol{F})$ can be regarded as unstable to the nucleation of composite precipitates represented by a continuously varying first rank laminate. The iteration process $W(\boldsymbol{F}) \to \overline{W}(\boldsymbol{F}) \to \overline{\overline{W}} \to \cdots$ brings additional flexibility to the binodal detection by allowing composite precipitates represented by a continuously parametrized rank-r laminates. Examples of such composite precipitates have been studied in [106, 107, 108, 135, 74, 73].*

Example 4.13.

As a simple illustration of a complete characterization of the binodal by studying nucleation of simple laminates, we consider again our test case (4.9). Let us begin with the system of equations (4.34) describing the jump set. Straightforward calculations show that the third equation in (4.34) follows from the other two, and that the system can be reduced to the following one

$$\operatorname{Tr} \boldsymbol{F} = \theta_-, \quad \boldsymbol{a} = [\![\theta]\!] \boldsymbol{n}, \quad [\![\Phi'(\theta)]\!] = 0, \quad [\![\Phi(\theta)]\!] - [\![\theta]\!] \{\!\{ \Phi'(\theta) \}\!\} = 0,$$

where $\Phi(\theta)$ is given in (4.28). We see that the jump set is characterized in terms of $\theta = \mathrm{Tr}\,\boldsymbol{F}$, where θ is a point where the tangent line to the graph of $\Phi(\theta)$ touches the graph at some other point, see Figure 2. The jump set consists of the surfaces $\mathrm{Tr}\,\boldsymbol{F} = \theta_1$ and $\mathrm{Tr}\,\boldsymbol{F} = \theta_2$. This is the same set of points identified by the nucleation conditions obtained in Section 4.2.1. This is not surprising, since the analysis in Section 4.2.1 showed that the shape of the precipitate in this case can be arbitrary, including a slab used for computing the jump set. We also observe that each $\boldsymbol{F} = \boldsymbol{F}_- \in \mathfrak{J}$ can be paired with $\boldsymbol{F}_+ = \boldsymbol{F}_- + [\![\theta]\!]\boldsymbol{n} \otimes \boldsymbol{n}$ for any unit vector $\boldsymbol{n}$.

Now a straightforward calculation gives the formula for $\overline{W}(\boldsymbol{F})$

$$\overline{W}(\boldsymbol{F}) = \begin{cases} W(\boldsymbol{F}), & \mathrm{Tr}\,\boldsymbol{F} \notin (\theta_1, \theta_2) \\ \overline{f}(\mathrm{Tr}\,\boldsymbol{\varepsilon}) + \mu \left| \boldsymbol{\varepsilon} - \dfrac{1}{d}(\mathrm{Tr}\,\boldsymbol{\varepsilon})\boldsymbol{I} \right|^2, & \mathrm{Tr}\,\boldsymbol{F} \in (\theta_1, \theta_2), \end{cases}$$

where

$$\overline{f}(\mathrm{Tr}\,\boldsymbol{\varepsilon}) = \frac{\theta_2 - \mathrm{Tr}\,\boldsymbol{\varepsilon}}{[\![\theta]\!]}\Phi(\theta_1) + \frac{\mathrm{Tr}\,\boldsymbol{\varepsilon} - \theta_1}{[\![\theta]\!]}\Phi(\theta_2) - \frac{\mu(d-1)}{d}(\mathrm{Tr}\,\boldsymbol{\varepsilon})^2.$$

One can show that in fact $\overline{W}(\boldsymbol{F}) = QW(\boldsymbol{F})$ [60], which means that, in this case, studying simple laminates is sufficient for a complete characterization of the binodal.

5 Bi-quadratic energy

In this section we apply our approach to a nontrivial example where a rather complete picture of the binodal can be obtained by studying several specific families of test functions. The spinodal in this example is degenerate, since the loss of rank-1 convexity occurs via an sharp non-smooth transition from one well to the other. The spinodal in this example can be identified as the surface of jump discontinuity of $W_{\boldsymbol{F}}(\boldsymbol{F})$, rather than via the theory of Section 4.1.

More specifically we consider the bi-quadratic energy density of the form

$$W(\boldsymbol{F}) = \min\{f_+(\boldsymbol{\varepsilon}), f_-(\boldsymbol{\varepsilon})\}, \quad \boldsymbol{\varepsilon} = \frac{1}{2}(\boldsymbol{F} + \boldsymbol{F}^T), \quad f_\pm(\boldsymbol{\varepsilon}) = \frac{1}{2}(\mathsf{C}_\pm\boldsymbol{\varepsilon}, \boldsymbol{\varepsilon}) + w_\pm, \tag{5.1}$$

We assume that the elastic tensors $\mathsf{C}_\pm$ are isotropic:

$$\mathsf{C}_\pm\boldsymbol{\xi} = \lambda_\pm(\mathrm{Tr}\,\boldsymbol{\xi})\boldsymbol{I} + 2\mu_\pm\boldsymbol{\xi}, \quad \text{for any } \boldsymbol{\xi} \in \mathrm{Sym}(\mathbb{R}^d),$$

and elliptic

$$\lambda_+ + 2\mu_+ > 0, \qquad \lambda_- + 2\mu_- > 0.$$

Additionally we assume that

$$\lambda_\pm + \mu_\pm \neq 0, \qquad [\![\mu]\!] \neq 0, \qquad k[\![\lambda]\!] + 2[\![\mu]\!] \neq 0. \tag{5.2}$$

This energy plays an important role both in the mathematical theory of composite materials [87, 52, 28, 29, 25] and in the modeling of martensitic phase transitions [78, 45, 46].

Even in this piecewise linear example we can not find all solutions to the system (4.12)–(4.13). However, we can obtain bounds on the binodal by computing in Section 5.1 nucleating solutions in $\widetilde{\mathcal{C}}_k$, $1 \le k \le d$ that have ellipsoidal k-dimensional cross-section. In Section 5.2 we also present an example of a solution in $\mathcal{C}_1 \setminus \widetilde{\mathcal{C}}_1$ in 2D.

While the calculations presented below illustrate the general theory of binodal developed in this paper, their origin lies (at least for positive definite $\mathsf{C}_\pm$) in the literature on optimal bounds for composite materials, e.g. [50, 51, 7]; the link with the theory of phase transitions is also well known [87, 55, 52, 25].

5.1 Isolated cylindrical inclusions

The goal of this section is to obtain bounds on the binodal in arbitrary dimensions using elliptical cylinders as test functions. Expanding on prior work [86, 85, 40, 20, 67, 78, 45, 46] we can compute the solutions of (4.12) for the bi-quadratic energy (5.1) corresponding to infinite elliptical cylinders explicitly. The explicit representation of these test functions in [81, 79, 80] allows us to estimate their decay at infinity and prove that they are in $\widetilde{\mathcal{C}}_k$, so that our general theory applies. In 2D these solutions can be viewed as limiting cases of composite strips computed in Section 5.2, as the period p goes to infinity.

For each $k \ge 1$ we will look for a solution of the system (4.12) in the form of an elliptical k-cylinder. We therefore define the sets $\mathfrak{N}_k^{\mathrm{ell}}$ as in Definition 4.8.

Definition 5.1. *We say that $\boldsymbol{\varepsilon}$ belongs to the* ***elliptical k-cylinder nucleation set*** $\mathfrak{N}_k^{\mathrm{ell}}$*, $k = 1, \dots, d$, if there exists an elliptical k-cylinder inclusion satisfying (4.12) and (4.13).*

Observe that for $k = 1$ such a cylinder is a plate, while for $k = d$, it is an ellipsoid. Moreover, general elliptical k-cylinders can be regarded as ellipsoids with some of the aspect ratios going to infinity [78, 44] This suggests that in order to map the entire binodal it is enough to consider only ellipsoids. However, the parts of the binodal identified by the elliptical cylinders are of the same dimension ($md - 1$) as the parts of the binodal identified by the ellipsoids. Thus, for the strategy of passing to the limits in the space of ellipsoid parameters to succeed one needs to test against *arbitrary* ellipsoids and then optimize the explicit results over orientations and aspect ratios, allowing infinite values of the parameters to capture plates and cylinders. It is a challenging technical problem. Our approach, that treats elliptical k and r-cylinders as distinct, when $k \neq r$, has the advantage of identifying singular optimal shapes directly.

If we align our coordinate system with the cylindrical inclusion in such a way that vectors $\boldsymbol{e}_1, \dots, \boldsymbol{e}_d$ are directed along the coordinate axes, then we can write $\boldsymbol{x} = (t_1, \dots, t_k, x_{k+1}, \dots, x_d)$. The test field $\boldsymbol{\phi}(\boldsymbol{x}) = \boldsymbol{\psi}(\boldsymbol{t})$ and we write the field $\boldsymbol{\varepsilon}$ at infinity in the block form

$$\boldsymbol{\varepsilon} = \begin{bmatrix} \varepsilon_0 & \boldsymbol{E}^T \\ \boldsymbol{E} & \varepsilon' \end{bmatrix},$$

where $\boldsymbol{\varepsilon}_0$ is a $k \times k$ matrix, $\boldsymbol{E}$ is a $(d-k) \times k$ matrix and $\boldsymbol{\varepsilon}'$ is a $(d-k) \times (d-k)$ matrix. We also use the notation

$$\lambda(\boldsymbol{t}) = \lambda_-(1 - \chi(\boldsymbol{t})) + \lambda_+\chi(\boldsymbol{t}), \quad \mu(\boldsymbol{t}) = \mu_-(1 - \chi(\boldsymbol{t})) + \mu_+\chi(\boldsymbol{t}),$$

where $\chi(\boldsymbol{t})$ is the characteristic function of the elliptical cylinder. One can see that the label "+" refers to the materials and fields inside the inclusion, while the label "−" refers to the materials and fields outside the inclusion. Finally, let $\mathsf{C}(\boldsymbol{t})$ be the local elasticity tensor defined by its action on an arbitrary strain $\boldsymbol{\xi}$ by

$$\mathsf{C}(\boldsymbol{t})\boldsymbol{\xi} = \lambda(\boldsymbol{t})(\operatorname{Tr}\boldsymbol{\xi})\boldsymbol{I} + 2\mu(\boldsymbol{t})\boldsymbol{\xi}, \qquad \text{for any } \boldsymbol{\xi} \in \operatorname{Sym}(\mathbb{R}^d).$$

We observe that the elastic tensor $\mathsf{C}(\boldsymbol{t})$ and the elastic constants $\lambda(\boldsymbol{t})$ and $\mu(\boldsymbol{t})$ are piecewise constant with a jump discontinuity across the boundary of the elliptical k-cylinder.

5.1.1 Euler-Lagrange equations

The isotropy of the materials cause Euler-Lagrange equation in (4.12) to decouple into separate PDEs for $\boldsymbol{\psi}_0(\boldsymbol{t}) = (\psi_1(\boldsymbol{t}), \dots, \psi_k(\boldsymbol{t}))$ and $\boldsymbol{\psi}'(\boldsymbol{t}) = (\boldsymbol{\psi}_{k+1}(\boldsymbol{t}), \dots, \psi_d(\boldsymbol{t}))$:

$$\begin{cases} \nabla \cdot \mathsf{C}(\boldsymbol{t}) \left(e(\boldsymbol{\psi}_0) + \boldsymbol{\varepsilon}_0 + \dfrac{[\![\lambda]\!] \operatorname{Tr}\boldsymbol{\varepsilon}'}{k[\![\lambda]\!] + 2[\![\mu]\!]} \boldsymbol{I}_k \right) = \boldsymbol{0}, \\ \nabla \cdot \mu(\boldsymbol{t})(\nabla\boldsymbol{\psi}' + 2\boldsymbol{E}) = 0. \end{cases} \tag{5.3}$$

The equations (5.3) decouple into equations of elasticity in $\mathbb{R}^k$ and an additional generalized anti-plane shear. The elastic strain field

$$e(\boldsymbol{\phi}) = \begin{bmatrix} e(\boldsymbol{\psi}_0) & \dfrac{1}{2}(\nabla\boldsymbol{\psi}')^T \\ \dfrac{1}{2}\nabla\boldsymbol{\psi}' & \boldsymbol{0} \end{bmatrix}$$

is smooth inside and outside of the elliptical k-cylinder

$$\sum_{i=1}^{k} \frac{t_k^2}{a_k^2} = 1, \tag{5.4}$$

but has a jump discontinuity across its boundary. Thus, in the application of the general theory we may replace the Noether-Eshelby equation $(4.12)_2$ with the Maxwell relation (4.21) on the boundary of the cylinder.

We know that both $e(\boldsymbol{\psi}_0)$ and $\nabla\boldsymbol{\psi}'(\boldsymbol{t})$ are uniform inside the ellipsoid [98]. The values of these fields are determined uniquely by the fields at infinity and the shape of the ellipsoid described by the $k \times k$ matrix $\boldsymbol{a}$ =diag$(a_1, \dots, a_k)$. Eshelby [40, 41] has presented the solution for 3D isotropic ellipsoidal inclusions in the isotropic external medium. We will use the elegant formulas that are valid in any dimensions and for general anisotropic media due to Kunin and Sosnina [80].

Recall the definition of the fourth order tensor $\mathsf{K}_{\mathsf{C}}(\boldsymbol{n})$, which is a Fourier space representation of the fundamental solution for the equations of linear elasticity in the general anisotropic medium C. Suppose $\boldsymbol{u}(\boldsymbol{t})$ solves

$$\nabla \cdot \mathsf{C}e(\boldsymbol{u}) = \nabla \cdot \boldsymbol{\tau}, \qquad \boldsymbol{t} \in \mathbb{R}^k,$$

where the symmetric external stress field $\boldsymbol{\tau}(\boldsymbol{t})$ is smooth and compactly supported. Then the Fourier transform of the strain will satisfy

$$\widehat{e(\boldsymbol{u})}(\boldsymbol{\omega}) = \mathsf{K}_{\mathsf{C}}(\boldsymbol{\omega})\widehat{\boldsymbol{\tau}}(\boldsymbol{\omega}).$$

Explicitly,

$$\mathsf{K}_{\mathsf{C}}(\boldsymbol{n})\boldsymbol{\xi} = \boldsymbol{A}_{\mathsf{C}}(\boldsymbol{n})^{-1}\boldsymbol{\xi}\boldsymbol{n} \odot \boldsymbol{n},$$

where $\boldsymbol{A}_{\mathsf{C}}(\boldsymbol{n})$ is the acoustic tensor of C.

THEOREM **5.2** (Kunin and Sosnina)**.**

(a) Suppose that $\boldsymbol{u} : \mathbb{R}^k \to \mathbb{R}^k$ *satisfies*

$$\nabla \cdot \mathsf{C}(\boldsymbol{t})(e(\boldsymbol{u}) + \boldsymbol{\varepsilon}^\infty) = \boldsymbol{0}$$

where $\mathsf{C}(\boldsymbol{t}) = (1 - \chi(\boldsymbol{t}))\mathsf{C}_- + \chi(\boldsymbol{t})\mathsf{C}_+$ *and* $\chi(\boldsymbol{t})$ *is the characteristic function of the ellipsoid (5.4). Then*

$$\boldsymbol{\varepsilon}^\infty = \boldsymbol{\varepsilon}^+ + \langle \mathsf{K}_{\mathsf{C}_-}(\boldsymbol{n})\rangle_{\boldsymbol{a}} [\![\mathsf{C}]\!] \boldsymbol{\varepsilon}^+, \tag{5.5}$$

where $\boldsymbol{\varepsilon}^+ = e(\boldsymbol{u}_+) + \boldsymbol{\varepsilon}^\infty$ *is the strain field in the inclusion, and*

$$\langle \mathsf{K}_{\mathsf{C}_-}(\boldsymbol{n})\rangle_{\boldsymbol{a}} = \fint_{\mathbb{S}^{k-1}} \mathsf{K}_{\mathsf{C}_-}(\boldsymbol{a}^{-1}\boldsymbol{n})dS(\boldsymbol{n}), \qquad \boldsymbol{a} = \mathrm{diag}(a_1, \ldots, a_k).$$

(b) Suppose that $\boldsymbol{v} : \mathbb{R}^k \to \mathbb{R}^p$ *satisfies*

$$\nabla \cdot \mu(\boldsymbol{t})(\nabla \boldsymbol{v} + \boldsymbol{e}^\infty) = \boldsymbol{0},$$

where $\mu(\boldsymbol{t}) = (1 - \chi(\boldsymbol{t}))\mu_- + \chi(\boldsymbol{t})\mu_+$. *Then*

$$\boldsymbol{e}^\infty = \boldsymbol{e}^+ + \frac{[\![\mu]\!]}{\mu_-}\boldsymbol{e}^+ \langle \Gamma(\boldsymbol{n})\rangle_{\boldsymbol{a}} \tag{5.6}$$

where $\boldsymbol{e}^+ = \nabla \boldsymbol{v}_+ + \boldsymbol{e}^\infty$ *is the strain field in the inclusion. Here*

$$\langle \Gamma(\boldsymbol{n})\rangle_{\boldsymbol{a}} = \fint_{\mathbb{S}^{k-1}} \Gamma(\boldsymbol{a}^{-1}\boldsymbol{n})dS(\boldsymbol{n}), \qquad \Gamma(\boldsymbol{\omega}) = \frac{\boldsymbol{\omega} \otimes \boldsymbol{\omega}}{|\boldsymbol{\omega}|^2}.$$

The proof of part (a) can be found in [80]. Part (b) is proved in exactly the same way (with simpler calculations). In particular, the explicit formulas for the solution shows that both $\boldsymbol{\psi}_0(\boldsymbol{t})$ and $\boldsymbol{\psi}'(\boldsymbol{t})$ are bounded and $\nabla\boldsymbol{\psi}_0 \in L^2(\mathbb{R}^k;\mathbb{R}^{k\times k})$ and $\nabla\boldsymbol{\psi}' \in L^2(\mathbb{R}^k;\mathbb{R}^{d-k\times k})$. Hence, the corresponding test function $\boldsymbol{\phi} \in \widetilde{\mathcal{C}}_k$, and our general theory applies.

Remark 5.3. *The tensor* $\langle \mathsf{K}_{\mathsf{C}_-}(\boldsymbol{n})\rangle_{\boldsymbol{a}}$ *has the property that*

$$\mathsf{S} = \langle \mathsf{K}_{\mathsf{C}_-}(\boldsymbol{n})\rangle_{\boldsymbol{a}}\mathsf{C}_-$$

is the Eshelby tensor [40] for the ellipsoidal inhomogeneity relating the eigenstrain $\boldsymbol{\varepsilon}^* = [\![\mathsf{C}^{-1}]\!]\boldsymbol{\sigma}^+$ *and the inhomogeneity strain* $\boldsymbol{\varepsilon}^d = \boldsymbol{\varepsilon}^+ - \boldsymbol{\varepsilon}^\infty$.

Theorem 5.2 provides a relation between the strain at infinity and the uniform field in the inclusion. For instance, the explicit Fourier space representation of the field in the exterior of the inclusion can be written as

$$\widehat{e(\boldsymbol{u})}(\boldsymbol{\omega}) = -\widehat{\chi}(\boldsymbol{\omega})\mathsf{K}_{\mathsf{C}_-}(\boldsymbol{\omega})[\![\mathsf{C}]\!]\boldsymbol{\varepsilon}^+, \qquad \widehat{\nabla\boldsymbol{v}}(\boldsymbol{\omega}) = -\frac{[\![\mu]\!]}{\mu_-}\widehat{\chi}(\boldsymbol{\omega})\boldsymbol{e}^+\Gamma(\boldsymbol{\omega}).$$

For our purposes, however, we would only need the relations (5.5) and (5.6).

5.1.2 Noether-Eshelby equations

In this problem the Noether-Eshelby equation provides additional conditions only at the discontinuities of $\nabla\boldsymbol{\phi}$ and reduces to the Maxwell relation (4.21). In [78] Kublanov and Freidin studied the ellipsoidal inclusions in $3D$ space that satisfy the Maxwell condition, where they also computed the Eshelby tensor explicitly for such ellipsoids. Here we generalize some of their results to elliptical cylinders with arbitrary dimension k of cross-section in $\mathbb{R}^d$.

In [56] we have shown that the Maxwell relation for the energy (5.1) takes the form

$$[\![w]\!] + \frac{1}{2}([\![\mathsf{C}]\!]\boldsymbol{\varepsilon}_+,\boldsymbol{\varepsilon}_+) + \frac{1}{2}(\mathsf{K}_{\mathsf{C}_-}(\boldsymbol{n})\boldsymbol{q}_+,\boldsymbol{q}_+) = 0, \tag{5.7}$$

where $\boldsymbol{q}_+ = -[\![\mathsf{C}]\!]\boldsymbol{\varepsilon}_+$ and $\boldsymbol{n}$ is the outward unit normal on the boundary of the inclusion. For isotropic materials $\mathsf{C}_\pm$ we can choose the coordinate axes aligned with the ellipsoid's principal directions and the generators of the elliptical cylinder. In that case the normal $\boldsymbol{n}$ has the last $d-k$ components equal to zero, while the first k components form an element of the unit sphere $\mathbb{S}^{k-1}$. We will denote this $\boldsymbol{n} \in \mathbb{S}^{k-1}$ for short. It will be convenient to write the matrix $\boldsymbol{q}_+$ in the block form

$$\boldsymbol{q}_+ = \begin{bmatrix} \boldsymbol{q}_0 & \boldsymbol{p}^T \\ \boldsymbol{p} & \boldsymbol{q}' \end{bmatrix},$$

where $\boldsymbol{q}_0$ is $k \times k$, $\boldsymbol{p}$ is $(d-k)\times k$ and $\boldsymbol{q}'$ is $(d-k)\times(d-k)$. Hence, the Maxwell relation (5.7) becomes

$$\frac{|\boldsymbol{q}_0\boldsymbol{n}|^2 + |\boldsymbol{p}\boldsymbol{n}|^2}{\mu_-} - \frac{(\lambda_- + \mu_-)(\boldsymbol{q}_0\boldsymbol{n},\boldsymbol{n})^2}{\mu_-(\lambda_- + 2\mu_-)} + [\![\lambda]\!](\operatorname{Tr}\boldsymbol{\varepsilon}_+)^2 + 2[\![\mu]\!]|\boldsymbol{\varepsilon}_+|^2 + 2[\![w]\!] = 0 \tag{5.8}$$

for all $\boldsymbol{n} \in \mathbb{S}^{k-1}$.

LEMMA **5.4.** *Let $\alpha \neq 0$. The function*

$$f(\boldsymbol{n}) = |\boldsymbol{q}_0\boldsymbol{n}|^2 + |\boldsymbol{p}\boldsymbol{n}|^2 - \alpha(\boldsymbol{q}_0\boldsymbol{n}, \boldsymbol{n})^2$$

is constant on $\mathbb{S}^{k-1}$ if and only if $\boldsymbol{q}_0 = q_0\boldsymbol{I}_k$ and $\boldsymbol{p}^T\boldsymbol{p} = p_0^2\boldsymbol{I}_k$. In particular, this implies that $\boldsymbol{p} = \boldsymbol{0}$, if $k > d/2$.

Proof. Let

$$f(\boldsymbol{n}) = f_1(\boldsymbol{n}) + f_2(\boldsymbol{n}) - \alpha f_3(\boldsymbol{n}),$$

where

$$f_1(\boldsymbol{n}) = (\boldsymbol{q}_0^2\boldsymbol{n}, \boldsymbol{n}), \quad f_2(\boldsymbol{n}) = (\boldsymbol{p}^T\boldsymbol{p}\boldsymbol{n}, \boldsymbol{n}), \quad f_3(\boldsymbol{n}) = (\boldsymbol{q}_0\boldsymbol{n}, \boldsymbol{n})^2.$$

The function $f(\boldsymbol{n})$ is constant on the sphere $\mathbb{S}^{k-1}$ if and only if its differential is zero on at any $\boldsymbol{n} \in \mathbb{S}^{k-1}$. Let $\boldsymbol{n}_0$ be an eigenvector of $\boldsymbol{q}_0$ (and therefore of $\boldsymbol{q}_0^2$). Then $df_1(\boldsymbol{n}_0) = df_3(\boldsymbol{n}_0) = 0$. Hence, we must have $df_3(\boldsymbol{n}_0) = 0$. Therefore, $\boldsymbol{n}_0$ must be an eigenvector of $\boldsymbol{p}^T\boldsymbol{p}$. Hence, $\boldsymbol{q}_0$ and $\boldsymbol{p}^T\boldsymbol{p}$ have a common orthonormal eigen-basis. Suppose, $\boldsymbol{n}_1$ and $\boldsymbol{n}_2$ are orthogonal unit eigenvectors corresponding to the eigenvalues ν_1 and ν_2 of $\boldsymbol{q}_0$ and eigenvalues τ_1 and τ_2 of $\boldsymbol{p}^T\boldsymbol{p}$. Let $\phi(\theta) = f(\boldsymbol{n}_1\cos\theta + \boldsymbol{n}_2\sin\theta)$. We compute

$$\phi(\theta) = (\nu_1^2 + \tau_1)\cos^2\theta + (\nu_2 + \tau_2)\sin^2\theta - \alpha(\nu_1\cos^2\theta + \nu_2\sin^2\theta)^2.$$

Now it is easy to see that $\phi(\theta)$ is constant if and only if $\nu_1 = \nu_2$ and $\tau_1 = \tau_2$. We conclude that both $\boldsymbol{q}_0$ and $\boldsymbol{p}^T\boldsymbol{p}$ must be multiples of the identity, since the pair of eigenvectors was chosen arbitrarily. Conversely, if $\boldsymbol{q}_0 = q_0\boldsymbol{I}_k$ and $\boldsymbol{p}^T\boldsymbol{p} = p_0^2\boldsymbol{I}_k$ then $f(\boldsymbol{n}) = (1-\alpha)q_0^2 + p_0^2$. ☐

The assumption (5.2) ensures applicability of the lemma to (5.8). We conclude that

$$\boldsymbol{\varepsilon}_+ = \begin{bmatrix} e(\boldsymbol{\psi}_0^+) + \boldsymbol{\varepsilon}_0 & \frac{1}{2}(\nabla\boldsymbol{\psi}'_+)^T + \boldsymbol{E}^T \\ \frac{1}{2}\nabla\boldsymbol{\psi}'_+ + \boldsymbol{E} & \boldsymbol{\varepsilon}' \end{bmatrix} = \begin{bmatrix} \varepsilon_0^+\boldsymbol{I}_k & \boldsymbol{E}_+^T \\ \boldsymbol{E}_+ & \boldsymbol{\varepsilon}'_+ \end{bmatrix}, \qquad \boldsymbol{E}_+^T\boldsymbol{E}_+ = E_0^2\boldsymbol{I}_k, \tag{5.9}$$

where the scalars ε_0^+ and E_0 satisfy the Maxwell relation

$$\frac{([\![k\lambda + 2\mu]\!]\varepsilon_0^+ + [\![\lambda]\!]\mathrm{Tr}\,\boldsymbol{\varepsilon}')^2}{\lambda_- + 2\mu_-} + [\![\lambda]\!](\varepsilon_0^+ k + \mathrm{Tr}\,\boldsymbol{\varepsilon}')^2 + 2k[\![\mu]\!](\varepsilon_0^+)^2 + \frac{4[\![\mu]\!](k\mu_- + [\![\mu]\!])}{\mu_-}E_0^2 + 2[\![\mu]\!]|\boldsymbol{\varepsilon}'|^2 + 2[\![w]\!] = 0. \tag{5.10}$$

Applying Theorem 5.2 to (5.3) and using (5.9) we obtain

$$\begin{cases} \boldsymbol{\varepsilon}_0 = \varepsilon_0^+\boldsymbol{I}_k + \dfrac{\varepsilon_0^+[\![k\lambda + 2\mu]\!] + [\![\lambda]\!]\mathrm{Tr}\,\boldsymbol{\varepsilon}'}{\lambda_- + 2\mu_-}\langle\Gamma(\boldsymbol{n})\rangle_{\boldsymbol{a}}, \\ \boldsymbol{E} = \boldsymbol{E}_+\left(\boldsymbol{I}_k + \dfrac{[\![\mu]\!]}{\mu_-}\langle\Gamma(\boldsymbol{n})\rangle_{\boldsymbol{a}}\right). \end{cases} \tag{5.11}$$

We note that the explicit expressions for $\langle\Gamma(\boldsymbol{n})\rangle_{\boldsymbol{a}}$ is available for $k=1$ ($\langle\Gamma(\boldsymbol{n})\rangle_{\boldsymbol{a}}=1$), $k=2$ ($\langle\Gamma(\boldsymbol{n})\rangle_{\boldsymbol{a}}=\mathrm{cof}(\boldsymbol{a})/\mathrm{Tr}\,\boldsymbol{a}$) and $k=3$, when it can be expressed in terms of the elliptic integrals. However, we do not need to know $\langle\Gamma(\boldsymbol{n})\rangle_{\boldsymbol{a}}$ explicitly, we only need the set of diagonal matrices

$$\mathcal{G}=\{\langle\Gamma(\boldsymbol{n})\rangle_{\boldsymbol{a}}:\boldsymbol{a}=\mathrm{diag}(a_1,\ldots,a_k),\ a_i>0,\ i=1,\ldots,k\}.$$

Lemma **5.5.**

$$\mathcal{G}=\{\boldsymbol{A}=\mathrm{diag}(A_1,\ldots,A_k),\ A_i>0,\ i=1,\ldots,k,\ \mathrm{Tr}\,\boldsymbol{A}=1\}.$$

The proof of the lemma is in the Appendix G.

We now apply Lemma 5.5 by taking the trace of the first equation in (5.11). We obtain

$$\varepsilon_0^+=\frac{(\lambda_-+2\mu_-)\mathrm{Tr}\,\boldsymbol{\varepsilon}_0-[\![\lambda]\!]\mathrm{Tr}\,\boldsymbol{\varepsilon}'}{k\lambda_++2k\mu_-+2[\![\mu]\!]}. \tag{5.12}$$

The denominator in (5.12) is positive if either $[\![\lambda]\!]>0$ or $[\![\mu]\!]<0$. It could change sign if $[\![\lambda]\!]<0$ and $[\![\mu]\!]>0$. We therefore place the material with larger λ or smaller μ inside the inclusion. In the well-ordered case ($\lambda_+>\lambda_-$, $\mu_+>\mu_-$) , either material can be placed inside the inclusion, while in the non well-ordered case only the material with larger λ and smaller μ can be placed inside.

5.1.3 Optimal orientation

In our example the optimal orientation equation (4.13) becomes

$$\boldsymbol{Q}\int_{\mathbb{R}^k}(\mathsf{C}(\boldsymbol{t})(\boldsymbol{\varepsilon}^\infty+e(\boldsymbol{\phi}))-\mathsf{C}_-\boldsymbol{\varepsilon}^\infty)\nabla\boldsymbol{\psi}d\boldsymbol{t}=\boldsymbol{0}. \tag{5.13}$$

We can rewrite the left-hand side in (5.13) as the sum of two terms T_1 and T_2

$$T_1=\boldsymbol{Q}\int_{\mathbb{R}^k}\chi(\boldsymbol{t})([\![\mathsf{C}]\!]\boldsymbol{\varepsilon}^\infty)\nabla\boldsymbol{\psi}d\boldsymbol{t},\qquad T_2=\boldsymbol{Q}\int_{\mathbb{R}^k}(\mathsf{C}(\boldsymbol{t})e(\boldsymbol{\phi}))\nabla\boldsymbol{\psi}d\boldsymbol{t}.$$

We compute

$$T_1=\left(2[\![\mu]\!]\boldsymbol{E}\nabla\boldsymbol{\psi}_0^++[\![\lambda]\!](\mathrm{Tr}\,\boldsymbol{\varepsilon}_0+\mathrm{Tr}\,\boldsymbol{\varepsilon}')\nabla\boldsymbol{\psi}'_++2[\![\mu]\!]\boldsymbol{\varepsilon}'\nabla\boldsymbol{\psi}'_+\right)\int_{\mathbb{R}^k}\chi(\boldsymbol{t})d\boldsymbol{t}.$$

$$T_2=\int_{\mathbb{R}^k}\{\mu(\boldsymbol{t})\nabla\boldsymbol{\psi}'\nabla\boldsymbol{\psi}_0+\lambda(\boldsymbol{t})(\nabla\cdot\boldsymbol{\psi}_0)\nabla\boldsymbol{\psi}'\}d\boldsymbol{t}.$$

Using integration by parts we can rewrite T_2 as

$$T_2=-\int_{\mathbb{R}^k}\boldsymbol{\psi}'\otimes\nabla\cdot(\mathsf{C}(\boldsymbol{t})e(\boldsymbol{\psi}_0))d\boldsymbol{t}+\int_{\mathbb{R}^k}\nabla\cdot(\mu(\boldsymbol{t})\nabla\boldsymbol{\psi}')\otimes\boldsymbol{\psi}_0d\boldsymbol{t}.$$

Using equations (5.3) we get

$$\nabla \cdot (\mathsf{C}(\boldsymbol{t})e(\boldsymbol{\psi}_0)) = -\nabla \cdot (\chi(\boldsymbol{t})[\![\mathsf{C}]\!]\widehat{\boldsymbol{\varepsilon}}_0), \qquad \nabla \cdot (\mu(\boldsymbol{t})\nabla\boldsymbol{\psi}') = -2[\![\mu]\!]\nabla \cdot (\chi(\boldsymbol{t})\boldsymbol{E}),$$

where

$$\widehat{\boldsymbol{\varepsilon}}_0 = \boldsymbol{\varepsilon}_0 + \frac{[\![\lambda]\!]\mathrm{Tr}\,\boldsymbol{\varepsilon}'}{k[\![\lambda]\!] + 2[\![\mu]\!]}\boldsymbol{I}_k.$$

Thus, we obtain

$$T_2 = \int_{\mathbb{R}^k} \chi(\boldsymbol{t})\{-\nabla\boldsymbol{\psi}'([\![\mathsf{C}]\!]\widehat{\boldsymbol{\varepsilon}}_0) + 2[\![\mu]\!]\boldsymbol{E}(\nabla\boldsymbol{\psi}_0)^T\}d\boldsymbol{t}.$$

Computing $[\![\mathsf{C}]\!]\widehat{\boldsymbol{\varepsilon}}_0$ and combining with T_1 we write (5.13) as

$$\boldsymbol{E}e(\boldsymbol{\psi}_0^+) + \frac{1}{2}\boldsymbol{\varepsilon}'\nabla\boldsymbol{\psi}'_+ - \frac{1}{2}\nabla\boldsymbol{\psi}'_+\boldsymbol{\varepsilon}_0 = \mathbf{0}. \tag{5.14}$$

Substituting the values

$$e(\boldsymbol{\psi}_0^+) = \varepsilon_0^+\boldsymbol{I}_k - \boldsymbol{\varepsilon}_0, \qquad \frac{1}{2}\nabla\boldsymbol{\psi}'_+ = \boldsymbol{E}_+ - \boldsymbol{E},$$

obtained from (5.9), into (5.14) we get

$$(\varepsilon_0^+\boldsymbol{I}_k - \boldsymbol{\varepsilon}')\boldsymbol{E} = \boldsymbol{E}_+\boldsymbol{\varepsilon}_0 - \boldsymbol{\varepsilon}'\boldsymbol{E}_+. \tag{5.15}$$

Substituting the second equation in (5.11) into (5.15) we obtain

$$\frac{[\![\mu]\!]}{\mu_-}(\varepsilon_0^+\boldsymbol{I}_k - \boldsymbol{\varepsilon}')\boldsymbol{E}_+\langle\Gamma(\boldsymbol{n})\rangle_{\boldsymbol{a}} = \boldsymbol{E}_+(\boldsymbol{\varepsilon}_0 - \varepsilon_0^+\boldsymbol{I}_k).$$

Applying the first equation in (5.11) and the invertibility of $\langle\Gamma(\boldsymbol{n})\rangle_{\boldsymbol{a}}$ we finally conclude

$$[(\lambda_-[\![\mu]\!] - k\mu_-[\![\lambda]\!])\varepsilon_0^+ - \mu_-[\![\lambda]\!]\mathrm{Tr}\,\boldsymbol{\varepsilon}']\boldsymbol{E}_+ = (\lambda_- + 2\mu_-)[\![\mu]\!]\boldsymbol{\varepsilon}'\boldsymbol{E}_+. \tag{5.16}$$

The equations (5.9) and (5.16) say that, provided $E_0 \neq 0$, the k columns of the $(d-k)\times k$ matrix $\boldsymbol{E}_+/E_0$ are orthonormal eigenvectors of the $(d-k)\times(d-k)$ matrix $\boldsymbol{\varepsilon}'$. All of them correspond to the same eigenvalue

$$\nu = \frac{(\lambda_-[\![\mu]\!] - k\mu_-[\![\lambda]\!])\varepsilon_0^+ - \mu_-[\![\lambda]\!]\mathrm{Tr}\,\boldsymbol{\varepsilon}'}{(\lambda_- + 2\mu_-)[\![\mu]\!]}. \tag{5.17}$$

5.1.4 Explicit bounds

If $E_0 = 0$ then $\boldsymbol{E}_+ = \mathbf{0}$ and the relation (5.16) is identically satisfied. In that case the equation for the sets $\mathfrak{N}_k^{\mathrm{ell}}$ introduced in Definition 5.1 is provided by the relation (5.10), which becomes

$$\frac{(\lambda_- + 2\mu_-)([\![k\lambda + 2\mu]\!]\mathrm{Tr}\,\boldsymbol{\varepsilon}_0 + k[\![\lambda]\!]\mathrm{Tr}\,\boldsymbol{\varepsilon}')^2}{[\![k\lambda + 2\mu]\!](k\lambda_+ + 2k\mu_- + 2[\![\mu]\!])} + \frac{2[\![\lambda]\!][\![\mu]\!](\mathrm{Tr}\,\boldsymbol{\varepsilon}')^2}{[\![k\lambda + 2\mu]\!]} + 2[\![\mu]\!]|\boldsymbol{\varepsilon}'|^2 + 2[\![w]\!] = 0. \tag{5.18}$$

Equation (5.18) provides a characterization of the union of $\binom{d}{k}$ surfaces in the space of eigenvalues of $\boldsymbol{\varepsilon}$. Different surfaces in this union are obtained by choosing k of the d eigenvalues of $\boldsymbol{\varepsilon}$ forming the diagonal of the $k \times k$ diagonal matrix $\boldsymbol{\varepsilon}_0$. Another union of $\binom{d}{k}$ surfaces are obtained by exchanging "+" and "−" subscripts in (5.18). The entire collection of $2\binom{d}{k}$ surfaces comprises the part of the set $\mathfrak{N}_k^{\rm ell}$ corresponding to $E_0 = 0$.

If $E_0 \neq 0$, then the optimality of orientation condition (5.16) requires $\boldsymbol{\varepsilon}'$ to have k equal eigenvalues. Together with the relation (5.10) this places $\boldsymbol{\varepsilon}$ on a co-dimension k surface in $\mathrm{Sym}(\mathbb{R}^d)$. Such surfaces cannot be candidates for the binodal when $k > 1$ and are therefore discarded, leaving only the case $k = 1$. In this case $\langle \Gamma(\boldsymbol{n}) \rangle_{\boldsymbol{a}} = 1$ and the matrices $\boldsymbol{E}$ and $\boldsymbol{E}_+$ are vectors in $\mathbb{R}^{d-1}$, related via (5.11)

$$\boldsymbol{E} = \frac{\mu_+}{\mu_-}\boldsymbol{E}_+. \tag{5.19}$$

If we choose one of the coordinate axes to be aligned with $\boldsymbol{E}$ then, according to (5.16), $\boldsymbol{\varepsilon}$ must have the following structure

$$\boldsymbol{\varepsilon} = \begin{bmatrix} \varepsilon_0 & \frac{\mu_+}{\mu_-}E_0 & \mathbf{0} \\ \frac{\mu_+}{\mu_-}E_0 & \nu & \mathbf{0} \\ \mathbf{0} & \mathbf{0} & \boldsymbol{\varepsilon}'' \end{bmatrix}, \tag{5.20}$$

where ν is given by (5.17) with $k = 1$. Writing it in terms of ε_0 and $\boldsymbol{\varepsilon}''$, using (5.12) we obtain

$$\nu = \frac{(\lambda_- [\![\mu]\!] - \mu_- [\![\lambda]\!])\varepsilon_0 - \mu_+ [\![\lambda]\!] \mathrm{Tr}\,\boldsymbol{\varepsilon}''}{\mu_+ [\![\lambda + 2\mu]\!] + \lambda_+ [\![\mu]\!]}. \tag{5.21}$$

In order to write the equation for $\mathfrak{N}_1^{\rm ell}$ in terms of the eigenvalues of $\boldsymbol{\varepsilon}$ we introduce the notation

$$\boldsymbol{\varepsilon}_1 = \begin{bmatrix} \varepsilon_0 & \frac{\mu_+}{\mu_-}E_0 \\ \frac{\mu_+}{\mu_-}E_0 & \nu \end{bmatrix}.$$

The eigenvalues of $\boldsymbol{\varepsilon}$ are split into two groups: the group of $d-2$ eigenvalues, comprising the diagonal of $\boldsymbol{\varepsilon}''$, and the group containing the two eigenvalues of $\boldsymbol{\varepsilon}_1$. It will be convenient to introduce variables

$$X = \frac{\mathrm{Tr}\,\boldsymbol{\varepsilon}_1}{\sqrt{2}}, \qquad Y^2 = \frac{1}{2}((\mathrm{Tr}\,\boldsymbol{\varepsilon}_1)^2 - 4\det\boldsymbol{\varepsilon}_1), \qquad Z = \frac{\mathrm{Tr}\,\boldsymbol{\varepsilon}''}{\sqrt{2}},$$

which are well-known functions of the eigenvalues. Then the formula (5.12) becomes

$$\varepsilon_0^+ = \frac{(\mu_- [\![\lambda + 2\mu]\!] + \lambda_- [\![\mu]\!])\varepsilon_0 - \sqrt{2}[\![\lambda]\!][\![\mu]\!] Z}{\mu_+ [\![\lambda + 2\mu]\!] + \lambda_+ [\![\mu]\!]}. \tag{5.22}$$

From the equation $\varepsilon_0 + \nu = \operatorname{Tr} \boldsymbol{\varepsilon}_1$ we find

$$\varepsilon_0 = \frac{(\mu_+ [\![\lambda + 2\mu]\!] + \lambda_+ [\![\mu]\!])X + \mu_+ [\![\lambda]\!] Z}{\sqrt{2}[\![\mu]\!](\lambda_+ + \mu_+)}. \tag{5.23}$$

We also have

$$2E_0^2 = \left(\frac{\mu_-}{\mu_+}\right)^2 \left(Y^2 - \left(\mu_+ \frac{[\![\lambda + \mu]\!] X + [\![\lambda]\!] Z}{[\![\mu]\!](\lambda_+ + \mu_+)}\right)^2\right). \tag{5.24}$$

If we now substitute (5.21), (5.22) and (5.24) into (5.10), taking into account (5.23), we obtain a representation for the $E_0 \neq 0$ part of $\mathfrak{N}_1^{\text{ell}}$ in terms of the eigenvalues of $\boldsymbol{\varepsilon}$:

$$\frac{(\lambda_- + \mu_-)[\![\lambda + \mu]\!]}{\lambda_+ + \mu_+} X^2 + 2\frac{(\lambda_- + \mu_-)[\![\lambda]\!]}{\lambda_+ + \mu_+} XZ + \frac{[\![\lambda]\!](\lambda_- + \mu_+)}{\lambda_+ + \mu_+} Z^2 + \frac{[\![\mu]\!]\mu_-}{\mu_+} Y^2 + [\![\mu]\!] |\boldsymbol{\varepsilon}''|^2 = -[\![w]\!]. \tag{5.25}$$

We interpret (5.25) as the union of $\binom{d}{2}$ surfaces. Each of these surfaces is characterized by two (out of d) eigenvalues corresponding to $\boldsymbol{\varepsilon}_1$. Another union of $\binom{d}{2}$ surfaces is obtained from (5.25) by interchanging "+" and "−" subscripts in the well-ordered case. The entire collection of $2\binom{d}{2}$ surfaces comprises the part of the set $\mathfrak{N}_1^{\text{ell}}$ corresponding to $E_0 \neq 0$.

When $k > 1$ (and hence $E_0 = 0$), we have only used the fact that $\operatorname{Tr} \langle \Gamma(\boldsymbol{n}) \rangle_{\boldsymbol{a}} = 1$. The positive definiteness of $\langle \Gamma(\boldsymbol{n}) \rangle_{\boldsymbol{a}}$ gives us the validity domain for the equation (5.18). Substituting (5.12) into (5.11) and solving for $\langle \Gamma(\boldsymbol{n}) \rangle_{\boldsymbol{a}}$ we obtain

$$\frac{(\lambda_- + 2\mu_-)\boldsymbol{I}_k}{k\lambda_+ + 2k\mu_- + 2[\![\mu]\!]} \leq \frac{[\![k\lambda + 2\mu]\!]\boldsymbol{\varepsilon}_0 + [\![\lambda]\!](\operatorname{Tr} \boldsymbol{\varepsilon}')\boldsymbol{I}_k}{[\![k\lambda + 2\mu]\!] \operatorname{Tr} \boldsymbol{\varepsilon}_0 + k[\![\lambda]\!] \operatorname{Tr} \boldsymbol{\varepsilon}'} \leq \frac{(\lambda_- + 2\mu_+ + k[\![\lambda]\!])\boldsymbol{I}_k}{k\lambda_+ + 2k\mu_- + 2[\![\mu]\!]}. \tag{5.26}$$

This statement is equivalent to the inequalities $\mathbf{0} \leq \langle \Gamma(\boldsymbol{n}) \rangle_{\boldsymbol{a}} \leq \boldsymbol{I}_k$ understood in the sense of quadratic forms.

It is easy to check that the upper bound in (5.26) is a consequence of the lower bound, due to the fact that

$$\frac{\lambda_- + 2\mu_-}{k\lambda_+ + 2k\mu_- + 2[\![\mu]\!]} > 0,$$

and we conclude that for $k > 1$ (5.18) is the equation of $\mathfrak{N}_k^{\text{ell}}$, provided

$$\frac{[\![k\lambda + 2\mu]\!]\boldsymbol{\varepsilon}_0 + [\![\lambda]\!](\operatorname{Tr} \boldsymbol{\varepsilon}')\boldsymbol{I}_k}{[\![k\lambda + 2\mu]\!] \operatorname{Tr} \boldsymbol{\varepsilon}_0 + k[\![\lambda]\!] \operatorname{Tr} \boldsymbol{\varepsilon}'} \geq \frac{(\lambda_- + 2\mu_-)\boldsymbol{I}_k}{k\lambda_+ + 2k\mu_- + 2[\![\mu]\!]} \tag{5.27}$$

in the sense of quadratic forms. Equation (5.18) and inequality (5.27) reduce to the results of Kublanov and Freidin [78], when $k = d = 3$.

If the materials are well-ordered, we may interchange the materials (i.e. consider an inclusion of phase "−" in the matrix of phase "+"). In that case the inequalities in (5.26) and (5.27) are reversed, while the subscripts "+" and "−" are interchanged.

Notice that when $k = 1$ we have $\langle \Gamma(\boldsymbol{n}) \rangle_{\boldsymbol{a}} = 1$ and there are no extra inequalities in the case $E_0 = 0$. However, when $E_0 \neq 0$, equation (5.24) implies that the values of the variables (X, Y, Z) must satisfy

$$|Y| \geq \mu_+ \left| \frac{[\![\lambda + \mu]\!] X + [\![\lambda]\!] Z}{[\![\mu]\!](\lambda_+ + \mu_+)} \right| \tag{5.28}$$

This is the range of the validity of equation (5.25).

Let us verify that all solutions to (4.12) satisfy the non-degeneracy condition (4.26) of Corollary 4.7. An easy calculation shows that

$$W^{\circ}_{\boldsymbol{\varepsilon}}(\boldsymbol{\varepsilon}, e(\boldsymbol{\psi})) = [\![\mathsf{C}]\!]\boldsymbol{\varepsilon}^{+}\chi(\boldsymbol{t}). \tag{5.29}$$

Hence, $\partial J_k(\boldsymbol{F}, \boldsymbol{\phi})/\partial \boldsymbol{F} = \boldsymbol{0}$ if and only if $\boldsymbol{\varepsilon}^{+} = \boldsymbol{0}$. However, $\boldsymbol{\varepsilon}^{+} = \boldsymbol{0}$ contradicts (5.10).

Remark 5.6. *It will be shown in [56] that the surface patch $\mathfrak{N}_2^{ell}$ given by (5.18), (5.26) is indeed a part of the binodal when $\mathrm{d} = 2$. If we choose $\boldsymbol{F} \in \mathfrak{N}_2^{ell}$ and the corresponding elliptical inclusion, then the field $\boldsymbol{\varepsilon}^{\infty} + e(\boldsymbol{\phi})$ will stay strictly away from the singular boundaries of the quadratic energy wells[7]. Hence, if we choose $\widetilde{\boldsymbol{F}} \notin \overline{\mathfrak{B}}$ sufficiently close to $\boldsymbol{F}$ and solve (5.30) then the solution will also be a nontrivial solution of $(4.12)_1$, with $W(\boldsymbol{F})$ given by (5.1). Therefore, the "bifurcation" in $(4.12)_1$ alone is not sufficient to obtain any bounds on the binodal region.*

5.2 Interacting cylindrical inclusions

In this section we give an example of the test field $\boldsymbol{\phi} \in \mathcal{C}_1 \setminus \widetilde{\mathcal{C}}_1$ satisfying (4.12)–(4.13). More specifically, we construct a 1-parameter family of energetically equivalent $\mathcal{C}_1$ test fields interpolating between the $\mathcal{C}_2$ test fields (corresponding to elliptical inclusions) and the rank-two laminates discussed in Section 3.2.3.

5.2.1 Euler-Lagrange equations

We are looking for equilibrium configurations where the materials "+" and "−" occupy complementary subdomains Ω_+ and Ω_- that are periodic with period 1 in y-direction. We further assume that the material "+" occupies a compact subset in the fundamental region $Y_1 = \mathbb{R} \times [-1/2, 1/2]$ with smooth boundary Σ. The first equation in (4.12) is

$$\nabla \cdot \big(\mathsf{C}(\boldsymbol{x})e(\boldsymbol{u})\big) = \boldsymbol{0}, \qquad \boldsymbol{x} \in \mathbb{R}^2, \tag{5.30}$$

understood in the sense of distributions. Here

$$e(\boldsymbol{u})_{ij} = \frac{1}{2}\left(\frac{\partial u_i}{\partial x_j} + \frac{\partial u_j}{\partial x_i}\right).$$

The equation (5.30) can be written as the standard Lamé system in $\Omega_{\pm}$ together with the interface conditions

$$[\![\boldsymbol{u}]\!] = \boldsymbol{0}, \qquad [\![\mathsf{C}e(\boldsymbol{u})]\!]\boldsymbol{n} = \boldsymbol{0}, \qquad \boldsymbol{x} \in \Sigma. \tag{5.31}$$

[7] By the regularity of the quasicovex envelope theorem [16] the optimal fields must stay strictly away from the singularities of $W(\boldsymbol{F})$. However, our results cannot guarantee that the field $\boldsymbol{\varepsilon}^{\infty} + e(\boldsymbol{\phi})$ is indeed optimal.

The method of complex potentials [99] allows one to characterize the set of solutions to (5.30)–(5.31) completely in 2D. Accordingly, the vector $\boldsymbol{u} = (u_1, u_2) \in \mathbb{R}^2$ is written as a complex number $u = u_1 + iu_2$. If $\boldsymbol{u}$ solves the Lamé system then

$$u(z) = A\phi(z) - B(\overline{\psi}(z) + z\overline{\Phi}(z)), \tag{5.32}$$

where

$$\Phi(z) = \phi'(z), \qquad A = \frac{1}{\kappa} + \frac{1}{2\mu}, \qquad B = \frac{1}{2\mu}.$$

Also, any 2×2 matrix $\boldsymbol{M}$ can be written as a pair of complex numbers $\boldsymbol{M} = [p, q]$, according to the rule

$$\boldsymbol{M} = \begin{bmatrix} p_1 & -p_2 \\ p_2 & p_1 \end{bmatrix} + \begin{bmatrix} q_1 & q_2 \\ q_2 & -q_1 \end{bmatrix},$$

where $p = p_1 + ip_2$ and $q = q_1 + iq_2$. Then, the complex representation of the vector $\boldsymbol{Mv}$, $\boldsymbol{v} \in \mathbb{R}^2$, is $pv + q\bar{v}$, and

$$\nabla \boldsymbol{u} = \left[\frac{\partial u}{\partial z}, \frac{\partial u}{\partial \overline{z}}\right]. \tag{5.33}$$

Applying (5.33) to (5.32) we obtain $\nabla \boldsymbol{u} = [A\Phi - B\overline{\Phi}, -2B\overline{\Pi}]$, where

$$\Pi(z) = \frac{1}{2}(\Psi(z) + \overline{z}\Phi'(z)), \qquad \Psi(z) = \psi'(z).$$

We also obtain

$$e(\boldsymbol{u}) = \left[\frac{\mathfrak{Re}\Phi(z)}{\kappa}, -\frac{\overline{\Pi}(z)}{\mu}\right], \qquad \boldsymbol{\sigma} = [2\mathfrak{Re}\Phi(z), -2\overline{\Pi}(z)].$$

The continuity of displacements $[\![\boldsymbol{u}]\!] = \boldsymbol{0}$ can be conveniently written in differential form, via the representation (5.32):

$$[\![A\Phi - B\overline{\Phi}]\!]\dot{z} - 2[\![B\overline{\Pi}]\!]\dot{\overline{z}} = 0, \tag{5.34}$$

where $\dot{z}$ is the derivative of the parametrization $z(t)$ of the interface Γ. The continuity of tractions reads

$$[\![\mathfrak{Re}\Phi]\!]\dot{z} + [\![\overline{\Pi}]\!]\dot{\overline{z}} = 0, \tag{5.35}$$

since the complex representation of the unit normal $\boldsymbol{n}$ is $-i\dot{z}/|\dot{z}|$. In terms of the variables $\dot{z} = |\dot{z}|e^{i\alpha}$, $\Phi(z) = X$ and $\Pi(z)e^{2i\alpha} = Y$, the system (5.34)–(5.35) can be written as

$$\begin{cases} [\![AX - B\overline{X}]\!] - 2[\![B\overline{Y}]\!] = 0, \\ [\![\mathfrak{Re}X]\!] + [\![\overline{Y}]\!] = 0. \end{cases} \tag{5.36}$$

5.2.2 Noether-Eshelby equations

Under the assumptions of the smoothness of the interfaces the second equation in (4.12) can be replaced by the Maxwell relation (4.21), as discussed in Section 4.2.1.

$$[\![W]\!] - (\{\!\!\{ \mathsf{C}e(\boldsymbol{u})\}\!\!\}, [\![e(\boldsymbol{u})]\!]) = 0, \qquad \boldsymbol{x} \in \Sigma, \tag{5.37}$$

which in the X and Y variables we can be written as

$$[\![\frac{2}{\kappa}]\!]\mathfrak{Re}(X_+)\mathfrak{Re}(X_-) + [\![\frac{2}{\mu}]\!]\mathfrak{Re}(Y_+\overline{Y}_-) = [\![w]\!]. \tag{5.38}$$

5.2.3 Optimal orientation

In addition, the necessary condition (4.11), though not computable by itself, implies an easily verifiable additional condition (4.22), as discussed in Section 4.2.1. It can be written in terms of X, Y as

$$[\![\mathfrak{Re}X]\!][\![AX - B\overline{X}]\!] + 2[\![\mathfrak{Re}X]\!][\![B\overline{Y}]\!] + [\![\overline{Y}]\!][\![A\overline{X} - BX]\!] + 2[\![\overline{Y}]\!][\![B\overline{Y}]\!] = 0.$$

If we eliminate $[\![\overline{Y}]\!]$ and $[\![B\overline{Y}]\!]$ by means of (5.36) we obtain

$$[\![\mathfrak{Re}X]\!][\![(A+B)\mathfrak{Im}X]\!] = 0. \tag{5.39}$$

Hence, there are two possibilities. Either $[\![\mathfrak{Re}X]\!] = 0$, corresponding to $[\![\boldsymbol{\sigma}]\!] = \boldsymbol{0}$ or $[\![(A + B)\mathfrak{Im}X]\!] = 0$, corresponding to $\boldsymbol{a} = \lambda\boldsymbol{n}$ and $[\![\boldsymbol{\sigma}]\!] = \beta\boldsymbol{n}^\perp \otimes \boldsymbol{n}^\perp$ for some scalars λ and β.

Case $[\![\mathfrak{Re}X]\!] = 0$. In this case we get

$$\begin{cases} \mathfrak{Re}X_+ = \mathfrak{Re}X_- = \mathfrak{Re}X, \\ Y_+ = Y_- = [\![\frac{1}{\mu}]\!]^{-1}\left([\![\frac{1}{\kappa}]\!]\mathfrak{Re}X - i[\![\left(\frac{1}{\kappa}+\frac{1}{\mu}\right)\mathfrak{Im}X]\!]\right), \\ [\![\frac{1}{\kappa}]\!][\![\frac{1}{\kappa}+\frac{1}{\mu}]\!](\mathfrak{Re}X)^2 + [\![\left(\frac{1}{\kappa}+\frac{1}{\mu}\right)\mathfrak{Im}X]\!]^2 = \frac{1}{2}[\![\frac{1}{\mu}]\!][\![w]\!]. \end{cases} \tag{5.40}$$

Then, the function

$$f(z) = \begin{cases} \mathfrak{Re}\Phi_+(z), & z \text{ in } + \text{ region} \\ \mathfrak{Re}\Phi_-(z), & z \text{ in } - \text{ region} \end{cases}$$

is bounded and harmonic on $\mathbb{R}^2$. Hence, it is a constant. We conclude that $\Phi'_\pm(z) = 0$ and hence the functions $\mathfrak{Im}X_\pm$, and therefore $Y_\pm = \frac{1}{2}\Psi_\pm(z)\dot{z}/\dot{\overline{z}}$ are constants on Σ. Hence, we obtain $\psi_+(z) = 2Y_+\overline{z} + \gamma_+$ on Σ. By assumption region "+" contains a compact inclusion D with smooth boundary. Then we must have $Y_+ = 0$, since

$$0 = \int_{\partial D} \psi_+(z)dz = 4iY_+|D|. \tag{5.41}$$

This contradicts (5.40).

Case $[\![(A+B)\mathfrak{Im}X]\!]=0$. Then the function

$$f(z)=\begin{cases}\left(\dfrac{1}{\kappa_+}+\dfrac{1}{\mu_+}\right)\mathfrak{Im}\Phi_+(z), & z \text{ in } + \text{ region}\\ \left(\dfrac{1}{\kappa_-}+\dfrac{1}{\mu_-}\right)\mathfrak{Im}\Phi_-(z), & z \text{ in } - \text{ region}\end{cases}$$

must be both bounded and harmonic. Therefore, it is constant. Hence, $\Phi_\pm(z)$ is constant in the "$\pm$" region. We can assume without loss of generality, that $\Phi_-(z)$ is a real constant. Hence, $\Phi_+(z)$ is also a real constant. It follows from (5.36) that $Y_\pm$ are constants on Σ. By assumption, region "+" contains a compact inclusion D, then we must have $Y_+=0$ due to (5.41). Hence, from (5.36) we get

$$\mathfrak{Re}X_+=\frac{\kappa_+(\kappa_-+\mu_-)}{\kappa_-(\kappa_++\mu_-)}\mathfrak{Re}X_-,$$

while

$$X_-=\mathfrak{Re}\Phi_-(z)=\frac{1}{4}\mathrm{Tr}\,\boldsymbol{\sigma}_\infty=\frac{1}{2}\kappa_-\mathrm{Tr}\,\boldsymbol{\varepsilon}_\infty.$$

Substituting these relations into (5.38) we get

$$(\mathrm{Tr}\,\boldsymbol{\varepsilon}_\infty)^2=\frac{-2[\![w]\!](\mu_-+\kappa_+)}{[\![\kappa]\!](\kappa_-+\mu_-)}. \tag{5.42}$$

Hence, in terms of $\mathrm{Tr}\,\boldsymbol{\varepsilon}_\infty$ we obtain

$$\psi_+(z)=0,\quad \phi_+(z)=\frac{\kappa_+(\kappa_-+\mu_-)\mathrm{Tr}\,\boldsymbol{\varepsilon}_\infty}{2(\kappa_++\mu_-)}z,\quad \phi_-(z)=\frac{1}{2}(\mathrm{Tr}\,\boldsymbol{\varepsilon}_\infty)\kappa_-z. \tag{5.43}$$

We also have

$$\psi_-(z)=c\overline{z}+\gamma,\quad z\in\Sigma,\qquad c=\frac{\mu_-[\![k]\!]\mathrm{Tr}\,\boldsymbol{\varepsilon}_\infty}{\kappa_++\mu_-}. \tag{5.44}$$

The parameter γ is locally constant on Σ and can be chosen to be zero if Σ is connected. Observe that the trivial solution $\boldsymbol{u}=\boldsymbol{\varepsilon}_\infty\boldsymbol{x}$ corresponds to the complex potentials

$$\phi(z)=\frac{1}{2}(\mathrm{Tr}\,\boldsymbol{\varepsilon}_\infty)\kappa_-z,\qquad \psi(z)=bz,\qquad b=\mu_-(\varepsilon_\infty^{(22)}-\varepsilon_\infty^{(11)}-2i\varepsilon_\infty^{(12)}).$$

Hence, the function $p(z)=\psi_-(z)-bz$ must be i-periodic. Thus,

$$\psi_-(z+i)=\psi_-(z)+bi. \tag{5.45}$$

It is now easy to verify that the as yet unused condition (4.13) holds automatically for any solution of the Lamé system satisfying (5.43). In fact, we have $\widehat{\boldsymbol{P}}^*(z)=0$ for all z.

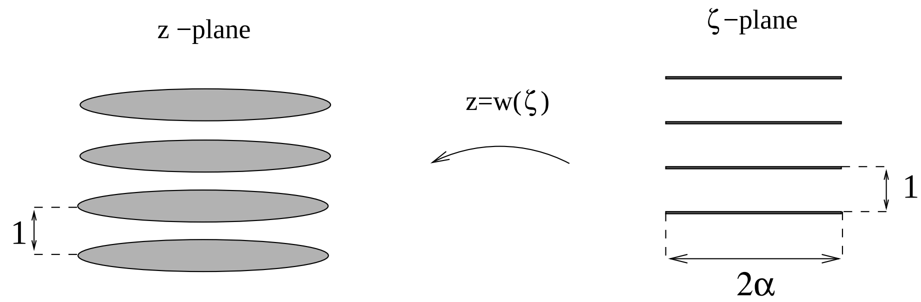

Figure 4: Conformal mapping of the exterior of the periodic array of slits onto the exterior of the periodic array of inclusions.

5.2.4 Optimal shapes

We are now in a position to look for i-periodic structure of inclusions satisfying (5.43) and (5.44). The analysis here is an adaptation of the analysis in [126, 127, 128, 129, 54] for the case of simply-periodic array of inclusions. Following [26, 54], we map the exterior of a periodic array of slits in the ζ plane conformally onto the region "$-$" in the z plane (see Figure 4). More precisely, let $z = w(\zeta)$ map the i-periodic array of slits

$$M_n = \{z = x + in : x \in [-\alpha, \alpha]\}, \quad n \in \mathbb{Z}$$

of length 2α (to be determined) in the ζ plane to the i-periodic array of inclusions with smooth boundary in the z plane. The map w must satisfy the following conditions:

$$w(\zeta + i) = w(\zeta) + i \tag{5.46}$$

At the endpoints of the slits $w(\zeta) = O(\sqrt{\zeta - \zeta_n})$ as $\zeta \to \zeta_n$, where $\zeta_n = \pm\alpha + in$ is an endpoint of the slit M_n, on account of the smoothness of the boundary of the inclusion in the z plane.

Let us now substitute $z = w(\zeta)$ in (5.44) and differentiate along the slit. Using notation $\Psi(\zeta) = \Psi_-(w(\zeta))$ we obtain:

$$\Psi(\zeta) w'(\zeta) = c\overline{w'}(\zeta), \quad \zeta \in M. \tag{5.47}$$

We can represent (5.47) using the following trick of Cherepanov [26]: Consider two analytic functions F and G chosen such that

$$F'(\zeta) = -\Psi(\zeta) w'(\zeta) + c w'(\zeta), \tag{5.48}$$

$$G'(\zeta) = -\Psi(\zeta) w'(\zeta) - c w'(\zeta). \tag{5.49}$$

Then (5.47) becomes

$$\left.\begin{aligned} \Re\mathrm{e} F'(\zeta) &= 0, \quad \zeta \in M_n, \\ \Im\mathrm{m} G'(\zeta) &= 0, \quad \zeta \in M_n. \end{aligned}\right\} \tag{5.50}$$

Besides (5.50) the analytic functions F and G have the following properties: they are i-periodic, since both $\Psi(\zeta)$ and $w(\zeta)$ are, and at the endpoints ζ_n of the slits M_n

$$F'(\zeta) = O(\frac{1}{\sqrt{\zeta - \zeta_n}}) \text{ and } G'(\zeta) = O(\frac{1}{\sqrt{\zeta - \zeta_n}}) \text{ as } \zeta \to \zeta_n; \tag{5.51}$$

also F' and G' are single valued and have no other singularities. Once such functions are found, using (5.48), (5.49) we can easily reconstruct $w(\zeta)$ and $\Psi(\zeta)$. The result is

$$w(\zeta) = \frac{1}{2c}(F(\zeta) - G(\zeta)) + C_0, \tag{5.52}$$

where C_0 is an arbitrary constant of integration, and

$$\Psi(\zeta) = -c\frac{F'(\zeta) + G'(\zeta)}{F'(\zeta) - G'(\zeta)}. \tag{5.53}$$

Now let's construct the functions F and G. Consider the function [26]

$$v(\zeta) = \sqrt{\frac{\cosh(2\pi\zeta) - 1}{\cosh(2\pi\zeta) - \lambda}}, \qquad \lambda = \cosh(2\pi\alpha). \tag{5.54}$$

We claim that $v(\zeta)$ has the following properties:

1. $v(\zeta)$ is single valued analytic function in the exterior of the periodic array of slits $\{M_n : n \in \mathbb{Z}\}$;

2. $v(\zeta)$ is i-periodic;

3. $v(\zeta) = O(\frac{1}{\sqrt{\zeta - \zeta_n}})$ as $\zeta \to \zeta_n$, and v is bounded everywhere else;

4. $\mathfrak{Re}(v(\zeta)) = 0$ on M_n.

To justify the claim we choose the branch of the square root such that $\sqrt{1} = 1$, with the branch cut along the negative real axis. Then the function $v(\zeta)$ has a branch cut wherever

$$\frac{\cosh(2\pi\zeta) - 1}{\cosh(2\pi\zeta) - \lambda} < 0. \tag{5.55}$$

This is equivalent to the condition that $\cosh(2\pi\zeta) \in (1, \lambda)$, which is satisfied only along the cuts M_n (this is how the function (5.54) was constructed). Thus, properties 1 and 4 are proved. Property 2 follows from the i-periodicity of $\cosh(2\pi\zeta)$. And property 3 follows from the fact that points ζ_n are simple points for $\cosh(2\pi\zeta)$ (the derivative $2\pi\sinh(2\pi\alpha) \neq 0$).

We look for the functions F' and G' in the form

$$\begin{cases} F' = r_1 v(\zeta) + id_1, \\ G' = ir_2 v(\zeta) + d_2, \end{cases} \tag{5.56}$$

where $r_j, d_j \in R$ are constants to be determined. It is easy to see that equations (5.50) are satisfied, as is the condition (5.51). In order to recover F and G from the above formulas we have to use the function

$$V(\zeta) = \int_{i/2}^{\zeta} v(z)dz. \tag{5.57}$$

This function is single valued in the exterior of the periodic system of the slits because $\oint_{\Gamma_R} v(\zeta)d\zeta = 0$, where Γ_R is a rectangle with vertexes $\pm R \pm i/2$. Indeed, the function $v(\zeta)$ is even and i-periodic. Therefore,

$$\int_{-R}^{R} v(x - i/2)dx = -\int_{R}^{-R} v(x + i/2)dx, \qquad i\int_{-1/2}^{1/2} v(R + iy)dy = -i\int_{1/2}^{-1/2} v(-R + iy)dy.$$

The i-periodicity of $v(\zeta)$ implies that $V(\zeta + i) - V(\zeta)$ is independent of ζ. Therefore,

$$V(\zeta + i) - V(\zeta) = \lim_{R\to\infty} i\int_{-1/2}^{1/2} v(R + iy)dy = i. \tag{5.58}$$

The periodicity condition (5.46) together with formulas (5.52), (5.56) and (5.58) implies

$$d_1 = r_2, \qquad r_1 - d_2 = 2c.$$

So that

$$w(\zeta) = rV(\zeta) + (1 - r)\zeta, \qquad r = \frac{r_1 - ir_2}{2c}. \tag{5.59}$$

Thus by (5.53)

$$\psi_2(w(\zeta)) = -c(\overline{r}V(\zeta) + (\overline{r} - 1)\zeta) + \text{const.} \tag{5.60}$$

Now using the translation law (5.45) for the potential ψ_- we obtain:

$$r = \frac{1}{2}(1 - \overline{q}), \qquad q = \frac{b}{c}. \tag{5.61}$$

We need to place further restriction on the value of parameter r (i.e. on $\boldsymbol{\varepsilon}_\infty$) so that the map $w(\zeta)$ given by (5.59) maps the exterior of the i-periodic array of slits $\{M_n : n \in \mathbb{Z}\}$ one-to-one and onto the exterior of the i-periodic array of inclusions $D_n = w(M_n)$. A necessary condition for univalence of $w(\zeta)$ is that $w'(\zeta) \neq 0$. In other words $v(\zeta) \neq (r - 1)/r$. The principal branch of the square root in (5.54) can take any value in the right half-plane $\mathfrak{Re}\, v \geq 0$. Hence, we require that $\mathfrak{Re}((r - 1)/r) < 0$. In other words $|r - 1/2| < 1/2$, or equivalently, $|q| < 1$, i.e.

$$|\varepsilon_\infty^{(22)} - \varepsilon_\infty^{(11)} - 2i\varepsilon_\infty^{(12)}|^2 < -\frac{2[\![w]\!][\![\kappa]\!]}{(\kappa_+ + \mu_-)(\kappa_- + \mu_-)}. \tag{5.62}$$

It is easy to show that $|q| < 1$ is also sufficient for univalence. Indeed, we only need to prove that $w(\zeta_1) \neq w(\zeta_2)$ for any $\zeta_1 \neq \zeta_2$, such that $\mathfrak{Im}(\zeta_j) \in (0, 1)$, $j = 1, 2$. Observe that we can connect the points ζ_1 and ζ_2 by straight line without crossing any slits. Thus, we can write

$$\frac{w(\zeta_1) - w(\zeta_2)}{\zeta_1 - \zeta_2} = 1 - r + r\int_0^1 v(t\zeta_1 + (1 - t)\zeta_2)dt$$

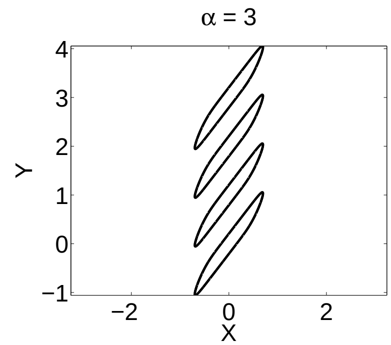

Figure 5: Periodic array of inclusions for $\alpha = 3$ and $q = -0.4\sqrt{2}(1+i)$.

If $w(\zeta_1) = w(\zeta_2)$ then we must have

$$\int_0^1 v(t\zeta_1 + (1-t)\zeta_2)dt = \frac{r-1}{r}.$$

However, the left-hand side is in the right half-plane $\mathfrak{Re}(v) > 0$, while the right-hand side is in the left half-plane, when $|q| < 1$. Thus, the map $w(\zeta)$ is univalent if and only if (5.62) holds.

The inequality (5.62) together with (5.42) describes a surface known to be in $\overline{\mathfrak{B}}$, since the non-degeneracy condition (4.26), that has the form (5.29) in our example, is obviously satisfied. The surface (5.42), (5.62) coincides with (5.18), (5.27) for $d = k = 2$.

We compute that for any $\xi \in [-\alpha, \alpha]$

$$V(\xi + 0i) = \frac{i}{\pi} \arccos\left(\frac{\cosh(\pi\xi)}{\cosh(\pi\alpha)}\right).$$

Therefore the parametric equations of the upper half of the inclusion are

$$x = \frac{1+q_1}{2}\xi - \frac{q_2}{2i}V(\xi), \qquad y = \frac{1-q_1}{2i}V(\xi) - \frac{q_2}{2}\xi, \qquad \xi \in [-\alpha, \alpha].$$

where $q = q_1 + iq_2$. The parameter α is arbitrary. The structure for $\alpha = 3$ and $q = -0.4\sqrt{2}(1+i)$ is pictured in Figure 5.

Now, for simplicity let us examine in more detail the case when the periodic direction is chosen to be the eigendirection of $\boldsymbol{\varepsilon}_\infty$. Then $b \in \mathbb{R}$, and hence $r \in (0,1)$. The parameter $\alpha > 0$ can be chosen arbitrarily. The resulting shapes are different for different values of α, yet all have the same energy. The equation of the upper half of the inclusion centered at the origin is

$$y = \frac{1-q}{2\pi} \arccos\left(\frac{\cosh\left(\frac{2\pi x}{1+q}\right)}{\cosh(\pi\alpha)}\right), \qquad x \in \left[-\frac{(1+q)\alpha}{2}, \frac{(1+q)\alpha}{2}\right].$$

When $\alpha \to 0$ the inclusions degenerate into the i-periodic array of small ellipses

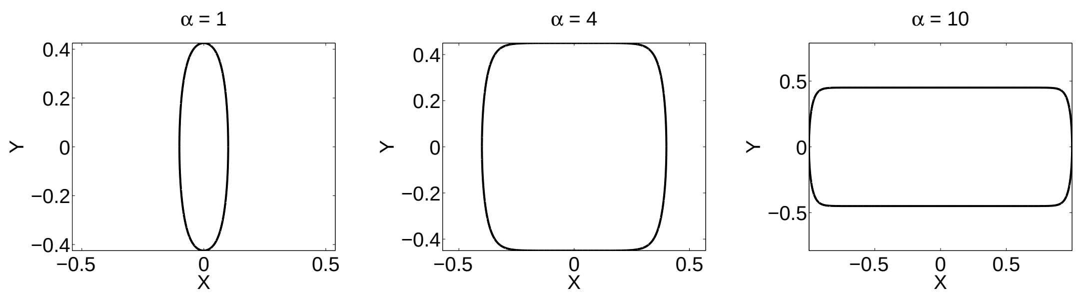

Figure 6: The shape of the component of a periodic array of inclusions for $q = -0.8$ and $\alpha = 1$, 4 and 10.

$$\frac{x^2}{(1+q)^2} + \frac{y^2}{(1-q)^2} = \frac{\alpha^2}{4}.$$

When $\alpha \to \infty$ the structure becomes a periodic array of horizontal layers of thickness r. However, for each large value α one needs to rescale the structure to keep the width of the inclusions constant, i.e. we change variables

$$X = \frac{2x}{(1+q)\alpha}, \qquad Y = \frac{2y}{(1+q)\alpha}.$$

In the new variables the array of inclusions is p-periodic, where

$$p = \frac{2i}{(1+q)\alpha}$$

is large, while the upper half of the inclusion centered at the origin has the equation

$$Y = \frac{1}{\pi\alpha}\frac{1-q}{1+q}\arccos\left(\frac{\cosh(\pi\alpha X)}{\cosh(\pi\alpha)}\right), \qquad X \in [-1, 1]. \tag{5.63}$$

When $\alpha \to \infty$ both the period p and the vertical dimensions of the inclusions will go to zero and the structure will converge to a second rank laminate with inner volume fraction r, which is also known to permit detection of this part of the binodal.

Figure 6 shows the shapes of single inclusions given by (5.63) for $q = -0.8$ and $\alpha = 1$, 4 and 10. For each fixed value α the decay of the elastic fields along the x-direction is exponential. Therefore, the corresponding test function $\boldsymbol{\phi} = \boldsymbol{u} - \boldsymbol{\varepsilon}_\infty \boldsymbol{x}$ is in the space $\mathcal{C}_1$.

In summary, for each fixed value $\boldsymbol{\varepsilon}_\infty$ satisfying (5.42) and (5.62), that are identical to (5.18), (5.27) for $d = k = 2$, we found a 1-parameter family of $\mathcal{C}_1$ test fields satisfying (4.12)–(4.13) degenerating into $\mathcal{C}_2$ test fields (corresponding to elliptical inclusions) when $\alpha \to 0$ and to rank-two laminates when $\alpha \to \infty$. In other words, each member of the solution family identifies exactly the same marginally stable value of $\boldsymbol{\varepsilon}_\infty$ as the simple elliptical inclusions, confirming previously obtained bounds. The isotropy and high non-convexity of this example contributes to the abundance of rank-1 connected pairs $\boldsymbol{F}_+$, $\boldsymbol{F}_-$ on the jump set [58], described in Section 4.2.2. This in turn provides sufficient flexibility for multiple structures to identify same marginally stable values of deformation gradients. For more general energies we expect fewer binodal points to be detectable through classical nucleation. For example in [53], essentially the same model with anisotropic tensors $\mathsf{C}_{\pm}$ was considered in $2d$. It was shown there that the regime analogous to (5.42), (5.62) can be detected only by second rank laminates, since the support of the optimal Young measure in (2.19) consists of specific three points which are inconsistent with classical nucleation.

5.3 Laminates

We have the following equations for $\boldsymbol{\varepsilon}$ on a second rank lamination set. The "micro-level" system is

$$\begin{cases} [\![\boldsymbol{\varepsilon}]\!] = \boldsymbol{b} \odot \boldsymbol{m} \\ [\![\mathsf{C}\boldsymbol{\varepsilon}]\!]\boldsymbol{m} = \boldsymbol{0} \\ [\![\mathsf{C}\boldsymbol{\varepsilon}]\!]\boldsymbol{b} = \boldsymbol{0} \\ [\![w]\!] + \dfrac{1}{2}([\![\mathsf{C}]\!]\boldsymbol{\varepsilon}_{\pm}, \boldsymbol{\varepsilon}_{\pm}) = \mp\dfrac{1}{2}(\mathsf{C}_{\mp}[\![\boldsymbol{\varepsilon}]\!], [\![\boldsymbol{\varepsilon}]\!]). \end{cases} \tag{5.64}$$

while the macro-level system is

$$\begin{cases} s\boldsymbol{\varepsilon}_{-} + (1-s)\boldsymbol{\varepsilon}_{+} - \boldsymbol{\varepsilon} = \boldsymbol{a} \odot \boldsymbol{n} \\ (s\mathsf{C}_{-}\boldsymbol{\varepsilon}_{-} + (1-s)\mathsf{C}_{+}\boldsymbol{\varepsilon}_{+} - \mathsf{C}_{\pm}\boldsymbol{\varepsilon})\boldsymbol{n} = \boldsymbol{0} \\ (s\mathsf{C}_{-}\boldsymbol{\varepsilon}_{-} + (1-s)\mathsf{C}_{+}\boldsymbol{\varepsilon}_{+} - \mathsf{C}_{\pm}\boldsymbol{\varepsilon})\boldsymbol{a} = \boldsymbol{0} \\ [\![w]\!] + \dfrac{1}{2}([\![\mathsf{C}]\!]\boldsymbol{\varepsilon}, \boldsymbol{\varepsilon}) = \mp\dfrac{1}{2}(\mathsf{C}_{\mp}\boldsymbol{a} \odot \boldsymbol{n}, \boldsymbol{a} \odot \boldsymbol{n}), \end{cases} \tag{5.65}$$

where the upper sign corresponds to the situation when $\boldsymbol{\varepsilon}$ lies in the "+" well, while the lower sign corresponds to the situation when $\boldsymbol{\varepsilon}$ lies in the "−" well. The detailed analysis of this system of equations in 2D shows that by studying laminates one can confirm the bounds obtained in the analysis of classical nuclei and obtain new bounds inaccessible by the methods based exclusively on solving the associated PDE problem [56].

6 Conclusions

Marginal stability plays an important role in nonlinear elasticity because the associated minimally stable states delineate failure thresholds. In this paper we systematically juxtaposed the conditions of marginal stability for weak and strong local minimizers in nonlinear elasticity. While the case of weak marginal stability, allowing one to determine the *spinodal*, can be studied in full detail, the case of strong marginal stability, bringing about the crucial notion of the *binodal*, is much less transparent. The reason is that binodal coincides with the boundary of the typically inscrutable quasiconvexity set. We have shown that in order to locate the binodal one does not have to solve the difficult minimization problem for a non-convex integral functional of non-linear elasticity. Instead, one needs to deal with an equivalence class of parametric variational inequalities with a possibility that a particular formulation delivers a tractable characterization. We used this freedom to obtain several characterizations of the binodal in terms of either PDEs or algebraic equations. In the former case the test functions are "well-behaved" members of a function space, in the latter they are weakly convergent sequences of gradients-generating laminate Young measures described by finitely many parameters. While the proposed explicit characterization is far from being exhaustive, we obtained a set of bounds which may be useful in applications where one has no hope of computing the explicit quasiconvex envelopes.

7 Acknowledgement

We thank R. Fosdick, R. Kohn and anonymous reviewers for helpful comments. This material is based upon work supported by the National Science Foundation under Grant No. 1008092 and the French ANR grant EVOCRIT (2008-2012).

A Proof of Lemma 3.3

We note that $\mathcal{S} = W^{1,\infty}(\mathbb{R}^d;\mathbb{R}^m) \cap \mathcal{S}_0$. It will be important to use the following embedding theorem for the space $\mathcal{S}_0$

THEOREM **A.1.** *Assume that $\boldsymbol{\phi} \in \mathcal{S}_0$ and $d \geq 3$. Then there exists a unique constant $\boldsymbol{c} \in \mathbb{R}^m$ such that $\boldsymbol{\phi} - \boldsymbol{c} \in L^{\frac{2d}{d-2}}(\mathbb{R}^d;\mathbb{R}^m)$.*

Proof. First, we remark that without loss of generality we may take $m = 1$. Now recall the well-known potential theory operators. The Riesz transforms R_j are defined by

$$\mathcal{F}(R_j f)(\boldsymbol{\xi}) = i\frac{\xi_j}{|\boldsymbol{\xi}|}\widehat{f}(\boldsymbol{\xi}),$$

where

$$\mathcal{F}(f)(\boldsymbol{\xi}) = \widehat{f}(\boldsymbol{\xi}) = \int_{\mathbb{R}^d} f(\boldsymbol{x})e^{2\pi i(\boldsymbol{x},\boldsymbol{\xi})}d\boldsymbol{x}$$

is the Fourier transform. The operators R_j map $L^2(\mathbb{R}^d)$ into $L^2(\mathbb{R}^d)$. The Riesz potential I_1 is defined by

$$\mathcal{F}(I_1 f)(\boldsymbol{\xi}) = \frac{\widehat{f}(\boldsymbol{\xi})}{2\pi|\boldsymbol{\xi}|}.$$

It maps $L^2(\mathbb{R}^d)$ into $L^{\frac{2d}{d-2}}(\mathbb{R}^d)$, [117].

If ϕ were smooth and compactly supported, we would have

$$\phi = I_1\left(\sum_{j=1}^{d} R_j\left(\frac{\partial\phi}{\partial x_j}\right)\right).$$

Hence, we define

$$\psi(\boldsymbol{x}) = I_1\left(\sum_{j=1}^{d} R_j(g_j)\right),$$

where $\boldsymbol{g} = \nabla\phi \in L^2(\mathbb{R}^d;\mathbb{R}^d)$.

Let $\eta(\boldsymbol{x})$ be an arbitrary smooth compactly supported function. By definition of the distributional derivative we have

$$\int_{\mathbb{R}^d}\left\{g_k\frac{\partial\eta}{\partial x_j} - g_j\frac{\partial\eta}{\partial x_k}\right\}d\boldsymbol{x} = -\langle\phi, \frac{\partial^2\eta}{\partial x_k\partial x_j}\rangle + \langle\phi, \frac{\partial^2\eta}{\partial x_j\partial x_k}\rangle = 0.$$

By Plancherel's identity

$$\int_{\mathbb{R}^d}(\widehat{g}_k\xi_j - \widehat{g}_j\xi_k)\overline{\widehat{\eta}}d\boldsymbol{\xi} = 0.$$

We conclude that

$$\widehat{g}_k(\boldsymbol{\xi})\xi_j = \widehat{g}_j(\boldsymbol{\xi})\xi_k \tag{A.1}$$

for a.e. $\boldsymbol{\xi} \in \mathbb{R}^d$. Thus,

$$-2\pi i\xi_k\widehat{\psi}(\boldsymbol{\xi}) = \sum_{j=1}^{d}\frac{\xi_k\xi_j\widehat{g}_j(\boldsymbol{\xi})}{|\boldsymbol{\xi}|^2} = \widehat{g}_k(\boldsymbol{\xi}),$$

due to (A.1). By Plancherel's identity

$$\int_{\mathbb{R}^d}\psi(\boldsymbol{x})\frac{\partial\eta}{\partial x_k}d\boldsymbol{x} = 2\pi i\int_{\mathbb{R}^d}\xi_k\widehat{\psi}\,\overline{\widehat{\eta}}d\boldsymbol{\xi} = -\int_{\mathbb{R}^d}\widehat{g}_k(\boldsymbol{\xi})\overline{\widehat{\eta}}d\boldsymbol{\xi} = -\int_{\mathbb{R}^d}g_k(\boldsymbol{x})\eta(\boldsymbol{x})d\boldsymbol{x}.$$

Therefore, $\nabla\psi = \boldsymbol{g} = \nabla\phi$ as distributions. The theorem is proved. □

The proof of Lemma 3.3 proceeds in different ways depending on the dimension d. If $d = 1$, then

$$\frac{1}{R}\int_R^{2R}|\boldsymbol{\phi}||\boldsymbol{\phi}'(x)|dx \le \frac{\|\boldsymbol{\phi}\|_\infty}{\sqrt{R}}\left(\int_R^{2R}|\boldsymbol{\phi}'(x)|^2dx\right)^{1/2} \to 0, \text{ as } R\to\infty.$$

$$\frac{1}{R^2}\int_R^{2R}|\boldsymbol{\phi}(x)|^2dx \le \frac{\|\boldsymbol{\phi}\|_\infty^2}{R} \to 0, \text{ as } R\to\infty.$$

Let $d = 2$. We estimate

$$\frac{1}{R}\int_{A_R}|\boldsymbol{\phi}||\nabla\boldsymbol{\phi}|d\boldsymbol{x} \le \|\boldsymbol{\phi}\|_\infty\sqrt{3\pi}\left(\int_{A_R}|\nabla\boldsymbol{\phi}|^2d\boldsymbol{x}\right)^{1/2} \to 0, \text{ as } R\to\infty.$$

By the Poincaré inequality

$$\int_{A_R}|\boldsymbol{\phi}(\boldsymbol{x}) - \langle\boldsymbol{\phi}\rangle_{A_R}|^2d\boldsymbol{x} \le C_0R^2\int_{A_R}|\nabla\boldsymbol{\phi}|^2d\boldsymbol{x},$$

where C_0 is the Poincaré constant for A_1. The boundedness of $\boldsymbol{\phi}$ implies that there exists a sequence $R = R_k$ such that

$$\lim_{k\to\infty} \langle \boldsymbol{\phi} \rangle_{A_{R_k}} = \boldsymbol{c}.$$

Hence, by the triangle inequality

$$\left(\int_{A_R} |\boldsymbol{\phi} - \boldsymbol{c}|^2 d\boldsymbol{x} \right)^{1/2} \leq \left(\int_{A_R} |\boldsymbol{\phi} - \langle \boldsymbol{\phi} \rangle_{A_R}|^2 d\boldsymbol{x} \right)^{1/2} + |A_R|^{1/2} |\langle \boldsymbol{\phi} \rangle_{A_R} - \boldsymbol{c}|.$$

Then,

$$\left(\frac{1}{R_k^2} \int_{A_{R_k}} |\boldsymbol{\phi} - \boldsymbol{c}|^2 d\boldsymbol{x} \right)^{1/2} \leq \left(C_0 \int_{A_{R_k}} |\nabla \boldsymbol{\phi}|^2 d\boldsymbol{x} \right)^{1/2} + \sqrt{3\pi} |\langle \boldsymbol{\phi} \rangle_{A_{R_k}} - \boldsymbol{c}| \to 0 \text{ as } n \to \infty.$$

Now assume that $d \geq 3$. By Theorem A.1 there exists a unique constant $\boldsymbol{c}$, such that $\boldsymbol{\phi} - \boldsymbol{c} \in L^{\frac{2d}{d-2}}(\mathbb{R}^d; \mathbb{R}^m)$. Using the inequality $ab \leq (a^2 + b^2)/2$ we get

$$\frac{1}{R} \int_{A_R} |\boldsymbol{\phi} - \boldsymbol{c}| |\nabla \boldsymbol{\phi}| d\boldsymbol{x} + \frac{1}{R^2} \int_{A_R} |\boldsymbol{\phi} - \boldsymbol{c}|^2 d\boldsymbol{x} \leq \frac{1}{2} \int_{A_R} |\nabla \boldsymbol{\phi}|^2 d\boldsymbol{x} + \frac{3}{2R^2} \int_{A_R} |\boldsymbol{\phi} - \boldsymbol{c}|^2 d\boldsymbol{x}.$$

By Hölder inequality

$$\frac{1}{R^2} \int_{A_R} |\boldsymbol{\phi} - \boldsymbol{c}|^2 d\boldsymbol{x} \leq \left(\int_{A_R} |\boldsymbol{\phi} - \boldsymbol{c}|^{\frac{2d}{d-2}} d\boldsymbol{x} \right)^{\frac{d-2}{d}} \to 0, \text{ as } R \to \infty.$$

The lemma is proved.

B Proof of Lemma 3.7

Let us begin with a technical lemma.

LEMMA **B.1.** *Suppose $\alpha(R) > 0$ is such that $\alpha(R) \to 0$, as $R \to \infty$. Then there exists a monotone increasing function $h(R)$ with $h(R)/R \to 0$, as $R \to \infty$, such that*

$$\lim_{R\to\infty} \left(\frac{R}{h(R)} \right) \alpha(R) = 0. \tag{B.1}$$

Proof. We define

$$h(R) = \max_{r<R} \left(r\sqrt{\alpha(r)} \right).$$

Then $h(R)$ is monotone increasing and $h(R)/R \to 0$, as $R \to \infty$. Indeed, for any $\epsilon > 0$

$$h(R) \leq \max_{r<\epsilon R} \left(r\sqrt{\alpha(r)} \right) + \max_{\epsilon R<r<R} \left(r\sqrt{\alpha(r)} \right) \leq \epsilon R\sqrt{\alpha(0)} + R\sqrt{\alpha(\epsilon R)}.$$

Therefore,

$$\overline{\lim_{R\to\infty}} \frac{h(R)}{R} \le \epsilon\sqrt{\alpha(0)}.$$

Hence, $h(R)/R \to 0$, as $R \to \infty$. By definition of $h(R)$ we have $h(R) \ge R\sqrt{\alpha(R)}$. Therefore,

$$\frac{R}{h(R)} \le \frac{1}{\sqrt{\alpha(R)}}.$$

Thus,

$$\left(\frac{R}{h(R)}\right)\alpha(R) \le \sqrt{\alpha(R)} \to 0, \text{ as } R \to \infty.$$

□

Now let us prove Lemma 3.7. First observe that for any $\boldsymbol{\phi} \in \mathcal{S}_0$

$$\lim_{R\to\infty}\int_{B_R} |\nabla\boldsymbol{\phi}|^2 d\boldsymbol{x} = \|\nabla\boldsymbol{\phi}\|_2^2,$$

while

$$\lim_{R\to\infty}\int_{A_R(h(R))} |\nabla\boldsymbol{\phi}|^2 d\boldsymbol{x} = 0.$$

Hence, we only need to prove that there exists $\boldsymbol{c} \in \mathbb{R}^m$ and a monotone increasing function $h(R) = o(R)$ such that

$$\lim_{R\to\infty}\frac{1}{h(R)^2}\int_{A_R(h(R))} |\boldsymbol{\phi} - \boldsymbol{c}|^2 d\boldsymbol{x} = 0. \tag{B.2}$$

Remark 3.6 implies that we need to prove (B.2) for $d \ge 3$. In that case, the constant $\boldsymbol{c} \in \mathbb{R}^m$ is chosen so that $\boldsymbol{\phi} - \boldsymbol{c} \in L^{\frac{2d}{d-2}}(\mathbb{R}^d;\mathbb{R}^m)$, which is possible by Theorem A.1. The Hölder inequality gives us

$$\frac{1}{h(R)^2}\int_{A_R(h(R))} |\boldsymbol{\phi} - \boldsymbol{c}|^2 d\boldsymbol{x} \le C\left(\frac{R}{h(R)}\right)^{\frac{2(d-1)}{d}}\left(\int_{A_R(h(R))} |\boldsymbol{\phi} - \boldsymbol{c}|^{\frac{2d}{d-2}} d\boldsymbol{x}\right)^{\frac{d-2}{d}}.$$

By Theorem A.1

$$\alpha(R) = \left(\int_{|\boldsymbol{x}|\ge R/2} |\boldsymbol{\phi} - \boldsymbol{c}|^{\frac{2d}{d-2}} d\boldsymbol{x}\right)^{\frac{d-2}{2(d-1)}} \to 0, \text{ as } R \to \infty.$$

We see that in each of the three cases we have a function $\alpha(R) \to 0$, as $R \to \infty$, which is independent of $h(R)$. The application of Lemma B.1 concludes the proof of Lemma 3.7.

C Proof of Theorem 3.9

Step 1: Asymptotics of $\int_{B_R} |\nabla\boldsymbol{\phi}|^2 d\boldsymbol{x}$.

We write $\boldsymbol{x} = \boldsymbol{p} + \boldsymbol{R}^T\boldsymbol{t}$ and $|\boldsymbol{x}|^2 = |\boldsymbol{p}|^2 + |\boldsymbol{t}|^2$. Therefore,

$$B_R \subset V_R = \{\boldsymbol{x} \in \mathbb{R}^d : \boldsymbol{x} = \boldsymbol{p} + \boldsymbol{R}^T\boldsymbol{t},\ |\boldsymbol{t}| \le R,\ |\boldsymbol{p}| \le R\}.$$

$$\int_{V_R} |\nabla\boldsymbol{\phi}|^2 d\boldsymbol{x} = \int_{\{|\boldsymbol{t}|<R\}} \int_{\{|\boldsymbol{p}|<R\}} \{|\boldsymbol{\psi_t}|^2 + |\boldsymbol{\psi_p}|^2\} d\boldsymbol{t} d\boldsymbol{p}.$$

If we make a change of variables $\boldsymbol{p} = R\boldsymbol{u}$ we obtain

$$\frac{1}{R^{d-k}} \int_{V_R} |\nabla\boldsymbol{\phi}|^2 d\boldsymbol{x} = \int_{\{|\boldsymbol{t}|<R\}} \int_{\{|\boldsymbol{u}|<1\}} \{|\boldsymbol{\psi_t}(\boldsymbol{t}, R\boldsymbol{u})|^2 + |\boldsymbol{\psi_p}(\boldsymbol{t}, R\boldsymbol{u})|^2\} d\boldsymbol{u} d\boldsymbol{t}.$$

Hence,

$$\frac{1}{R^{d-k}} \int_{V_R} |\nabla\boldsymbol{\phi}|^2 d\boldsymbol{x} \le \int_{\{|\boldsymbol{u}|<1\}} \int_{\mathbb{R}^k} \{|\boldsymbol{\psi_t}(\boldsymbol{t}, R\boldsymbol{u})|^2 + |\boldsymbol{\psi_p}(\boldsymbol{t}, R\boldsymbol{u})|^2\} d\boldsymbol{t} d\boldsymbol{u}.$$

By the Riemann-Lebesgue lemma we get

$$\overline{\lim_{R\to\infty}} \frac{1}{R^{d-k}} \int_{V_R} |\nabla\boldsymbol{\phi}|^2 d\boldsymbol{x} \le \omega_{d-k} \fint_{Q_{d-k}} \int_{\mathbb{R}^k} \{|\boldsymbol{\psi_t}(\boldsymbol{t}, \boldsymbol{p})|^2 + |\boldsymbol{\psi_p}(\boldsymbol{t}, \boldsymbol{p})|^2\} d\boldsymbol{t} d\boldsymbol{p},$$

where ω_n is the volume of the n-dimensional unit ball. Thus,

$$\overline{\lim_{R\to\infty}} \frac{1}{R^{d-k}} \int_{B_R} |\nabla\boldsymbol{\phi}|^2 d\boldsymbol{x} \le \omega_{d-k} \fint_{Q_{d-k}} \int_{\mathbb{R}^k} \{|\boldsymbol{\psi_t}(\boldsymbol{t}, \boldsymbol{p})|^2 + |\boldsymbol{\psi_p}(\boldsymbol{t}, \boldsymbol{p})|^2\} d\boldsymbol{t} d\boldsymbol{p}.$$

To get the reverse inequality we write

$$\int_{B_R} |\nabla\boldsymbol{\phi}|^2 d\boldsymbol{x} = \int_{\{|\boldsymbol{t}|<R\}} \int_{\{|\boldsymbol{p}|<r(R,\boldsymbol{t})\}} \{|\boldsymbol{\psi_t}|^2 + |\boldsymbol{\psi_p}|^2\} d\boldsymbol{p} d\boldsymbol{t},$$

where $r(R, \boldsymbol{t}) = \sqrt{R^2 - |\boldsymbol{t}|^2}$. If we make a change of variables $\boldsymbol{p} = r(R, \boldsymbol{t})\boldsymbol{u}$ we obtain

$$\int_{B_R} |\nabla\boldsymbol{\phi}|^2 d\boldsymbol{x} = \int_{\{|\boldsymbol{t}|<R\}} r(R, \boldsymbol{t})^{d-k} \int_{\{|\boldsymbol{u}|<1\}} \{|\boldsymbol{\psi_t}(\boldsymbol{t}, r(R, \boldsymbol{t})\boldsymbol{u})|^2 + |\boldsymbol{\psi_p}(\boldsymbol{t}, r(R, \boldsymbol{t})\boldsymbol{u})|^2\} d\boldsymbol{u} d\boldsymbol{t}.$$

By the Riemann-Lebesgue lemma we get

$$\lim_{R\to\infty} \int_{\{|\boldsymbol{u}|<1\}} \{|\boldsymbol{\psi_t}(\boldsymbol{t}, r(R, \boldsymbol{t})\boldsymbol{u})|^2 + |\boldsymbol{\psi_p}(\boldsymbol{t}, r(R, \boldsymbol{t})\boldsymbol{u})|^2\} d\boldsymbol{u} = \omega_{d-k} \fint_{Q_{d-k}} \{|\boldsymbol{\psi_t}(\boldsymbol{t}, \boldsymbol{p})|^2 + |\boldsymbol{\psi_p}(\boldsymbol{t}, \boldsymbol{p})|^2\} d\boldsymbol{p}$$

for a.e. $\boldsymbol{t} \in \mathbb{R}^k$. By Fatous's lemma we get

$$\underline{\lim_{R\to\infty}} \frac{1}{R^{d-k}} \int_{B_R} |\nabla\boldsymbol{\phi}|^2 d\boldsymbol{x} \ge \omega_{d-k} \int_{\mathbb{R}^k} \fint_{Q_{d-k}} \{|\boldsymbol{\psi_t}(\boldsymbol{t}, \boldsymbol{p})|^2 + |\boldsymbol{\psi_p}(\boldsymbol{t}, \boldsymbol{p})|^2\} d\boldsymbol{p} d\boldsymbol{t}.$$

Hence, we obtain the asymptotics of $\int_{B_R} |\nabla \boldsymbol{\phi}|^2 d\boldsymbol{x}$:

$$\lim_{R\to\infty} \frac{1}{R^{d-k}} \int_{B_R} |\nabla \boldsymbol{\phi}|^2 d\boldsymbol{x} = \omega_{d-k} \int_{\mathbb{R}^k} \fint_{Q_{d-k}} \{|\boldsymbol{\psi}_{\boldsymbol{t}}(\boldsymbol{t},\boldsymbol{p})|^2 + |\boldsymbol{\psi}_{\boldsymbol{p}}(\boldsymbol{t},\boldsymbol{p})|^2\} d\boldsymbol{p} d\boldsymbol{t}. \tag{C.1}$$

In particular, we get

$$\overline{\lim_{R\to\infty}} \fint_{B_R} |\nabla \boldsymbol{\phi}|^2 d\boldsymbol{x} \le \overline{\lim_{R\to\infty}} \frac{\omega_d}{R^d} \int_{V_R} |\nabla \boldsymbol{\phi}|^2 d\boldsymbol{x} = 0,$$

establishing (3.19).

Step 2: Proof of (3.17).

For any $h(R) = o(R)$ we have, using (C.1)

$$\frac{\displaystyle\int_{A_R(h(R))} |\nabla \boldsymbol{\phi}|^2 d\boldsymbol{x}}{\int_{B_R} |\nabla \boldsymbol{\phi}|^2 d\boldsymbol{x}} = \frac{\displaystyle\int_{B_R} |\nabla \boldsymbol{\phi}|^2 d\boldsymbol{x} - \int_{B_{R-h(R)}} |\nabla \boldsymbol{\phi}|^2 d\boldsymbol{x}}{\int_{B_R} |\nabla \boldsymbol{\phi}|^2 d\boldsymbol{x}} = 1 - \left(1 - \frac{h(R)}{R}\right)^{d-k} u_R,$$

where $u_R \to 1$, as $R \to \infty$. Thus, (3.17) is proved.

Step 3: Proof of (3.18). We have

$$\int_{A_R(h(R))} |\boldsymbol{\phi}|^2 d\boldsymbol{x} \le \int_{|\boldsymbol{t}|<R} \int_{|\boldsymbol{p}|<R} |\boldsymbol{\psi}(\boldsymbol{t},\boldsymbol{p})|^2 d\boldsymbol{p} d\boldsymbol{t}$$

The periodicity in $\boldsymbol{p}$ variable implies that for any domain $\Omega \subset \mathbb{R}^{d-k}$

$$\int_{\Omega} |\boldsymbol{\psi}(\boldsymbol{t},\boldsymbol{p})|^2 d\boldsymbol{p} \le v(\Omega) \fint_{Q_{d-k}} |\boldsymbol{\psi}(\boldsymbol{t},\boldsymbol{p})|^2 d\boldsymbol{p},$$

where $v(\Omega)$ is the $(d-k)$-volume of all period cells intersecting Ω. We further estimate that

$$v(\Omega) \le |\Omega + B_M|,$$

where M is the diameter of the period cell Q_{d-k}. When $R > M$ we obtain

$$v(\{|\boldsymbol{p}| \le R + M\}) \le \omega_{d-k}(2R)^{d-k}.$$

Hence, we get the estimate

$$\underline{\lim}_{R\to\infty} \frac{\displaystyle\frac{1}{h(R)^2} \int_{A_R(h(R))} |\boldsymbol{\phi}|^2 d\boldsymbol{x}}{\displaystyle\int_{B_R} |\nabla \boldsymbol{\phi}|^2 d\boldsymbol{x}} \le \frac{2^{d-k}}{\|\nabla \boldsymbol{\phi}\|^2_{L^2(Y)}} \underline{\lim}_{R\to\infty} \frac{1}{h(R)^2} \int_{|\boldsymbol{t}|<R} \fint_{Q_{d-k}} |\boldsymbol{\psi}(\boldsymbol{t},\boldsymbol{p})|^2 d\boldsymbol{p} d\boldsymbol{t}. \tag{C.2}$$

For convenience we introduce the truncated L^2 norm

$$\|\boldsymbol{f}\|^2_{2,R} = \int_{B_R} \int_{Q_{d-k}} |\boldsymbol{f}(\boldsymbol{t},\boldsymbol{p})|^2 d\boldsymbol{p} d\boldsymbol{t}$$

Lemma **C.1.** *For every* $\boldsymbol{\psi} \in \mathcal{S}_k(Q_{d-k})$ *there exists a constant* $\boldsymbol{c} \in \mathbb{R}^m$ *such that*

$$\varliminf_{R\to\infty} \frac{\|\boldsymbol{\psi} - \boldsymbol{c}\|_{2,R}^2}{R^2} = 0.$$

Proof. The proof of the Lemma is different depending on whether $k = 1$, $k = 2$ or $k \geq 3$.

If $k = 1$ we can use the assumption of uniform boundedness of $\boldsymbol{\psi}$ and conclude that

$$\frac{\|\boldsymbol{\psi}\|_{2,R}^2}{R^2} \leq \frac{2\|\boldsymbol{\psi}\|_\infty^2}{R} \to 0, \text{ as } R \to \infty.$$

If $k \geq 3$ then, according to Theorem A.1, for a.e. $\boldsymbol{p} \in Q_{d-k}$ there exists a unique vector $\boldsymbol{c}(\boldsymbol{p})$ such that

$$\int_{\mathbb{R}^k} |\boldsymbol{\psi}(\boldsymbol{t}, \boldsymbol{p}) - \boldsymbol{c}(\boldsymbol{p})|^{\frac{2k}{k-2}} < \infty.$$

However, we need a sharper statement

Lemma **C.2.** *There exists* $\boldsymbol{c} \in \mathbb{R}^m$ *such that* $\boldsymbol{c}(\boldsymbol{p}) = \boldsymbol{c}$ *for a.e.* $\boldsymbol{p} \in Q_{d-k}$.

Proof. Let

$$\langle\boldsymbol{\psi}\rangle_{Q_{d-k}}(\boldsymbol{t}) = \frac{1}{|Q_{d-k}|} \int_{Q_{d-k}} \boldsymbol{\psi}(\boldsymbol{t}, \boldsymbol{p}) d\boldsymbol{p}.$$

The Poincaré inequality implies

$$\|\boldsymbol{\psi} - \langle\boldsymbol{\psi}\rangle_{Q_{d-k}}(\boldsymbol{t})\|_{2,R}^2 \leq C\|\boldsymbol{\psi}_{\boldsymbol{p}}\|_{2,R}^2.$$

Therefore, $\|\boldsymbol{\psi} - \langle\boldsymbol{\psi}\rangle_{Q_{d-k}}(\boldsymbol{t})\|_{2,R}$ is bounded as $R \to \infty$. Next observe that $\langle\boldsymbol{\psi}\rangle_{Q_{d-k}}(\boldsymbol{t}) \in \mathcal{S}$ as a function of $\boldsymbol{t}$. Hence, there exists $\boldsymbol{c} \in \mathbb{R}^m$ such that $\langle\boldsymbol{\psi}\rangle_{Q_{d-k}}(\boldsymbol{t}) - \boldsymbol{c} \in L^{\frac{2k}{k-2}}(\mathbb{R}^k)$. It follows that

$$\|\boldsymbol{c}(\boldsymbol{p}) - \boldsymbol{c}\|_{2,R} \leq \|\boldsymbol{c}(\boldsymbol{p}) - \boldsymbol{\psi}\|_{2,R} + \|\boldsymbol{\psi} - \langle\boldsymbol{\psi}\rangle_{Q_{d-k}}(\boldsymbol{t})\|_{2,R} + \|\langle\boldsymbol{\psi}\rangle_{Q_{d-k}}(\boldsymbol{t}) - \boldsymbol{c}\|_{2,R}.$$

Let us apply the Hölder inequality to the first and third term on the left-hand side of the above inequality.

$$\|\boldsymbol{c}(\boldsymbol{p}) - \boldsymbol{\psi}\|_{2,R}^2 \leq CR^2 \int_{Q_{d-k}} \left(\int_{\mathbb{R}^k} |\boldsymbol{c}(\boldsymbol{p}) - \boldsymbol{\psi}|^{\frac{2k}{k-2}} d\boldsymbol{t} \right)^{\frac{k-2}{k}} d\boldsymbol{p}.$$

$$\|\langle\boldsymbol{\psi}\rangle_{Q_{d-k}}(\boldsymbol{t}) - \boldsymbol{c}\|_{2,R}^2 \leq CR^2|Q_{d-k}| \left(\int_{\mathbb{R}^k} |\langle\boldsymbol{\psi}\rangle_{Q_{d-k}}(\boldsymbol{t}) - \boldsymbol{c}|^{\frac{2k}{k-2}} d\boldsymbol{t} \right)^{\frac{k-2}{k}}.$$

We conclude that

$$\varlimsup_{R\to\infty} \frac{1}{R^2}\|\boldsymbol{c}(\boldsymbol{p}) - \boldsymbol{c}\|_{2,R}^2 < +\infty.$$

However, this would contradict

$$\|\boldsymbol{c}(\boldsymbol{p}) - \boldsymbol{c}\|_{2,R}^2 = |B_R| \int_{Q_{d-k}} |\boldsymbol{c}(\boldsymbol{p}) - \boldsymbol{c}|^2 d\boldsymbol{p},$$

unless $\boldsymbol{c}(\boldsymbol{p}) = \boldsymbol{c}$ for a.e. $\boldsymbol{p} \in Q_{d-k}$. $\square$

We will now establish Lemma C.1 in which the constant vector $\boldsymbol{c}$ is coming from Lemma C.2. For simplicity of notation $\boldsymbol{\psi}(\boldsymbol{t},\boldsymbol{p})$ will now stand for $\boldsymbol{\psi}-\boldsymbol{c}$. In order to prove Lemma C.1 we split the $\boldsymbol{t}$-integral in the definition of $\|\boldsymbol{\psi}\|_{2,R}$ into the integral over the ball $\{|\boldsymbol{t}|<\epsilon R\}$ and the annulus $\{\epsilon R<|\boldsymbol{t}|<R\}$. Then we apply the same Hölder inequality to both integrals and obtain the estimate

$$\frac{1}{R^2}\int_{|\boldsymbol{t}|<R}|\boldsymbol{\psi}(\boldsymbol{t},\boldsymbol{p})|^2d\boldsymbol{t}\le\omega_k^{\frac{k}{2}}\epsilon^2\left(\int_{|\boldsymbol{t}|<\epsilon R}|\boldsymbol{\psi}(\boldsymbol{t},\boldsymbol{p})|^{\frac{2k}{k-2}}d\boldsymbol{t}\right)^{\frac{k-2}{k}}$$
$$+\,\omega_k^{\frac{k}{2}}(1-\epsilon^k)^{\frac{k}{2}}\left(\int_{\epsilon R<|\boldsymbol{t}|<R}|\boldsymbol{\psi}(\boldsymbol{t},\boldsymbol{p})|^{\frac{2k}{k-2}}d\boldsymbol{t}\right)^{\frac{k-2}{k}}.$$

Lemma C.2 then implies that for a.e. $\boldsymbol{p}\in Q_{d-k}$

$$\overline{\lim_{R\to\infty}}\frac{1}{R^2}\int_{|\boldsymbol{t}|<R}|\boldsymbol{\psi}(\boldsymbol{t},\boldsymbol{p})|^2d\boldsymbol{t}\le\omega_k^{\frac{k}{2}}\epsilon^2\left(\int_{\mathbb{R}^k}|\boldsymbol{\psi}(\boldsymbol{t},\boldsymbol{p})|^{\frac{2k}{k-2}}d\boldsymbol{t}\right)^{\frac{k-2}{k}}.$$

Thus, for a.e. $\boldsymbol{p}\in Q_{d-k}$

$$\lim_{R\to\infty}\frac{1}{R^2}\int_{|\boldsymbol{t}|<R}|\boldsymbol{\psi}(\boldsymbol{t},\boldsymbol{p})|^2d\boldsymbol{t}=0. \tag{C.3}$$

By Hölder inequality and Theorem A.1

$$\frac{1}{R^2}\int_{|\boldsymbol{t}|<R}|\boldsymbol{\psi}(\boldsymbol{t},\boldsymbol{p})|^2d\boldsymbol{t}\le\omega_k^{\frac{2}{k}}\left(\int_{|\boldsymbol{t}|<R}|\boldsymbol{\psi}(\boldsymbol{t},\boldsymbol{p})|^{\frac{2k}{k-2}}d\boldsymbol{t}\right)^{\frac{k-2}{k}}\le C\int_{\mathbb{R}^k}|\boldsymbol{\psi}_{\boldsymbol{t}}(\boldsymbol{t},\boldsymbol{p})|^2d\boldsymbol{t}.$$

By the Lebesgue dominated convergence theorem $\|\boldsymbol{\psi}\|^2_{2,R}/R^2\to 0$, as $R\to\infty$, since the function

$$\Phi(\boldsymbol{p})=\int_{\mathbb{R}^k}|\boldsymbol{\psi}_{\boldsymbol{t}}(\boldsymbol{t},\boldsymbol{p})|^2d\boldsymbol{t}$$

is integrable over Q_{d-k}.

The case $k=2$ is the most delicate. Let us define

$$\boldsymbol{c}_R(\boldsymbol{p})=\quad ⨍_{|\boldsymbol{t}|<R}\boldsymbol{\psi}(\boldsymbol{t},\boldsymbol{p})d\boldsymbol{t}.$$

Let $R_n\to\infty$ be a strictly monotone sequence such that

$$\lim_{n\to\infty}\langle\boldsymbol{c}_{R_n}\rangle_{Q_{d-2}}=\boldsymbol{c}$$

for some vector $\boldsymbol{c}\in\mathbb{R}^m$. We claim that

$$\lim_{R\to\infty}\|\boldsymbol{c}_R(\boldsymbol{p})-\langle\boldsymbol{c}_R\rangle_{Q_{d-2}}\|_2d\boldsymbol{p}=0.$$

Indeed,

$$\|\boldsymbol{c}_R(\boldsymbol{p})-\langle\boldsymbol{c}_R\rangle_{Q_{d-2}}\|_2^2\le C\quad ⨍_{|\boldsymbol{t}|<R}\int_{Q_{d-2}}|\boldsymbol{\psi}(\boldsymbol{t},\boldsymbol{p})-\langle\boldsymbol{\psi}\rangle_{Q_{d-2}}(\boldsymbol{t})|^2d\boldsymbol{p}d\boldsymbol{t}.$$

Applying the Poincaré inequality for the inner integral we get

$$\|\boldsymbol{c}_R - \langle \boldsymbol{c}_R\rangle_{Q_{d-2}}\|_2^2 \le C \fint_{|\boldsymbol{t}|<R}\int_{Q_{d-2}} |\boldsymbol{\psi}_{\boldsymbol{p}}(\boldsymbol{t},\boldsymbol{p})|^2 d\boldsymbol{p}d\boldsymbol{t} \to 0, \quad \text{as } R\to\infty.$$

We now prove that

$$\lim_{n\to\infty} \frac{1}{R^2}\|\boldsymbol{\psi}(\boldsymbol{t},\boldsymbol{p}) - \boldsymbol{c}\|_{2,R}^2 = 0.$$

By triangle inequality we have

$$\|\boldsymbol{\psi}(\boldsymbol{t},\boldsymbol{p}) - \boldsymbol{c}\|_{2,R} \le \|\boldsymbol{\psi} - \boldsymbol{c}_R(\boldsymbol{p})\|_{2,R} + \|\boldsymbol{c}_R(\boldsymbol{p}) - \langle \boldsymbol{c}_R\rangle_{Q_{d-2}}\|_{2,R} + \|\langle \boldsymbol{c}_R\rangle_{Q_{d-2}} - \boldsymbol{c}\|_{2,R}.$$

We compute

$$\|\langle \boldsymbol{c}_R\rangle_{Q_{d-2}} - \boldsymbol{c}\|_{2,R}^2 = |Q_{d-2}|\pi R^2 |\langle \boldsymbol{c}_R\rangle_{Q_{d-2}} - \boldsymbol{c}|^2.$$

Hence,

$$\lim_{n\to\infty} \frac{1}{R_n^2}\|\langle \boldsymbol{c}_{R_n}\rangle_{Q_{d-2}} - \boldsymbol{c}\|_{2,R}^2 = 0.$$

$$\|\boldsymbol{c}_R(\boldsymbol{p}) - \langle \boldsymbol{c}_R\rangle_{Q_{d-2}}\|_{2,R}^2 = \pi R^2 \|\boldsymbol{c}_R - \langle \boldsymbol{c}_R\rangle_{Q_{d-2}}\|_2^2.$$

Therefore,

$$\lim_{R\to\infty} \frac{1}{R^2}\|\boldsymbol{c}_R(\boldsymbol{p}) - \langle \boldsymbol{c}_R\rangle_{Q_{d-2}}\|_{2,R}^2 = 0.$$

Finally, we have

$$\|\boldsymbol{\psi} - \boldsymbol{c}_R(\boldsymbol{p})\|_{2,R}^2 = \int_{Q_{d-2}}\int_{\{|\boldsymbol{t}|<\epsilon R\}} |\boldsymbol{\psi} - \boldsymbol{c}_R(\boldsymbol{p})|^2 d\boldsymbol{t}d\boldsymbol{p} + \int_{Q_{d-2}}\int_{\{\epsilon R<|\boldsymbol{t}|<R\}} |\boldsymbol{\psi} - \boldsymbol{c}_R(\boldsymbol{p})|^2 d\boldsymbol{t}d\boldsymbol{p}.$$

Using the uniform boundedness of $\boldsymbol{\psi}$ for the first term and the Poincaré inequality for the second term we get

$$\|\boldsymbol{\psi} - \boldsymbol{c}_R(\boldsymbol{p})\|_{2,R}^2 \le C\epsilon^2 R^2 \|\boldsymbol{\psi} - \boldsymbol{c}\|_\infty^2 + R^2 C_\epsilon \int_{Q_{d-2}}\int_{\{\epsilon R<|\boldsymbol{t}|<R\}} |\boldsymbol{\psi}_{\boldsymbol{t}}(\boldsymbol{t},\boldsymbol{p})|^2 d\boldsymbol{t}d\boldsymbol{p}.$$

Thus,

$$\overline{\lim_{R\to\infty}} \frac{1}{R^2}\|\boldsymbol{\psi} - \boldsymbol{c}_R(\boldsymbol{p})\|_{2,R}^2 \le C\epsilon^2 \|\boldsymbol{\psi} - \boldsymbol{c}\|_\infty^2.$$

The arbitrariness of $\epsilon > 0$ implies that

$$\lim_{R\to\infty} \frac{1}{R^2}\|\boldsymbol{\psi} - \boldsymbol{c}_R(\boldsymbol{p})\|_{2,R}^2 = 0.$$

Lemma C.1 is proved now. □

Let $R_n \to \infty$ be the monotone increasing sequence for which $\|\boldsymbol{\psi}-\boldsymbol{c}\|_{2,R_n}/R_n \to 0$, as $n \to \infty$. Let

$$\alpha(R) = \frac{\|\boldsymbol{\psi}-\boldsymbol{c}\|_{2,R_n}}{R_n}, \quad R_n \le R < R_{n+1}.$$

Then $\alpha(R) \to 0$, as $R \to \infty$. By Lemma B.1 there exists a monotone increasing function $h(R)$ such that $h(R)/R \to 0$, as $R \to \infty$ and

$$\lim_{R\to\infty} \left(\frac{R}{h(R)}\right) \alpha(R) = 0.$$

Hence,

$$\varlimsup_{R\to\infty} \left(\frac{\|\boldsymbol{\psi}-\boldsymbol{c}\|_{2,R}}{h(R)}\right)^2 \le \lim_{n\to\infty} \left(\frac{R_n}{h(R_n)}\alpha(R_n)\right)^2 = 0.$$

The estimate (C.2) together with (3.17) now implies (3.18). Thus, we have proved that $\mathcal{C}_k \subset \mathcal{S}_*$ for any $1 \le k \le d$.

Step 4: Proof of the formula (3.24). We have

$$\frac{1}{R^{d-k}} \int_{B_R} W^\circ(\boldsymbol{F}, \nabla\boldsymbol{\phi}) d\boldsymbol{x} = \int_{|\boldsymbol{u}|\le 1} \int_{|\boldsymbol{t}|\le R\sqrt{1-|\boldsymbol{u}|^2}} W^\circ(\boldsymbol{F}, \boldsymbol{\psi_t}(\boldsymbol{t}, R\boldsymbol{u})\boldsymbol{R} + \boldsymbol{\psi_p}(\boldsymbol{t}, R\boldsymbol{u})\boldsymbol{Q}) d\boldsymbol{t} d\boldsymbol{u}.$$

By the Riemann-Lebesgue lemma

$$\lim_{R\to\infty} \int_{|\boldsymbol{u}|\le 1} \int_{\mathbb{R}^k} W^\circ(\boldsymbol{F}, \boldsymbol{\psi_t}(\boldsymbol{t}, R\boldsymbol{u})\boldsymbol{R} + \boldsymbol{\psi_p}(\boldsymbol{t}, R\boldsymbol{u})\boldsymbol{Q}) d\boldsymbol{t} d\boldsymbol{u} =$$

$$\omega_{d-k} \quad ⨍_{Q_{d-k}} \int_{\mathbb{R}^k} W^\circ(\boldsymbol{F}, \boldsymbol{\psi_t}(\boldsymbol{t}, \boldsymbol{p})\boldsymbol{R} + \boldsymbol{\psi_p}(\boldsymbol{t}, \boldsymbol{p})\boldsymbol{Q}) d\boldsymbol{t} d\boldsymbol{p}.$$

Thus, in order to finish the proof of the theorem we need to show that

$$\rho = \lim_{R\to\infty} \int_{|\boldsymbol{u}|\le 1} \int_{|\boldsymbol{t}|\ge R\sqrt{1-|\boldsymbol{u}|^2}} W^\circ(\boldsymbol{F}, \boldsymbol{\psi_t}(\boldsymbol{t}, R\boldsymbol{u})\boldsymbol{R} + \boldsymbol{\psi_p}(\boldsymbol{t}, R\boldsymbol{u})\boldsymbol{Q}) d\boldsymbol{t} d\boldsymbol{u} = 0. \tag{C.4}$$

Recall that $\boldsymbol{\phi} \in W^{1,\infty}(\mathbb{R}^d; \mathbb{R}^m)$. Hence, there exists a number $C > 0$ depending on $\|\boldsymbol{\phi}\|_{1,\infty}$, but independent of R such that

$$\rho \le C \varlimsup_{R\to\infty} \int_{|\boldsymbol{u}|\le 1} \int_{|\boldsymbol{t}|\ge R\sqrt{1-|\boldsymbol{u}|^2}} \{|\boldsymbol{\psi_t}(\boldsymbol{t}, R\boldsymbol{u})|^2 + |\boldsymbol{\psi_p}(\boldsymbol{t}, R\boldsymbol{u})|^2\} d\boldsymbol{t} d\boldsymbol{u}.$$

For any $\epsilon \in (0, 1)$ we have

$$\int_{|\boldsymbol{u}|\le 1} \int_{|\boldsymbol{t}|\ge R\sqrt{1-|\boldsymbol{u}|^2}} \{|\boldsymbol{\psi_t}(\boldsymbol{t}, R\boldsymbol{u})|^2 + |\boldsymbol{\psi_p}(\boldsymbol{t}, R\boldsymbol{u})|^2\} d\boldsymbol{t} d\boldsymbol{u} = T_1(R, \epsilon) + T_2(R, \epsilon),$$

where

$$T_1(R, \epsilon) = \int_{|\boldsymbol{u}|\le 1-\epsilon} \int_{|\boldsymbol{t}|\ge R\sqrt{1-|\boldsymbol{u}|^2}} \{|\boldsymbol{\psi_t}(\boldsymbol{t}, R\boldsymbol{u})|^2 + |\boldsymbol{\psi_p}(\boldsymbol{t}, R\boldsymbol{u})|^2\} d\boldsymbol{t} d\boldsymbol{u}$$

$$T_2(R,\epsilon)=\int_{1-\epsilon<|\boldsymbol{u}|\le 1}\int_{|\boldsymbol{t}|\ge R\sqrt{1-|\boldsymbol{u}|^2}}\{|\boldsymbol{\psi_t}(\boldsymbol{t},R\boldsymbol{u})|^2+|\boldsymbol{\psi_p}(\boldsymbol{t},R\boldsymbol{u})|^2\}d\boldsymbol{t}d\boldsymbol{u}.$$

If $|\boldsymbol{u}|\le 1-\epsilon$ and $|\boldsymbol{t}|\ge R\sqrt{1-|\boldsymbol{u}|^2}$ then $|\boldsymbol{t}|\ge R\sqrt{\epsilon(2-\epsilon)}$. In particular, $|\boldsymbol{t}|\ge\sqrt{(2-\epsilon)/\epsilon}$, if $R>1/\epsilon$. Therefore, by the Riemann-Lebesgue lemma

$$\overline{\lim_{R\to\infty}}\, T_1(R,\epsilon)\le T_1^\infty(\epsilon)=\omega_{d-k}\;\;\fint_{Q_{d-k}}\int_{|\boldsymbol{t}|\ge\sqrt{(2-\epsilon)/\epsilon}}\{|\boldsymbol{\psi_t}(\boldsymbol{t},\boldsymbol{p})|^2+|\boldsymbol{\psi_p}(\boldsymbol{t},\boldsymbol{p})|^2\}d\boldsymbol{p}d\boldsymbol{t}.$$

Also, by the Riemann-Lebesgue lemma

$$\overline{\lim_{R\to\infty}}\, T_2(R,\epsilon)\le T_2^\infty(\epsilon)=|\{1-\epsilon<|\boldsymbol{u}|\le 1\}|\;\;\fint_{Q_{d-k}}\int_{\mathbb{R}^k}\{|\boldsymbol{\psi_t}(\boldsymbol{t},\boldsymbol{p})|^2+|\boldsymbol{\psi_p}(\boldsymbol{t},\boldsymbol{p})|^2\}d\boldsymbol{p}d\boldsymbol{t}.$$

We conclude that $\rho=0$, since

$$\lim_{\epsilon\to 0}T_1^\infty(\epsilon)=\lim_{\epsilon\to 0}T_2^\infty(\epsilon)=0.$$

D Proof of Theorem 3.14

We may assume, without loss of generality, that $\boldsymbol{n}=\boldsymbol{e}_1$. By Lemma 3.2 in [97], applied to the bounded domain $Q=[0,1]^d$, there exists a sequence of functions $\boldsymbol{u}_n(\boldsymbol{x})$ converging uniformly in Q to $\boldsymbol{u}_0(\boldsymbol{x})=x_1\boldsymbol{a}$ and such that $\|\nabla\boldsymbol{u}_n\|_\infty$ is a bounded sequence and for all $1\le j\le r$

$$\lim_{n\to\infty}|\{\boldsymbol{x}\in Q:\mathrm{dist}(\nabla\boldsymbol{u}_n(\boldsymbol{x}),\boldsymbol{H}_j)<1/n\}|=\lambda_j.$$

Let $\boldsymbol{p}_n(\boldsymbol{x})$ denote the function defined in the layer $0<x_1<1$, which is periodic with periods $\boldsymbol{e}_2,\ldots,\boldsymbol{e}_d$ and equal to $\boldsymbol{u}_n(\boldsymbol{x})$ on Q. Finally, we let

$$\boldsymbol{v}_n(\boldsymbol{x})=\begin{cases}\boldsymbol{a}, & \text{if } x_1\ge 1,\\ \boldsymbol{0}, & \text{if } x_1\le 0,\\ \boldsymbol{p}_n(\boldsymbol{x}), & \text{if } 0<x_1<1,\end{cases}$$

Clearly, $\boldsymbol{v}_n(\boldsymbol{x})\to\boldsymbol{\phi}_0(\boldsymbol{x})$ uniformly in $\mathbb{R}^d$. However, the functions $\boldsymbol{v}_n(\boldsymbol{x})$ have jump discontinuities across the surfaces $\Gamma_{j,k}=\{x_j=k, 0<x_1<1\}$, $j=2,\ldots,d$, $k\in\mathbb{Z}$, as well as the planes $\Pi_0=\{x_1=0\}$ and $\Pi_1=\{x_1=1\}$. Let $\epsilon_n=\|\boldsymbol{v}_n-\boldsymbol{\phi}_0\|_\infty$. Then $\epsilon_n\to 0$ as $n\to\infty$. Let

$$\Gamma=\Pi_0\cup\Pi_1\cup\left(\bigcup_{j=1}^d\left(\bigcup_{k\in\mathbb{Z}}\Gamma_{j,k}\right)\right)$$

be the entire singular set. When n is sufficiently large there is a $C^\infty(\mathbb{R}^d)$ function $\eta_n(\boldsymbol{x})$ that is periodic with periods $\boldsymbol{e}_2,\ldots,\boldsymbol{e}_d$, which is equal to 0 on Γ and 1 on $\{\boldsymbol{x}\in\mathbb{R}^d:\mathrm{dist}(\boldsymbol{x},\Gamma)>\sqrt{\epsilon_n}\}$, and such that $\|\nabla\eta_n\|_\infty\le C/\sqrt{\epsilon_n}$. It follows that the function

$$\boldsymbol{\phi}_n(\boldsymbol{x})=(1-\eta_n(\boldsymbol{x}))\boldsymbol{\phi}_0(\boldsymbol{x})+\eta_n(\boldsymbol{x})\boldsymbol{v}_n(\boldsymbol{x})$$

is Lipschitz continuous with

$$\|\nabla \boldsymbol{\phi}_n\|_\infty \leq \|\nabla \boldsymbol{\phi}_0\|_\infty + \|\nabla \boldsymbol{u}_n\|_\infty + C\sqrt{\epsilon_n}.$$

Obviously, $\boldsymbol{\phi}_n(\boldsymbol{x})$ converges uniformly to $\boldsymbol{\phi}_0(\boldsymbol{x})$. In addition $\nabla \boldsymbol{\phi}_n(\boldsymbol{x}) = 0$ whenever $x_1 < -\sqrt{\epsilon_n}$ or $x_1 > 1 + \sqrt{\epsilon_n}$. It follows that (3.19) holds. Observe that $\boldsymbol{\phi}_n(\boldsymbol{x})$ has periods $\boldsymbol{e}_2, \ldots, \boldsymbol{e}_d$, since both $\boldsymbol{v}_n(\boldsymbol{x})$ and $\eta_n(\boldsymbol{x})$ do. Thus, $\boldsymbol{\psi}_n \in \mathcal{S}_1^0$, where

$$\boldsymbol{\psi}_n(t, \boldsymbol{p}) = \boldsymbol{\phi}_n\left(t\boldsymbol{e}_1 + \sum_{j=2}^{d} p_j \boldsymbol{e}_j\right).$$

Hence, $\boldsymbol{\phi}_n \in \mathcal{C}_1$. To finish the proof of the theorem we need to establish (3.29). This is a consequence of the formula (3.24) and the relation

$$\lim_{n\to\infty} \int_{\mathbb{R}} \left(\int_{[0,1]^{d-1}} W^\circ(\boldsymbol{F}, \nabla \boldsymbol{\phi}_n) dx_2 \ldots dx_d \right) dx_1 = \lim_{n\to\infty} \int_Q W^\circ(\boldsymbol{F}, \nabla \boldsymbol{u}_n) d\boldsymbol{x} = J(\boldsymbol{F}, \nu).$$

E Proof of Lemma 4.4

The lemma is best proved in the $(\boldsymbol{t}, \boldsymbol{p})$ variables, where instead of $[0,1]^{d-k}$ periodic field $\boldsymbol{\psi}$ we use Q_{d-k} periodic field, that we denote $\boldsymbol{\psi}$ as well, so that

$$\boldsymbol{\phi}(\boldsymbol{x}) = \boldsymbol{\psi}(\boldsymbol{R}\boldsymbol{x}, \boldsymbol{Q}\boldsymbol{x}) \qquad \boldsymbol{\psi}(\boldsymbol{t}, \boldsymbol{p}) = \boldsymbol{\phi}(\boldsymbol{R}^T\boldsymbol{t} + \boldsymbol{Q}^T\boldsymbol{p}).$$

In terms of $\boldsymbol{\psi}$ equations (4.12) become

$$\begin{cases} \nabla_{\boldsymbol{t}} \cdot (\boldsymbol{P}(\boldsymbol{F} + \boldsymbol{\psi}_{\boldsymbol{t}}\boldsymbol{R} + \boldsymbol{\psi}_{\boldsymbol{p}}\boldsymbol{Q})\boldsymbol{R}^T) + \nabla_{\boldsymbol{p}} \cdot (\boldsymbol{P}(\boldsymbol{F} + \boldsymbol{\psi}_{\boldsymbol{t}}\boldsymbol{R} + \boldsymbol{\psi}_{\boldsymbol{p}}\boldsymbol{Q})\boldsymbol{Q}^T) = \boldsymbol{0}, \\ \nabla_{\boldsymbol{t}} \cdot (\boldsymbol{R}\boldsymbol{P}^*(\boldsymbol{F} + \boldsymbol{\psi}_{\boldsymbol{t}}\boldsymbol{R} + \boldsymbol{\psi}_{\boldsymbol{p}}\boldsymbol{Q})\boldsymbol{R}^T) = \nabla_{\boldsymbol{p}} \cdot (\boldsymbol{\psi}_{\boldsymbol{t}}^T \boldsymbol{P}(\boldsymbol{F} + \boldsymbol{\psi}_{\boldsymbol{t}}\boldsymbol{R} + \boldsymbol{\psi}_{\boldsymbol{p}}\boldsymbol{Q})\boldsymbol{Q}^T), \\ \nabla_{\boldsymbol{p}} \cdot (\boldsymbol{Q}\boldsymbol{P}^*(\boldsymbol{F} + \boldsymbol{\psi}_{\boldsymbol{t}}\boldsymbol{R} + \boldsymbol{\psi}_{\boldsymbol{p}}\boldsymbol{Q})\boldsymbol{Q}^T) = \nabla_{\boldsymbol{t}} \cdot (\boldsymbol{\psi}_{\boldsymbol{p}}^T \boldsymbol{P}(\boldsymbol{F} + \boldsymbol{\psi}_{\boldsymbol{t}}\boldsymbol{R} + \boldsymbol{\psi}_{\boldsymbol{p}}\boldsymbol{Q})\boldsymbol{R}^T) \end{cases} \tag{E.1}$$

while relation (4.18) reads

$$\begin{cases} \displaystyle\int_{\mathbb{R}^k} \int_{Q_{d-k}} \boldsymbol{R}\widehat{\boldsymbol{P}}^* \boldsymbol{R}^T d\boldsymbol{p} d\boldsymbol{t} = \boldsymbol{0}, \\ \displaystyle\int_{\mathbb{R}^k} \int_{Q_{d-k}} \boldsymbol{\psi}_{\boldsymbol{p}}^T \widehat{\boldsymbol{P}} \boldsymbol{R}^T d\boldsymbol{p} d\boldsymbol{t} = \boldsymbol{0}, \end{cases} \tag{E.2}$$

where

$$\widehat{\boldsymbol{P}} = \widehat{\boldsymbol{P}}(\boldsymbol{\psi}_{\boldsymbol{t}}\boldsymbol{R} + \boldsymbol{\psi}_{\boldsymbol{p}}\boldsymbol{Q}) = \boldsymbol{P}(\boldsymbol{F} + \boldsymbol{\psi}_{\boldsymbol{t}}\boldsymbol{R} + \boldsymbol{\psi}_{\boldsymbol{p}}\boldsymbol{Q}) - \boldsymbol{P}(\boldsymbol{F}).$$

Replacing $\widehat{\boldsymbol{P}}^*$ by its expression from (4.15) and using equations (E.1) we obtain

$$\nabla_{\boldsymbol{t}} \cdot (\boldsymbol{R}\widehat{\boldsymbol{P}}^* \boldsymbol{R}^T) = \nabla_{\boldsymbol{p}} \cdot (\boldsymbol{\psi}_{\boldsymbol{t}}^T \widehat{\boldsymbol{P}} \boldsymbol{Q}^T) - \nabla_{\boldsymbol{p}} \cdot (\boldsymbol{R}\boldsymbol{F}^T \boldsymbol{P}(\boldsymbol{F} + \boldsymbol{\psi}_{\boldsymbol{t}}\boldsymbol{R} + \boldsymbol{\psi}_{\boldsymbol{p}}\boldsymbol{Q})\boldsymbol{Q}^T), \tag{E.3}$$

since

$$\nabla_{\boldsymbol{t}} \cdot (\boldsymbol{R}\boldsymbol{N}(\boldsymbol{\psi_t}\boldsymbol{R} + \boldsymbol{\psi_p}\boldsymbol{Q})\boldsymbol{R}^T) = -\nabla_{\boldsymbol{t}} \cdot (\boldsymbol{\psi_t}^T\boldsymbol{P}(\boldsymbol{F})).$$

Let

$$\boldsymbol{f}_1(\boldsymbol{t}) = \int_{Q_{d-k}} \boldsymbol{R}\widehat{\boldsymbol{P}}^*\boldsymbol{R}^T d\boldsymbol{p},$$

$$\boldsymbol{f}_2(\boldsymbol{t}) = \int_{Q_{d-k}} \boldsymbol{\psi_p}^T\widehat{\boldsymbol{P}}\boldsymbol{R}^T d\boldsymbol{p} = \int_{Q_{d-k}} \boldsymbol{\psi_p}^T\boldsymbol{P}(\boldsymbol{F} + \boldsymbol{\psi_t}\boldsymbol{R} + \boldsymbol{\psi_p}\boldsymbol{Q})\boldsymbol{R}^T d\boldsymbol{p}.$$

Integrating (E.3) over Q_{d-k} and using the periodicity we obtain that $\nabla_{\boldsymbol{t}} \cdot \boldsymbol{f}_1(\boldsymbol{t}) = \boldsymbol{0}$. Similarly, Integrating the third equation in (E.1) over Q_{d-k} we conclude that $\nabla_{\boldsymbol{t}} \cdot \boldsymbol{f}_2(\boldsymbol{t}) = \boldsymbol{0}$. We estimate

$$|\widehat{\boldsymbol{P}}^*| \le C(|\boldsymbol{\psi_t}|^2 + |\boldsymbol{\psi_p}|^2), \qquad |\boldsymbol{\psi_p}^T\widehat{\boldsymbol{P}}| \le C(|\boldsymbol{\psi_t}|^2 + |\boldsymbol{\psi_p}|^2),$$

since $\boldsymbol{\psi_t}$ and $\boldsymbol{\psi_p}$ are assumed to be uniformly bounded. Then $\boldsymbol{\phi} \in \mathcal{C}_k$ implies that $\{\boldsymbol{f}_1, \boldsymbol{f}_2\} \subset L^1(\mathbb{R}^k)$. The statement of the lemma follows from

$$\int_{\mathbb{R}^k} \boldsymbol{f}_1(\boldsymbol{t})d\boldsymbol{t} = \boldsymbol{0}, \qquad \int_{\mathbb{R}^k} \boldsymbol{f}_2(\boldsymbol{t})d\boldsymbol{t} = \boldsymbol{0},$$

which is a consequence of a simple observation that any L^1 divergence-free vector field $\boldsymbol{f}(\boldsymbol{t})$ on $\mathbb{R}^k$ must satisfy $\int_{\mathbb{R}^k} \boldsymbol{f} d\boldsymbol{t} = \boldsymbol{0}$. Indeed, $\boldsymbol{f} \in L^1$ implies that its Fourier transform $\widehat{\boldsymbol{f}}(\boldsymbol{\omega})$ is continuous. $\nabla \cdot \boldsymbol{f} = 0$ implies that $\boldsymbol{\omega} \cdot \widehat{\boldsymbol{f}}(\boldsymbol{\omega}) = 0$ for any $\boldsymbol{\omega} \in \mathbb{R}^k$. Fixing $\boldsymbol{\omega} \neq \boldsymbol{0}$ we obtain

$$\frac{\boldsymbol{\omega} \cdot \widehat{\boldsymbol{f}}(\epsilon\boldsymbol{\omega})}{|\boldsymbol{\omega}|} = \frac{\epsilon\boldsymbol{\omega} \cdot \widehat{\boldsymbol{f}}(\epsilon\boldsymbol{\omega})}{|\epsilon\boldsymbol{\omega}|} = 0.$$

Passing to the limit as $\epsilon \to 0$ and using continuity of $\widehat{\boldsymbol{f}}(\boldsymbol{\omega})$ we obtain $\boldsymbol{\omega} \cdot \widehat{\boldsymbol{f}}(\boldsymbol{0}) = 0$. Thus $\widehat{\boldsymbol{f}}(\boldsymbol{0}) = \boldsymbol{0}$, since $\boldsymbol{\omega} \in \mathbb{R}^k \setminus \{\boldsymbol{0}\}$ was arbitrary.

F Proof of Theorem 4.6

When the subspace $\mathcal{L}$ described by $\boldsymbol{R}$ is fixed we can simplify our notation by regarding first k components of $\boldsymbol{x}$ as $\boldsymbol{t}$ and the remaining components as $\boldsymbol{p}$. Then $\nabla\boldsymbol{\phi} = [\boldsymbol{\psi_t}, \boldsymbol{\psi_p}]$. We then have the corresponding splitting of $\boldsymbol{P} = [\boldsymbol{P}_1, \boldsymbol{P}_2]$ and

$$\boldsymbol{P}^* = W(\boldsymbol{F} + [\boldsymbol{\psi_t}, \boldsymbol{\psi_p}]) \begin{bmatrix} \boldsymbol{I}_k & \boldsymbol{0} \\ \boldsymbol{0} & \boldsymbol{I}_{d-k} \end{bmatrix} - \begin{bmatrix} \boldsymbol{\psi_t}^T \\ \boldsymbol{\psi_p}^T \end{bmatrix} [\boldsymbol{P}_1, \boldsymbol{P}_2] = \begin{bmatrix} \boldsymbol{P}_1^* & -\boldsymbol{\psi_t}^T\boldsymbol{P}_2 \\ -\boldsymbol{\psi_p}^T\boldsymbol{P}_1 & \boldsymbol{P}_2^* \end{bmatrix}.$$

Similarly, splitting the $\boldsymbol{t}$ and $\boldsymbol{p}$ components we have

$$\widehat{\boldsymbol{P}}(\boldsymbol{H}) = [\widehat{\boldsymbol{P}}_1, \widehat{\boldsymbol{P}}_2], \qquad \widehat{\boldsymbol{P}}_i = \boldsymbol{P}_i(\boldsymbol{F} + [\boldsymbol{\psi_t}, \boldsymbol{\psi_p}]) - \boldsymbol{P}_i(\boldsymbol{F}),\ i = 1, 2.$$

$$\widehat{\boldsymbol{P}}^*(\boldsymbol{H}) = \begin{bmatrix} \widehat{\boldsymbol{P}}_1^* & -\boldsymbol{\psi}_{\boldsymbol{t}}^T \widehat{\boldsymbol{P}}_2 \\ -\boldsymbol{\psi}_{\boldsymbol{p}}^T \widehat{\boldsymbol{P}}_1 & \widehat{\boldsymbol{P}}_2^* \end{bmatrix},$$

where

$$\widehat{\boldsymbol{P}}_1^* = W^\circ(\boldsymbol{F}, [\boldsymbol{\psi}_{\boldsymbol{t}}, \boldsymbol{\psi}_{\boldsymbol{p}}])\boldsymbol{I}_k - \boldsymbol{\psi}_{\boldsymbol{t}}^T \widehat{\boldsymbol{P}}_1. \qquad \widehat{\boldsymbol{P}}_2^* = W^\circ(\boldsymbol{F}, [\boldsymbol{\psi}_{\boldsymbol{t}}, \boldsymbol{\psi}_{\boldsymbol{p}}])\boldsymbol{I}_{d-k} - \boldsymbol{\psi}_{\boldsymbol{p}}^T \widehat{\boldsymbol{P}}_2.$$

Next we use the generalized Calpeyron's theorem [59] for $\widehat{W}(\boldsymbol{H})$:

$$\int_{|\boldsymbol{t}|\le R} \int_{Q_{d-k}} \widehat{W}(\nabla\boldsymbol{\phi}) d\boldsymbol{p} d\boldsymbol{t} = \frac{1}{d}(T_1 + T_2), \tag{F.1}$$

where

$$T_1 = \int_{|\boldsymbol{t}|=R} \int_{Q_{d-k}} \{(\widehat{\boldsymbol{P}}_1^* \boldsymbol{n}_{\boldsymbol{t}}, \boldsymbol{t}) - (\boldsymbol{\psi}_{\boldsymbol{p}}^T \widehat{\boldsymbol{P}}_1 \boldsymbol{n}_{\boldsymbol{t}}, \boldsymbol{p}) + (\widehat{\boldsymbol{P}}_1 \boldsymbol{n}_{\boldsymbol{t}}, \boldsymbol{\psi})\} d\boldsymbol{p} dS(\boldsymbol{t}),$$

$$T_2 = \int_{|\boldsymbol{t}|\le R} \int_{\partial Q_{d-k}} \{(\widehat{\boldsymbol{P}}_2^* \boldsymbol{n}_{\boldsymbol{p}}, \boldsymbol{p}) - (\boldsymbol{\psi}_{\boldsymbol{t}}^T \widehat{\boldsymbol{P}}_2 \boldsymbol{n}_{\boldsymbol{p}}, \boldsymbol{t}) + (\widehat{\boldsymbol{P}}_2 \boldsymbol{n}_{\boldsymbol{p}}, \boldsymbol{\psi})\} dS(\boldsymbol{p}) d\boldsymbol{t}.$$

Next we observe that

$$\int_{\partial Q_{d-k}} \boldsymbol{\psi}_{\boldsymbol{t}}^T \widehat{\boldsymbol{P}}_2 \boldsymbol{n}_{\boldsymbol{p}} dS(\boldsymbol{p}) = \boldsymbol{0}, \qquad \int_{\partial Q_{d-k}} (\widehat{\boldsymbol{P}}_2 \boldsymbol{n}_{\boldsymbol{p}}, \boldsymbol{\psi}) dS(\boldsymbol{p}) = 0,$$

since $\boldsymbol{\psi}_{\boldsymbol{t}}^T \widehat{\boldsymbol{P}}_2$ and $(\widehat{\boldsymbol{P}}_2)^T \boldsymbol{\psi}$ are Q_{d-k}-periodic. By divergence theorem we obtain

$$\int_{\partial Q_{d-k}} (\widehat{\boldsymbol{P}}_2^* \boldsymbol{n}_{\boldsymbol{p}}, \boldsymbol{p}) dS(\boldsymbol{p}) = \int_{Q_{d-k}} \{(\nabla_{\boldsymbol{p}} \cdot \widehat{\boldsymbol{P}}_2^*, \boldsymbol{p}) + \operatorname{Tr} \widehat{\boldsymbol{P}}_2^*\} d\boldsymbol{p}.$$

The Noether-Eshelby equation gives

$$\nabla_{\boldsymbol{p}} \cdot \widehat{\boldsymbol{P}}_2^* = \nabla_{\boldsymbol{t}} \cdot (\boldsymbol{\psi}_{\boldsymbol{p}}^T \widehat{\boldsymbol{P}}_1),$$

We also compute

$$\operatorname{Tr} \widehat{\boldsymbol{P}}_2^* = (d-k)\widehat{W} - \operatorname{Tr}(\boldsymbol{\psi}_{\boldsymbol{p}}^T \widehat{\boldsymbol{P}}_2)$$

Hence, we obtain

$$T_2 = (d-k) \int_{|\boldsymbol{t}|\le R} \int_{Q_{d-k}} \widehat{W}(\nabla\boldsymbol{\phi}) d\boldsymbol{p} d\boldsymbol{t} + T_2',$$

where

$$T_2' = \int_{|\boldsymbol{t}|=R} \int_{Q_{d-k}} (\boldsymbol{\psi}_{\boldsymbol{p}}^T \widehat{\boldsymbol{P}}_1 \boldsymbol{n}_{\boldsymbol{t}}, \boldsymbol{p}) d\boldsymbol{p} dS(\boldsymbol{t}) - \int_{|\boldsymbol{t}|\le R} \int_{Q_{d-k}} \operatorname{Tr}(\boldsymbol{\psi}_{\boldsymbol{p}}^T \widehat{\boldsymbol{P}}_2) d\boldsymbol{p} d\boldsymbol{t}.$$

Substituting this back into (F.1) we obtain

$$\int_{|\boldsymbol{t}|\le R} \int_{Q_{d-k}} \widehat{W}(\nabla\boldsymbol{\phi}) d\boldsymbol{p} d\boldsymbol{t} = \frac{1}{k}(\widehat{T}_1(R) + \widehat{T}_2(R)),$$

where

$$\widehat{T}_1(R) = \int_{|\boldsymbol{t}|=R}\int_{Q_{d-k}} \{(\widehat{\boldsymbol{P}}_1^*\boldsymbol{n}_{\boldsymbol{t}}, \boldsymbol{t}) + (\widehat{\boldsymbol{P}}_1\boldsymbol{n}_{\boldsymbol{t}}, \boldsymbol{\psi})\}d\boldsymbol{p}dS(\boldsymbol{t}),$$

$$\widehat{T}_2(R) = -\int_{|\boldsymbol{t}|\le R}\int_{Q_{d-k}} \mathrm{Tr}\,(\boldsymbol{\psi}_{\boldsymbol{p}}^T\widehat{\boldsymbol{P}}_2)d\boldsymbol{p}d\boldsymbol{t}.$$

We observe that due to (4.17)

$$\lim_{R\to\infty}\widehat{T}_2(R) = -\mathrm{Tr}\left(\int_{Y_k}\boldsymbol{\psi}_{\boldsymbol{p}}^T\widehat{\boldsymbol{P}}_2 d\boldsymbol{p}d\boldsymbol{t}\right) = 0.$$

To finish the proof of the theorem we need to show that $\widehat{T}_1(R)\to 0$, as $R\to\infty$.

We have $|\widehat{\boldsymbol{P}}| \le C|\nabla\boldsymbol{\phi}|$ and $|\widehat{\boldsymbol{P}}^*| \le C|\nabla\boldsymbol{\phi}|^2$, due to the uniform boundedness of $\nabla\boldsymbol{\phi}$, where the constant C depends on $\boldsymbol{\phi}$, but is independent of R. Thus, $|\widehat{T}_1(R)| \le CK(R)$ for a.e. $R > 1$, where

$$K(R) = \int_{|\boldsymbol{t}|=R}\int_{Q_{d-k}} \{R|\nabla\boldsymbol{\phi}|^2 + |\boldsymbol{\phi}-\boldsymbol{c}||\nabla\boldsymbol{\phi}|\}d\boldsymbol{p}dS(\boldsymbol{t}),$$

where $\boldsymbol{c}\in\mathbb{R}^m$ can be chosen arbitrarily. We have, after an application of the Cauchy-Schwartz inequality

$$\frac{1}{R}\int_R^{2R}K(r)dr \le 2\int_{R<|\boldsymbol{t}|<2R}\int_{Q_{d-k}}|\nabla\boldsymbol{\phi}|^2 d\boldsymbol{p}d\boldsymbol{t} + \frac{\|\boldsymbol{\phi}-\boldsymbol{c}\|_{2,2R}}{R}\left(\int_{R<|\boldsymbol{t}|<2R}\int_{Q_{d-k}}|\nabla\boldsymbol{\phi}|^2 d\boldsymbol{p}d\boldsymbol{t}\right)^{1/2}.$$

If $k = 1$ or $k = 2$ then the boundedness of $\boldsymbol{\phi}$ implies that

$$\lim_{R\to\infty}\frac{1}{R}\int_R^{2R}K(r)dr = 0. \tag{F.2}$$

If $k \ge 3$ then Lemma C.1 guarantees the choice of the constant $\boldsymbol{c}\in\mathbb{R}^m$ such that (F.2) holds. Therefore,

$$\varliminf_{R\to\infty} K(R) = 0.$$

Hence,

$$\left|\int_Y \widehat{W}(\nabla\boldsymbol{\phi})d\boldsymbol{x}\right| \le C\varliminf_{R\to\infty}K(R) = 0.$$

The theorem is proved.

G Proof of Lemma 5.5

We will prove that $\mathcal{G} = \mathcal{G}_0$, where

$$\mathcal{G}_0 = \{\boldsymbol{A} = \mathrm{diag}(A_1,\ldots,A_k),\ A_i > 0,\ i = 1,\ldots,k,\ \mathrm{Tr}\,\boldsymbol{A} = 1\}.$$

If we write $\langle\Gamma(\boldsymbol{n})\rangle_{\boldsymbol{a}}$ in components

$$(\langle\Gamma(\boldsymbol{n})\rangle_{\boldsymbol{a}})_{ij} = \quad ⨍_{\mathbb{S}^{k-1}} \frac{n_i n_j}{a_i a_j \sum_{s=1}^k a_s^{-2} n_s^2} dS(\boldsymbol{n}).$$

we immediately see that $\mathcal{G} \subset \mathcal{G}_0$.

To each $\boldsymbol{a} = (a_1, \ldots, a_k) \in \mathbb{R}^k$ we associate (without relabeling) the diagonal matrix $\boldsymbol{a}$ =diag$(a_1, \ldots, a_k)$. Let $\Delta = \{(a_1, \ldots, a_k) : a_i > 0,\ \sum_{i=1}^k a_i = 1\}$. Then the smooth map $F(\boldsymbol{a}) = \langle\Gamma(\boldsymbol{n})\rangle_{\boldsymbol{a}}$ maps Δ into itself. To prove the reverse inclusion $\mathcal{G}_0 \subset \mathcal{G}$ we need to show that the map $F : \Delta \to \Delta$ is surjective. We first show that the differential of the map F is non-degenerate. This implies, via the inverse function theorem that $F(\Delta)$ is an open subset of Δ.

In order to simplify the calculation we first change variables $\boldsymbol{b} = \boldsymbol{a}^{-1}/\mathrm{Tr}\,(\boldsymbol{a}^{-1})$. Then

$$F(\boldsymbol{a}) = G\left(\frac{\boldsymbol{a}^{-1}}{\mathrm{Tr}\,\boldsymbol{a}^{-1}}\right), \qquad G(\boldsymbol{b}) = \quad ⨍_{\mathbb{S}^{k-1}} \frac{\boldsymbol{bn} \otimes \boldsymbol{bn}}{|\boldsymbol{bn}|^2} dS(\boldsymbol{n}).$$

We compute

$$dF(\boldsymbol{a})\boldsymbol{\eta} = -dG\left(\frac{\boldsymbol{a}^{-1}}{\mathrm{Tr}\,\boldsymbol{a}^{-1}}\right) \frac{\boldsymbol{a}^{-1}\mathrm{Tr}\,(\boldsymbol{a}^{-1}\boldsymbol{\eta}\boldsymbol{a}^{-1}) - \boldsymbol{a}^{-1}\boldsymbol{\eta}\boldsymbol{a}^{-1}\mathrm{Tr}\,\boldsymbol{a}^{-1}}{(\mathrm{Tr}\,\boldsymbol{a}^{-1})^2},$$

where $\boldsymbol{\eta}$ is a diagonal trace-free matrix. If

$$\boldsymbol{a}^{-1}\mathrm{Tr}\,(\boldsymbol{a}^{-1}\boldsymbol{\eta}\boldsymbol{a}^{-1}) - \boldsymbol{a}^{-1}\boldsymbol{\eta}\boldsymbol{a}^{-1}\mathrm{Tr}\,\boldsymbol{a}^{-1} = \boldsymbol{0}$$

then $\boldsymbol{\eta} = \lambda\boldsymbol{a}$ for some scalar λ. Taking traces we conclude that $\lambda = 0$. Hence, the map

$$\boldsymbol{\eta} \mapsto \frac{\boldsymbol{a}^{-1}\mathrm{Tr}\,(\boldsymbol{a}^{-1}\boldsymbol{\eta}\boldsymbol{a}^{-1}) - \boldsymbol{a}^{-1}\boldsymbol{\eta}\boldsymbol{a}^{-1}\mathrm{Tr}\,\boldsymbol{a}^{-1}}{(\mathrm{Tr}\,\boldsymbol{a}^{-1})^2}$$

is a non-degenerate linear transformation on the space of diagonal trace-free matrices. Hence, dF is non-degenerate if and only if dG is non-degenerate. We compute explicitly

$$dG\boldsymbol{\eta} = 2 \quad ⨍_{\mathbb{S}^{k-1}} \left\{\frac{\boldsymbol{\eta n} \odot \boldsymbol{bn}}{|\boldsymbol{bn}|^2} - \frac{\boldsymbol{bn} \otimes \boldsymbol{bn}}{|\boldsymbol{bn}|^4}(\boldsymbol{bn}, \boldsymbol{\eta n})\right\} dS(\boldsymbol{n}),$$

where $\boldsymbol{\eta}$ is diagonal and $\mathrm{Tr}\,\boldsymbol{\eta} = 0$. Suppose $dG\boldsymbol{\eta} = 0$ for some non-zero $\boldsymbol{\eta}$ The Lemma will be proved if we show that only for $\boldsymbol{\eta} = \boldsymbol{0}$. If this is not the case then we have $\mathrm{Tr}\,(\boldsymbol{\eta}\boldsymbol{b}^{-1}dG\boldsymbol{\eta}) = 0$. We compute (using commutativity of the diagonal matrix multiplication)

$$\mathrm{Tr}\,(\boldsymbol{\eta}\boldsymbol{b}^{-1}dG\boldsymbol{\eta}) = 2 \quad ⨍_{\mathbb{S}^{k-1}} \frac{|\boldsymbol{\eta n}|^2|\boldsymbol{bn}|^2 - (\boldsymbol{bn}, \boldsymbol{\eta n})^2}{|\boldsymbol{bn}|^4} dS(\boldsymbol{n}).$$

The Cauchy-Schwartz inequality implies that the integrand is non-negative. For it to be zero we would need $\boldsymbol{\eta n} = \alpha(\boldsymbol{n})\boldsymbol{bn}$ for almost all $\boldsymbol{n} \in \mathbb{S}^{k-1}$. The equivalent relation $\boldsymbol{b}^{-1}\boldsymbol{\eta n} =$

$\alpha(\boldsymbol{n})\boldsymbol{n}$ means that every unit vector is an eigenvector of $\boldsymbol{b}^{-1}\boldsymbol{\eta}$. Hence, there is a constant α_0 such that $\boldsymbol{\eta} = \alpha_0\boldsymbol{b}$. Taking the trace, we obtain $\alpha_0 = 0$ and the non-degeneracy of dG is proved.

The lemma will follow, if we show that if $\boldsymbol{a}_n \to \boldsymbol{a}^\circ \in \partial\Delta$ and $F(\boldsymbol{a}_n) \to \boldsymbol{f}^\circ$, as $n \to \infty$ then $\boldsymbol{f}^\circ \in \partial\Delta$. Let $1 \le i, j \le k$ be a pair of indexes such that $a_i^\circ = 0$ and $a_j^\circ \neq 0$. Such a pair exists, since $\boldsymbol{a}^\circ \in \partial\Delta$. We claim that $f_j^\circ = 0$, finishing the proof of the lemma. We estimate

$$F_j(\boldsymbol{a}) \le \quad \fint_{\mathbb{S}^{k-1}} \frac{a_j^{-2}n_j^2}{a_j^{-2}n_j^2 + a_i^{-2}n_i^2} dS(\boldsymbol{n}) = \quad \fint_{\mathbb{S}^{k-1}} \frac{a_i^2 n_j^2}{a_i^2 n_j^2 + a_j^2 n_i^2} dS(\boldsymbol{n}).$$

Now, by the Lebesgue bounded convergence theorem,

$$f_j^\circ = \lim_{n\to\infty} F_j(\boldsymbol{a}_n) = 0.$$

Lemma 5.5 is now proved.

References

[1] R. Abeyaratne and J. Guo-Hua. Dilatationally nonlinear elastic materials—I. Some theory. *International Journal of Solids and Structures*, 25(10):1201 – 1219, 1989.

[2] S. Agmon, A. Douglis, and L. Nirenberg. Estimates near the boundary for solutions of elliptic partial differential equations satisfying general boundary conditions. I. *Comm. Pure Appl. Math.*, 12:623–727, 1959.

[3] S. Agmon, A. Douglis, and L. Nirenberg. Estimates near the boundary for solutions of elliptic partial differential equations satisfying general boundary conditions. II. *Comm. Pure Appl. Math.*, 17:35–92, 1964.

[4] M. Alava, P. Nukala, and S. Zapperi. Statistical models of fracture. *Advances in Physics*, 55(3-4):349–476, 2006.

[5] G. Allaire. *Shape optimization by the homogenization method*, volume 146 of *Applied Mathematical Sciences*. Springer-Verlag, New York, 2002.

[6] G. Allaire and R. V. Kohn. Explicit optimal bounds on the elastic energy of a two-phase composite in two space dimensions. *Quart. Appl. Math.*, LI(4):675–699, Dec. 1993.

[7] G. Allaire and R. V. Kohn. Optimal bounds on the effective behavior of a mixture of two well-ordered elastic materials. *Quart. Appl. Math.*, LI(4):643–674, Dec. 1993.

[8] S. S. Antman. *Nonlinear problems of elasticity*, volume 107 of *Applied Mathematical Sciences*. Springer, New York, second edition, 2005.

[9] M. Baker and J. L. Ericksen. Inequalities restricting the form of the stress-deformation relations for isotropic elastic solids and Reiner-Rivlin fluids. *J. Washington Acad. Sci.*, 44:33–35, 1954.

[10] J. Ball. Strict convexity, strong ellipticity, and regularity in the calculus of variations. In *Math. Proc. Camb. Phil. Soc*, volume 87, pages 501–513. Cambridge Univ Press, 1980.

[11] J. Ball, K. Koumatos, and H. Seiner. Nucleation of austenite in mechanically stabilized martensite by localized heating. *Journal of Alloys and Compounds*, 2011.

[12] J. M. Ball. Convexity conditions and existence theorems in nonlinear elasticity. *Arch. Ration. Mech. Anal.*, 63(4):337–403, 1976/77.

[13] J. M. Ball. Discontinuous equilibrium solutions and cavitation in nonlinear elasticity. *Philos. Trans. Roy. Soc. London Ser. A*, 306(1496):557–611, 1982.

[14] J. M. Ball. A version of the fundamental theorem for Young measures. In *PDEs and continuum models of phase transitions (Nice, 1988)*, volume 344 of *Lecture Notes in Phys.*, pages 207–215. Springer, Berlin-New York, 1989.

[15] J. M. Ball. Some open problems in elasticity. In *Geometry, mechanics, and dynamics*, pages 3–59. Springer, New York, 2002.

[16] J. M. Ball, B. Kirchheim, and J. Kristensen. Regularity of quasiconvex envelopes. *Calc. Var. Partial Differential Equations*, 11(4):333–359, 2000.

[17] J. M. Ball and J. E. Marsden. Quasiconvexity at the boundary, positivity of the second variation and elastic stability. *Arch. Ration. Mech. Anal.*, 86(3):251–277, 1984.

[18] J. M. Ball and F. Murat. Remarks on Chacon's biting lemma. *Proc. Amer. Math. Soc.*, 107(3):655–663, 1989.

[19] P. W. Bates and P. C. Fife. The dynamics of nucleation for the Cahn-Hilliard equation. *SIAM J. Appl. Math.*, 53(4):990–1008, 1993.

[20] V. L. Berdichevsky. Seed of a melt in a solid. *Dokl. Acad. Nauk SSSR*, 27:80–84, 1983.

[21] V. L. Berdichevsky. *Variational principles of continuum mechanics. I Fundamentals.* Springer-Verlag, Berlin, 2009.

[22] V. L. Berdichevsky. *Variational principles of continuum mechanics. II Applications.* Springer-Verlag, Berlin, 2009.

[23] M. A. Biot. *Mechanics of incremental deformations.* John Wiley & Sons Inc., New York, 1965.

[24] B. Budiansky, J. Hutchinson, and J. Lambropoulos. Continuum theory of dilatant transformation toughening in ceramics. *International Journal of Solids and Structures*, 19(4):337 – 355, 1983.

[25] I. Chenchiah and K. Bhattacharya. The relaxation of two-well energies with possibly unequal moduli. *Arch. Rat. Mech. Anal.*, 187(3):409–479, 2008.

[26] G. P. Cherepanov. Inverse problems of the plane theory of elasticity. *J. Appl. Math. and Mech.*, 38(6):963–979, 1974.

[27] A. Cherkaev. *Variational methods for structural optimization*. Springer-Verlag, New York, 2000.

[28] A. Cherkaev and I. Kucuk. Detecting stress fields in an optimal structure. I. Two-dimensional case and analyzer. *Struct. Multidiscip. Optim.*, 26(1-2):1–15, 2004.

[29] A. Cherkaev and I. Kucuk. Detecting stress fields in an optimal structure. II. Three-dimensional case. *Struct. Multidiscip. Optim.*, 26(1-2):16–27, 2004.

[30] A. Cherkaev and Y. Zhang. Optimal anisotropic three-phase conducting composites: Plane problem. *International Journal of Solids and Structures*, 48(20):2800–2813, Oct. 2011.

[31] M. Chipot and D. Kinderlehrer. Equilibrium configurations of crystals. *Arch. Rational Mech. Anal.*, 103(3):237–277, 1988.

[32] P. G. Ciarlet. *Mathematical elasticity. Vol. I: Three-dimensional elasticity*, volume 20 of *Studies in Mathematics and its Applications*. North-Holland Publishing Co., Amsterdam, 1988.

[33] M. G. Crandall and P. H. Rabinowitz. Bifurcation from simple eigenvalues. *J. Functional Analysis*, 8:321–340, 1971.

[34] B. Dacorogna. Quasiconvexity and relaxation of nonconvex problems in the calculus of variations. *J. Funct. Anal.*, 46(1):102–118, 1982.

[35] B. Dacorogna. Necessary and sufficient conditions for strong ellipticity of isotropic functions in any dimension. *Discrete And Continuous Dynamical Systems, Series B*, 1(2):257–263, 2001.

[36] G. Dolzmann. *Variational methods for crystalline microstructure: analysis and computation*, volume 1803 of *Lecture Notes in Mathematics*. Springer Verlag, 2003.

[37] W. S. Edelstein and R. L. Fosdick. A note on non-uniqueness in linear elasticity theory. *Zeitschrift für Angewandte Mathematik und Physik (ZAMP)*, 19:906–912, 1968. 10.1007/BF01602270.

[38] G. Erdmann. Über die unstetige Lösungen in der Variationsrechnung. *J. Reine Angew. Math.*, 82:21–30, 1877.

[39] J. L. Ericksen and R. A. Toupin. Implications of Hadamard's conditions for elastic stability with respect to uniqueness theorems. *Canad. J. Math.*, 8:432–436, 1956.

[40] J. D. Eshelby. The determination of the elastic field of an ellipsoidal inclusion, and related problems. *Proceedings of the Royal Society of London. Series A, Mathematical and Physical Sciences*, 241:376–396, 1957.

[41] J. D. Eshelby. The elastic field outside an ellipsoidal inclusion. *Proceedings of the Royal Society of London. Series A, Mathematical and Physical Sciences*, 252:561–569, 1959.

[42] J. D. Eshelby. Energy relations and energy momentum tensor in continuum mechanics. In M. Kanninen, W. Adler, A. Rosenfeld, and R. Jaffee, editors, *Inelastic behavior of solids*, pages 77–114. McGraw-Hill, New York, 1970.

[43] J. D. Eshelby. The elastic energy-momentum tensor. *Journal of Elasticity*, 5(3-4):321–335, 1975.

[44] A. B. Freidin. On new phase inclusions in elastic solids. *Z. Angew. Math. Mech.*, 87(2):102–116, 2007.

[45] A. B. Freidin and A. M. Chiskis. Zones of phase transitions in non-linear elastic isotropic materials. Part 1. Basic relations. *Izv Akad Nauk MTT (Mechanics of Solids)*, 4:91–109, 1994. In Russian.

[46] A. B. Freidin and A. M. Chiskis. Zones of phase transitions in non-linear elastic isotropic materials. Part 2. Incompressible materials with a potentials solely dependent on one of the invariants of the strain tensor. *Izv Akad Nauk MTT (Mechanics of Solids)*, 5:49–61, 1994. In Russian.

[47] I. M. Gelfand and S. V. Fomin. *Calculus of variations.* Prentice-Hall, 1963.

[48] G. Geymonat, S. Müller, and N. Triantafyllidis. Homogenization of non-linearly elastic materials, microscopic bifurcation and macroscopic loss of rank-one convexity. *Arch. Ration. Mech. Anal.*, 122(3):231–290, 1993.

[49] M. Giaquinta and S. Hildebrandt. *Calculus of variations. I The Lagrangian formalism*, volume 310 of *Grundlehren der Mathematischen Wissenschaften.* Springer-Verlag, Berlin, 1996.

[50] L. V. Gibiansky and A. V. Cherkaev. Design of composite plates of extremal rigidity. Report 914, Ioffe Physicotechnical Institute, Leningrad, USSR, 1984.

[51] L. V. Gibiansky and A. V. Cherkaev. Microstructures of composites of extremal rigidity and exact estimates of the associated energy density. Report 1115, Ioffe Physicotechnical Institute, Leningrad, USSR, 1987.

[52] Y. Grabovsky. Nonsmooth analysis and quasi-convexification in elastic energy minimization problems. *Structural Optimization*, 10(3/4):217–221, Dec. 1995.

[53] Y. Grabovsky. Bounds and extremal microstructures for two-component composites: A unified treatment based on the translation method. *Proc. Roy. Soc. London, Series A.*, 452(1947):945–952, 1996.

[54] Y. Grabovsky and R. V. Kohn. Anisotropy of the vigdergauz microstructure. *J. Appl. Mech.*, 62(4):1063–1065, 1995.

[55] Y. Grabovsky and R. V. Kohn. Microstructures minimizing the energy of a two phase elastic composite in two space dimensions. I: the confocal ellipse construction. *J. Mech. Phys. Solids*, 43(6):933–947, 1995.

[56] Y. Grabovsky, V. Kucher, and L. Truskinovsky. Probing the limits of rank-one convexity. in preparation.

[57] Y. Grabovsky and L. Truskinovsky. The flip side of buckling. *Cont. Mech. Thermodyn.*, 19(3-4):211–243, 2007.

[58] Y. Grabovsky and L. Truskinovsky. Roughening instability of broken extremals. *Arch. Rat. Mech. Anal.*, 200(1):183–202, 2011.

[59] Y. Grabovsky and L. Truskinovsky. Generalized clapeyron's theorem. in preparation.

[60] Y. Grabovsky and L. Truskinovsky. Metastability in an elastic material with incompatible energy wells: an example. in preparation.

[61] Y. Grabovsky and L. Truskinovsky. Metastability in the presence of phase boundaries. in preparation.

[62] M. E. Gurtin. *Configurational forces as basic concepts of continuum physics*, volume 137 of *Applied Mathematical Sciences*. Springer-Verlag, New York, 2000.

[63] S. Gutiérrez. Laminations in linearized elasticity: the isotropic non-very strongly elliptic case. *J. Elasticity*, 53(3):215–256, 1998/99.

[64] R. Hill. On uniqueness and stability in the theory of finite elastic strain. *J. Mech. Phys. Solids*, 5:229–241, 1957.

[65] R. Hill. On the elasticity and stability of perfect crystals at finite strain. *Math. Proc. Cambridge Philos. Soc.*, 77:225–240, 1975.

[66] E. Hohlfeld and L. Mahadevan. Unfolding the sulcus. *Phys. Rev. Lett.*, 106:105702, Mar 2011.

[67] I. M. Kaganova and A. L. Roytburd. Equilibrium between elastically-interacting phases. *Sov. Phys. JETP*, 67(6):1173–1183, 1988.

[68] A. G. Khachaturyan. *Theory of structural transformation in solids.* Wiley, New York, 1983.

[69] D. Kinderlehrer. Remarks about equilibrium configurations of crystals. In *Material instabilities in continuum mechanics (Edinburgh, 1985–1986)*, Oxford Sci. Publ., pages 217–241. Oxford Univ. Press, New York, 1988.

[70] D. Kinderlehrer and P. Pedregal. Characterizations of Young measures generated by gradients. *Arch. Ration. Mech. Anal.*, 115(4):329–365, 1991.

[71] J. K. Knowles and E. Sternberg. On the ellipticity of the equations of nonlinear elastostatics for a special material. *Journal of Elasticity*, 5:341–361, 1975.

[72] J. K. Knowles and E. Sternberg. On the failure of ellipticity and the emergence of discontinuous deformation gradients in plane finite elastostatics. *J. Elasticity*, 8(4):329–379, 1978.

[73] H. Knüpfer, R. Kohn, and F. Otto. Nucleation barriers for the cubic-to-tetragonal transformation. *Comm Pure Appl Math*, 66(6):867–904, 2013.

[74] H. Knüpfer and R. V. Kohn. Minimal energy for elastic inclusions. *Proceedings of the Royal Society A: Mathematical, Physical and Engineering Science*, 467(2127):695–717, 2011.

[75] R. V. Kohn. The relaxation of a double-well energy. *Continuum Mech. Thermodyn.*, 3:193–236, 1991.

[76] R. V. Kohn and G. Strang. Optimal design and relaxation of variational problems. *Comm. Pure Appl. Math.*, 39:113–137, 139–182 and 353–377, 1986.

[77] J. Kristensen. On the non-locality of quasiconvexity. *Annales de l'Institut Henri Poincare (C) Non Linear Analysis*, 16(1):1 – 13, 1999.

[78] L. B. Kublanov and A. B. Freidin. Nuclei of a solid phase in a deformable material. *Prikl. Mat. Mekh.*, 52(3):493–501, 1988.

[79] I. Kunin, G. Mirenkova, and E. Sosnina. An ellipsoidal crack and needle in an anisotropic elastic medium: Pmm vol. 37, n 3, 1973, pp. 524–531. *Journal of Applied Mathematics and Mechanics*, 37(3):501–508, 1973.

[80] I. Kunin and E. Sosnina. Stress concentration on an ellipsoidal inhomogeneity in an anisotropic elastic medium. *Prikladnaia Matematika i Mekhanika*, 37:306–315, 1973.

[81] I. Kunin and E. G. Sosnina. Ellipsoidal inhomogeneity in an elastic medium. In *Soviet Physics Doklady*, volume 16, page 534, 1971.

[82] J. Langer. Metastable states. *Physica*, 73(1):61 – 72, 1974.

[83] H. Le Dret. An example of H^1-unboundedness of solutions to strongly elliptic systems of partial differential equations in a laminated geometry. *Proc. Roy. Soc. Edinburgh Sect. A*, 105:77–82, 1987.

[84] J. Li, T. Zhu, S. Yip, K. J. V. Vliet, and S. Suresh. Elastic criterion for dislocation nucleation. *Materials Science and Engineering: A*, 365(1–2):25 – 30, 2004.

[85] I. M. Lifshits and L. S. Gulida. On nucleation under local melting. *Dokl. Akad. Nauk SSSR*, 87(4):523–526, 1952. in Russian, English version available.

[86] I. M. Lifshits and L. S. Gulida. On the theory of local melting. *Dokl. Akad. Nauk SSSR*, 87(3):377–380, 1952. in Russian, English version available.

[87] J. Lu. *Elastic energy minimization and the shape of coherent precipitates*. PhD thesis, New York University, New York, NY, 1993.

[88] K. A. Lurie. Optimum control of conductivity of a fluid moving in a channel in a magnetic field. *J. Appl. Math. Mech.*, 28(2):316–327, 1964.

[89] K. A. Lurie. *Applied optimal control theory of distributed systems*. Plenum Press, New York, 1993.

[90] C. Maloney and A. Lemaître. Universal breakdown of elasticity at the onset of material failure. *Physical review letters*, 93(19):195501, 2004.

[91] G. A. Maugin. *Material inhomogeneities in elasticity*. Chapman and Hall, Ltd., London, 1993.

[92] J. C. Michel, O. Lopez-Pamies, P. Ponte Castañeda, and N. Triantafyllidis. Microscopic and macroscopic instabilities in finitely strained porous elastomers. *J. Mech. Phys. Solids*, 55(5):900–938, 2007.

[93] A. Mielke and P. Sprenger. Quasiconvexity at the boundary and a simple variational formulation of Agmon's condition. *J. Elasticity*, 51(1):23–41, 1998.

[94] C. B. Morrey, Jr. Quasi-convexity and the lower semicontinuity of multiple integrals. *Pacific J. Math.*, 2:25–53, 1952.

[95] M. Morse. *The calculus of variations in the large*, volume 18. Amer Mathematical Society, 1934.

[96] S. Müller, J. Sivaloganathan, and S. J. Spector. An isoperimetric estimate and $W^{1,p}$-quasiconvexity in nonlinear elasticity. *Calc. Var. Partial Differential Equations*, 8(2):159–176, 1999.

[97] S. Müller and V. Šverák. Convex integration for Lipschitz mappings and counterexamples to regularity. *Ann. of Math. (2)*, 157(3):715–742, 2003.

[98] T. Mura. *Micromechanics of defects in solids*. Springer, 1987.

[99] N. I. Muskhelishvili. *Some basic problems of the mathematical theory of elasticity*. P. Noordhoff Ltd., Groningen-Holland, 1953.

[100] E. Noether. Invariante variationsprobleme. *Nachr. v. d. Ges. d. Wiss. zu Göttingen*, pages 235–257, 1918. English translation in "Transport Theory and Statistical Mechanics" 1(3):183-207, 1971.

[101] R. Ogden. *Non-linear elastic deformations*. Dover Pubns, 1997.

[102] P. Pedregal. *Parametrized measures and variational principles*. Progress in Nonlinear Differential Equations and their Applications, 30. Birkhäuser Verlag, Basel, 1997.

[103] P. Pedregal. Fully explicit quasiconvexification of the mean-square deviation of the gradient of the state in optimal design. *Electron. Res. Announc. Amer. Math. Soc.*, 7:72–78 (electronic), 2001.

[104] K. A. Pericak-Spector, J. Sivaloganathan, and S. J. Spector. An explicit radial cavitation solution in nonlinear elasticity. *Math. Mech. Solids*, 7(1):87–93, 2002.

[105] G. Puglisi and L. Truskinovsky. Thermodynamics of rate-independent plasticity. *Journal of the Mechanics and Physics of Solids*, 53(3):655–679, 2005.

[106] A. Roytburd and J. Slutsker. Deformation of adaptive materials. Part I: Constrained deformation of polydomain crystals. *Journal of the Mechanics and Physics of Solids*, 47:2299–2329, 1999.

[107] A. Roytburd and J. Slutsker. Deformation of adaptive materials. Part II: Adaptive composite. *Journal of the Mechanics and Physics of Solids*, 47:2331–2349, 1999.

[108] A. Roytburd and J. Slutsker. Deformation of adaptive materials. Part III: Deformation of crystals with polytwin product phases. *Journal of the Mechanics and Physics of Solids*, 49(8):1795–1822, Aug 2001.

[109] O. Salman and L. Truskinovsky. On the critical nature of plastic flow: One and two dimensional models. *International Journal of Engineering Science*, 59:219–254, 2012.

[110] J. Sethna. Crackling noise and avalanches: Scaling, critical phenomena, and the renormalization group. *Les Houches*, 85:257–288, 2007.

[111] M. Šilhavý. *The mechanics and thermodynamics of continuous media.* Springer-Verlag, Berlin, 1997.

[112] H. C. Simpson and S. J. Spector. On barrelling instabilities in finite elasticity. *J. Elasticity*, 14(2):103–125, 1984.

[113] H. C. Simpson and S. J. Spector. On the positivity of the second variation in finite elasticity. *Arch. Ration. Mech. Anal.*, 98(1):1–30, 1987.

[114] H. C. Simpson and S. J. Spector. Necessary conditions at the boundary for minimizers in finite elasticity. *Arch. Ration. Mech. Anal.*, 107(2):105–125, 1989.

[115] H. C. Simpson and S. J. Spector. On bifurcation in finite elasticity: buckling of a rectangular rod. *J. Elasticity*, 92(3):277–326, 2008.

[116] J. Sokolowski and J.-P. Zolesio. *Introduction to Shape Optimization. Shape Sensitivity Analysis.* Springer-Verlag, 1992.

[117] E. M. Stein. *Singular integrals and differentiability properties of functions.* Princeton Mathematical Series, No. 30. Princeton University Press, Princeton, N.J., 1970.

[118] C. A. Stuart. Radially symmetric cavitation for hyperelastic materials. *Ann. Inst. H. Poincaré Anal. Non Linéaire*, 2(1):33–66, 1985.

[119] T. Tanaka, S.-T. Sun, Y. Hirokawa, S. Katayama, J. Kucera, Y. Hirose, and T. Amiya. Mechanical instability of gels at the phase transition. *Nature*, 325(6107):796–798, 02 1987.

[120] L. Tartar. *The general theory of homogenization*, volume 7 of *Lecture Notes of the Unione Matematica Italiana.* Springer-Verlag, Berlin, 2009. A personalized introduction.

[121] C. Truesdell and W. Noll. *The non-linear field theories of mechanics.* Springer-Verlag, Berlin, third edition, 2004.

[122] L. Truskinovsky and G. Zanzotto. Ericksen's bar revisited: energy wiggles. *J. Mech. Phys. Solids*, 44(8):1371–1408, 1996.

[123] L. M. Truskinovsky. Dynamics of nonequilibrium phase boundaries in a heat conducting non-linearly lastic medium. *Prikl. Mat. Mekh.*, 51(6):1009–1019, 1987.

[124] J. van der Waals. The equilibrium between a solid body and a fluid phase, especially in the neighbourhood of the critical state. In *KNAW, Proceedings*, volume 6, pages 1903–1904, 1903.

[125] L. Van Hove. Sur l'extension de la condition de Legendre du calcul des variations aux intégrales multiples à plusieurs fonctions inconnues. *Nederl. Akad. Wetensch., Proc.*, 50:18–23, 1947. (Indagationes Math. 9, 3–8, 1947).

[126] S. B. Vigdergauz. Integral equation of the inverse problem of the plane theory of elasticity. *Prikladnaia Matematika i Mekhanika (PMM)*, 40(3):518–521, 1976.

[127] S. B. Vigdergauz. On a case of the inverse problem of two-dimensional theory of elasticity. *Prikladnaia Matematika i Mekhanika (PMM)*, 41(5):927–933, 1977.

[128] S. B. Vigdergauz. Regular structures with extremal elastic properties. *MTT*, 24(3):57–63, 1989.

[129] S. B. Vigdergauz. Two-dimensional grained composites of extreme rigidity. *ASME J. Appl. Mech.*, 61(2):390–394, 1994.

[130] L. C. Young. Generalized curves and the existence of an attained absolute minimum in the calculus of variations. *Comptes Rendue Soc. Sciences & Lettres Varsovie, cl. III*, 30:212–234, 1937.

[131] L. C. Young. Generalized surfaces in the calculus of variations. *Ann. of Math. (2)*, 43(1):84–103, 1942.

[132] L. C. Young. *Lectures on the calculus of variations and optimal control theory.* W. B. Saunders Co., Philadelphia, 1969. Foreword by Wendell H. Fleming.

[133] M. Zaiser. Scale invariance in plastic flow of crystalline solids. *Advances in Physics*, 55(1-2):185–245, 2006.

[134] L. Zee and E. Sternberg. Ordinary and strong ellipticity in the equilibrium theory of incompressible hyperelastic solids. *Archive for Rational Mechanics and Analysis*, 83:53–90, 1983. 10.1007/BF00281087.

[135] Z. Zhang, R. D. James, and S. Müller. Energy barriers and hysteresis in martensitic phase transformations. *Acta Materialia*, 57(15):4332 – 4352, 2009.